Environmental drivers of space-time dynamics of vegetation in Bardia National Park, Nepal

Author: Jitse Bijlmakers

Program: M.Sc. thesis - Earth Surface and Water - Utrecht University

Supervisors: prof. dr. Derek Karssenberg, prof. dr. Jasper Griffioen & dr. Wiebe Nijland

Student Nr: 5748305

Contact: jitsebijlmakers@xs4all.nl / j.bijlmakers@students.uu.nl

Date: 01-08-2020

Acknowledgments

Wholeheartedly I would like to thank my supervisors Derek and Jasper for the opportunity to participate in this project of tiger conservation in Nepal, and for their trust in the students and room for initiatives. I am grateful to be able to contribute one of the very tiny bricks to fully understanding their habitat and enriching their opportunities of life in the future, along with other endangered fauna living in Bardia National Park.

Moreover, I would like to thank Florian and Ties, two fellow students at Utrecht University. Together we conducted fieldwork and explored scientific perspectives of hydrology on flora and fauna in the Terai as learning master students.

In addition, I would like to thank Shyam, Laxmi, Rabin, guide Tilak BK and all the staff at NTNC Bardia for their warm hospitality, insightful help in the field and showing the ways of Nepali culture and life. Lastly, I am grateful of Dipesh Sharma from Kathmandu, because of your help on aerial photography and captivating enthusiasm in the field of nature conservation.

Front page: View from tiger tower (Bagh Machan). In the front Saccharum spontaneum dominated tall grasslands grow, behind which dryer types of grassland are present. At the right grassland is located that was cut short. Behind the grasses, riverine forest is present. Location is northwest from the Khauraha phanta.

Abstract

In the Terai Arc Landscape a number of endangered faunal species, including the elusive Bengal Tiger (*Panthera tigris tigris*), depend on sub-tropical tall grassland habitats. In Bardia National Park, Nepal, these grasslands are predominantly located close to the Geruwa river, the eastern branch of the Lower Karnali system. The presence of these grasslands is associated with disturbances, such as fluvial processes, forest fires and anthropogenic cutting and burning. In the last decades, these grassland habitats are observed to be vulnerable to encroachment of woody species. In 2009, a change in the hydrology occurred: the dominant discharge branch of the Karnali river, bifurcating at Chisapani, shifted from the eastern branch (Geruwa river) to the western branch (Kauriala river), with reduced discharges along the western border of Bardia National Park as a consequence. This study mapped the development of the vegetation pattern during the last decades in the western part of Bardia National Park and related environmental drivers to the observed vegetation dynamics to gain insight in underlying processes and drivers of change. The environmental drivers considered are precipitation, discharge, flood extent and forest fires. Land cover dynamics derived from annual land cover maps, for which remotely sensed imagery (Landsat) together with data from the field is combined in a supervised Random Forest classification model. In the annual land cover maps, two levels of detail are considered: the level 1 classification, from 1993 to 2019, has 4 classes and the level 2 classification, from 2013 to 2019, has 8 classes. Accuracies obtained for the level 1 and level 2 classification are +- 85 % and 72%, respectively. Landscape fragmentation metrics are used to quantify the development of grassland patches. These metrics indicate that the grassland patches decreased in number and perimeter length, indicating a decrease of heterogeneity of grassland in the landscape. In relation with environmental drivers, peak discharges coincide with successional resets before the shift in river course in 2009. After 2009, this was not observed, because the discharge through the Geruwa river has decreased. Since then coverage of vegetation close to the Geruwa river increased, mainly involving the expansion of alluvial tall grasslands (*Saccharum spontaneum* dominant). For precipitation, only extreme precipitation events have a signal of successional resets in the classifications. We could not show direct relations between the used forest fire dataset and changes in land cover. For grassland (*phantas*) of which is known that yearly burning takes place, succession to later successional stages is prevented and they have been present for a longer time than other grassland patches.

Contents

Digitally supplied: appendices with GEE scripts, RStudio scripts and used in- and output data.

1. Introduction

In the outer reaches of the Himalayas the Terai Arc Landscape (TAL) stretches along the border of the countries Nepal and India. This sub-tropical belt encompasses an elongated lowland region known for its characteristic jungle flora and fauna. In the TAL settlements and agriculture alternate with forests providing shelter for wildlife and rivers draining the Himalayas. It is the most densely populated region of Nepal, in which the fertile soil supports agriculture and livelihood for more than half of the population of the country (CBS, 2014). In this diverse environment rare and threatened endemic species roam in national parks, such as the Greater One-horned Rhinoceros (*rhinoceros unicornis*), Asian elephant (*Elephas maximus*) and the Royal Bengal Tiger (*Panthera tigris tigris*) (Prajapati, 2008; Thapa et al., 2013; DNPWC and DFSC, 2018). To protect wildlife, conservational effort has been taken place in the Terai Arc Landscape, deemed as the number one tiger conservation unit by government of Nepal and WWF. Since 1973, National Parks such as Chitwan National Park (CNP) and Bardia National Park (BNP) have been established in the Terai belt to conserve these unique environments. Together with 12 other countries the Government of Nepal has signed a treaty in 2010 (St. Petersburg Declaration) to double the global tiger numbers by 2022 (DNPWC and DFSC, 2018). Important aspects in establishing healthy tiger numbers are space and sufficient prey, such as ungulates and primates (Støen and Wegge, 1996; DNPWC and DFSC, 2018). The habitat usage of ungulates in Bardia National Park is studied by Dinerstein (1979b) finding that only one of the six ungulate species present has a preference for the homogeneous *Shorea robusta* climax vegetation that covers around 70% of the park, while the other species are dependent on the more heterogeneous riverine forests and grasslands. In the similar National Park of Chitwan the landscape metric habitat heterogeneity is positively correlated with the principle prey for tigers (Bhattarai and Kindlmann, 2012). Not only for ungulates, but also other endangered faunal species such as the Rhino, Hispid hare, Indian hare and the Bengal Florican rely on early successional habitats. These early to mid-successional stages of vegetational development are of prime importance for wildlife habitats in Parks such as Bardia and Chitwan (Eisenberg and Seidensticker, 1976; Seidensticker, 1976; Dinerstein, 1979b).

The presence of the grasslands is associated with disturbances that prohibit successional growth of vegetation to later successional stages. These disturbances include fluvial processes, fires, cutting and grazing (Seidensticker, 1976; Dinerstein, 1979b; Lehmkuhl, 1989, 1994). Fluvial processes in the west part of Bardia National Park are largely originating from the Karnali river, the largest tributary of the Ganges river, located on the western border of the park. The Babai river is dominant in fluvial processes in the eastern part of the park (Adhakari, 2013). Next to fluvial processes, forest fires are common in Bardia Park and mainly occur at the end of the dry season. On top of that, anthropogenic disturbances occur in BNP, which are either originating from local inhabitants or are a part of park management strategies.

Grazing of cattle and cutting and burning by local inhabitants, that retards successional growth of vegetation, has been reduced since Bardia is established as a national park. Each year, during a short period in the dry season, locals are permitted to harvest thatch grass used as building material. Additional cutting and burning is carried out as part of park management strategies since the mid 1990's to prevent encroachment and maintain habitat diversity (Brown, 1997).

Several aspects on changes in the vegetation cover, transition between vegetation types and impact of environmental factors such as hydrology and forest fires are not fully understood in Bardiya National Park.

Of concern in Bardia National Park is that the grasslands have been threatened by encroachment of woody species (Peet et al., 1999a; Jnawali and Wegge, 2000), which follows the natural trajectory for grasslands (Clements, 1916) . In earlier times in BNP the grasslands were more widespread, and the area of these early successional habitats in the region have been declining (Peet et al., 1999a; Odden, 2007). This decline poses a threat to the endangered and rare fauna populations dependent on them.

Near the Karnali river, possibly an equilibrium is maintained between the coverage of grass-dominated communities and the tree-dominated successional stages (Wegge et al., 1999). This equilibrium in vegetation cover and whether it changed has not been extensively studied in the park.

Next to that, Lehmkuhl (1999) suggests with an exploratory successional model of vegetation types in Chitwan National Park, with similar conditions and floral and faunal species, that the aerial change of grass communities differ from higher successional stages of grassland communities. Tall grass species *Saccharum spontaneum*, which is dominant in the floodplain grassland assemblages, covers fresh alluvium faster than the rate of succession from *Saccharum spontaneum* to other ecological important grassland assemblages and vegetation types. He states the clear need for development of models that predict change in coverage of grassland types due to fluvial disturbances.

From a hydrological viewpoint, a change has occurred in the river course of the Karnali river during the 2009 monsoon season. The river changed its dominant discharge channel to the western Kauriala branch (Van Kooten, *unpublished*; Sinclair et al., 2017). Combined with gravel mining and construction of an irrigation system the water supply to the Geruwa river and BNP could be affected (Bheri Babai Diversion Multipurpose Project, no date; Department of Irrigation Nepal, 2017). Ground water near the Karnali floodplain is largely controlled by the Karnali river. The impact of the changing Karnali branch to the Kauriala branch potentially lowers the groundwater head (Berghuis, 2019). A reduced groundwater head could favor higher successional levels of vegetation and therefore loss of habitats important for wildlife.

From a methodology perspective, in Bardia National Park, barely any remote sensing work on the vegetation patterns has been conducted and no scientific work has been published that measured the mechanics of the space-time dynamics using satellite imagery of the park. Dinerstein (1979a) drew a map of a part of the study area and Sharma (1999) presented a vegetation map with GIS of the study area in 1999, using the classes Sal forest, savannah grassland, successional forest, tall grass floodplains and riverbeds. A shift to later successional stages of vegetation was observed (Sharma, 1999; Odden, 2007). Later, Nagarkoti (2012) created a land cover map similar to the extent of Dinerstein but with fewer classes and no changes of land cover have been assessed between them.

These gaps of knowledge in the development of the vegetation patterns and impact of environmental factors in Bardia National Park highlights the interest in understanding the spatial and temporal patterns of land cover based on frequent land cover maps created with remote sensing and GIS. This enables insight in the impact of environmental disturbances with focus on fluvial processes on the successional pattern of the vegetation in the park.

1.1 Objectives and Research Questions

The main objective is to map the development of the vegetation pattern in Bardia Park during the last decades and relate environmental drivers to the observed vegetation dynamics to gain insight in underlying processes and drivers of change. The main question that will be answered in this study is: What are possible causes of changes in the vegetation pattern near the Karnali floodplain in Bardia National Park? Sub questions to be answered are:

I. What is the development of the land cover pattern in the past decades near the Karnali river in Bardia National Park?
II. What is the spatio-temporal variation in the environmental drivers in Bardia National Park?
III. When and where did successional resets happen and what caused these resets?
IV. How do environmental drivers relate to changes in the vegetation pattern in Bardia National Park?

On the large timescale, from 1964 to 2019, it is expected to see a decrease in early successional vegetation and an increase in shrub and forest area, based on literature (Dinerstein, 1979b; Peet et al., 1999a; Odden, 2007) and experiences of staff of the National Park. On short timescales, removal of grass and riverine forest is expected during high discharge years, and in the years thereafter an increase in floodplain grasslands is expected, following the proposed successional trajectory of vegetation for the park and observational data (Dinerstein, 1979a; Lehmkuhl, 1989; Peet, 1997).

The answers to the research questions can be found in the changes in the vegetation pattern derived from a time series of the landcover of the study area. From this land cover series vegetation indices will be calculated, such as changes between years, transitions between classes and metrics of habitat fragmentation. The transitions of class types provides detailed information on dynamics between land cover classes and underlying processes (Kennedy et al., 2014). Landscape fragmentation metrics assist in quantifying the land cover pattern obtained from the classification and provide insight into the spatial development of the classes (McGarigal, 2014).

These indices will be related to environmental factors derived from a rainfall, a discharge, a flood extent and a forest fire dataset. Additionally, the findings of the study area are compared to two similar, close by environments where the change of coverage of the classes is compared. These two regions are the landcover near the Kauriala river, the western branch of the Lower Karnali river and near the Babai river, east in Bardia National Park, because of its hydrologic importance for the National Park.

The designated method for studying these space-time dynamics are remote sensing and Geographic Information Systems (GIS), which have been proven useful for monitoring moist grasslands in other areas in the Terai Arc Landscape (Acharya, 2002; Sarma et al., 2008; Biswas, 2010), vegetation mapping in Chitwan (Thapa, 2011) and morphological changes of rivers (Thorne et al., 1993; Yang et al., 1999). The outline of this study to use remotely sensed Landsat imagery for reconstruction of a time series of land cover of the National park. During fieldwork, the Bardia National Park was visited to collect ground truth data of vegetation types for supervised classification of Landsat satellite imagery for the time series creation. Next to that, archives were visited to acquire aerial photographs of 1964 and a topographic map of 1927 that can be used to evaluate presence of settlements in the park and changes in the land

cover over a longer time span. The time of fieldwork has been done during November and December 2019, falling in a dry period providing adequate circumstances for fieldwork because of the lack of clouds resulting in more reliable satellite imagery. The acquirement date for the satellite imagery is as close as possible to the field date, to reduce the chance of changes in the landscape between the image acquirement date and sample date.

The structure of the report is as follows: first, the study area is described, secondly a literature review is provided containing key properties of the studied ecosystem and used methodology. Thirdly, the methodology contains the data collection of remote sensing and field samples, the classification of the interannual image composites and the analysis of the derived land cover data in respects to environmental drivers. In chapter 4, the results are presented in the order of land cover time series, analysis of the development of the vegetation pattern, environmental indices and the relation between the vegetation pattern and environmental drivers in space and time. Furthermore, a short historical and regional analysis of the study area is conducted. Chapter 5 contains a discussion of the results followed by chapter 6 with the conclusion.

1.2 Study area: Karnali floodplain of Bardia National Park

Nepal is located between 80°4' to 88°12' East longitude and 26°22'to 30°27' and North latitude as a landlocked country. When traversing the country, diverse environments are encountered, with subtropical jungles in the south to majestic peaks of the Himalaya in the north. The Terai Arc Landscape, a uniform subtropical belt stretching from west to east along the toes of the Himalaya in Nepal and India, is one of the regions with the highest population density, and also tiger density (DNPWC and DFSC, 2018). In the far South West of Nepal the Royal Bardia National park (figure 1), a former hunting reserve, was established as the Royal Karnali Wildlife Reserve in 1976 holding an area of 368 km^2. In 1984 it has been expanded with the Babai valley to the east, and received the status of National Park in 1988 (Brown, 1997). Bardia National Park has a core zone area of 968 km^2, surrounded by a buffer zone of 507 km^2 falling in IUCN category II (DNPWC and DFSC, 2018).

Three distinct seasons are present in the region. From June to September a monsoon is present activating intermittent and ephemeral streams, recharging groundwater and providing 90% of the discharge for the Karnali river (USAID, 2018). From late September to February a cool post-monsoon with almost absent precipitation is present in the region. From February to mid-June a hot and dry pre-monsoon is present (USAID, 2018). Temperatures reach a maximum of 45 degrees Celsius in the hot season and fall to 10 degrees Celsius in January (Bolton, 1976). The mean annual precipitation is 1560 mm (DHM, 2017). Important for the hydrology in Bardia National Park is the Karnali river system, called the Lower Karnali south of Chisapani. The Karnali river lies on an alluvial mega fan (USAID 2018) and avulsions are often present. The lower Karnali system is divided in a Geruwa branch in the east and Kauriala river in the west, joining together in India as a tributary to the Ganges river. Prior to 2009 the eastern branch Geruwa was dominant in discharge over the Kauriala branch. Since 2009 the system has shifted to the Kauriala river resulting in a decreased low flow discharge in the Geruwa river. The distribution of discharge is considered 80% for the Kauriala river and 20% for the Geruwa branch during low discharges. During high flow the discharge distribution is modelled to be evenly distributed over the two branches (Van Kooten, 2019; Sinclair et al., 2017).

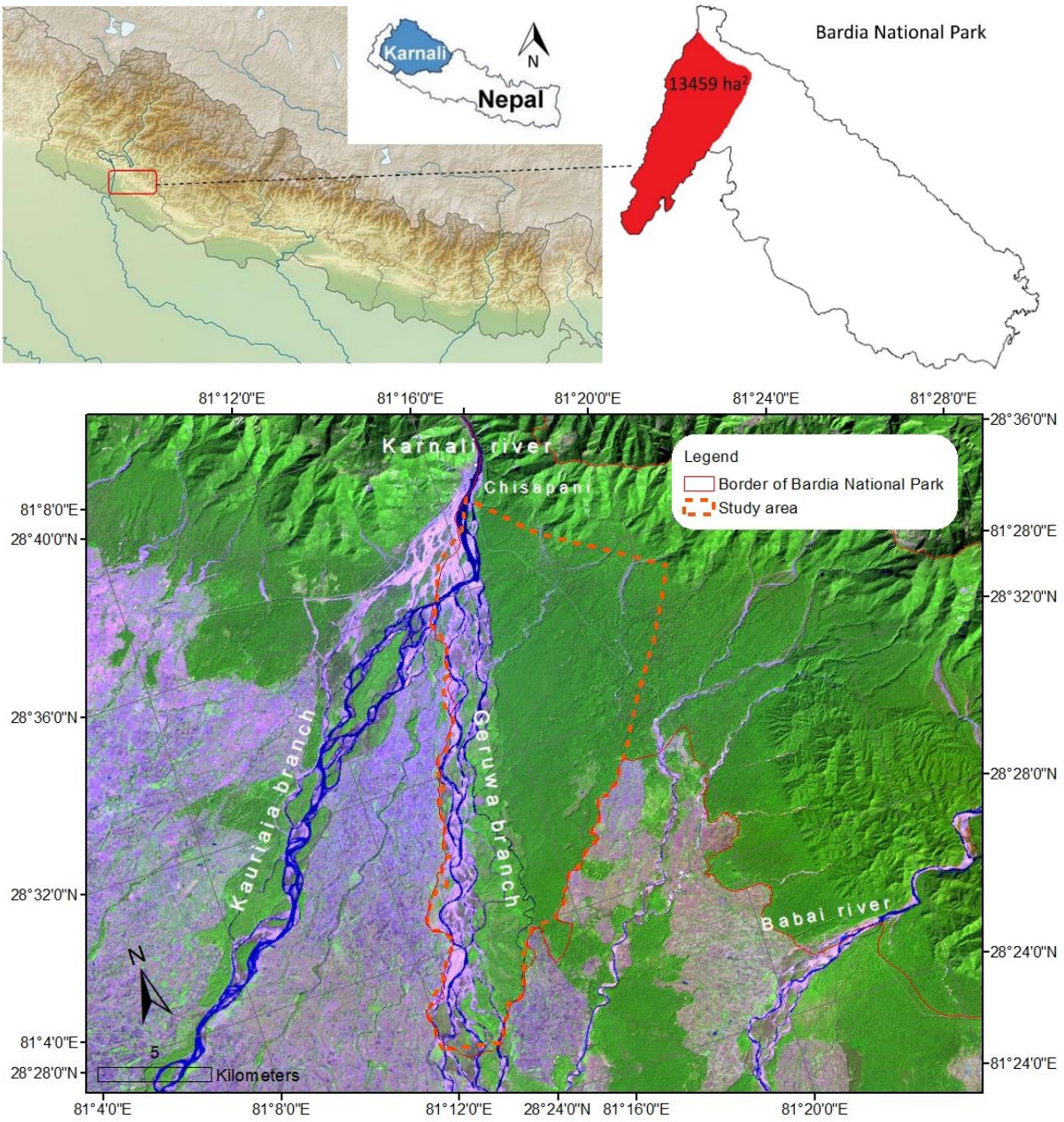

Figure 1: Top left: Location of Nepal with Karnali catchment in blue. Top right: Delineation of Bardia National Park, with study area colored in red. Bottom: Bardia National Park. The mega fan of the Karnali river is located at the western border of Bardia National Park. The Babai valley is in the eastern part of the park. This is a false color composite (RGB = 652 for Landsat 8 imagery, 2019)

2. Literature review

2.1 Properties of ecosystem

2.1.1 Types of vegetation

Dinerstein (1979a) described six major vegetation associations in the park, later modified by Jnawali and Wegge (1993) into seven types: Sal forests, Khair-Sissoo forest, moist riverine forest, mixed hardwood forest, wooded grasslands, previously cultivated fields and tall floodplain grasslands.

Firstly, the Sal forest is discriminated. In India these forests have been studied extensively, due to their central role in the forest ecosystems (Puri, 1961; Champion and Seth, 1968). In Bardia National Park in Sal forest, a moist deciduous forest, the canopy is dominated by *Shorea robusta* (sal) and *Terminalia tomentosa*, with mainly seedlings and small *Buchanania* trees in the understory. *Shorea robusta* is fire resistant and is the most dominant tree species in BNP. Subtypes of Sal forests are dry Sal forests on soils with higher clay content and flat terrain and hill Sal forest on soils with probably reduced fertility and more excessive drainage, where the *Shorea robusta* trees being less dominant (Dinerstein, 1979a). Secondly, the Khair-Sissoo forest is prevalent along the river courses and on floodplain islands in the Terai due to their ability to withstand floods, which in the western part of BNP is concentrated along the eastern Karnali branch. This association is dominated by species as *Dalbergia sissoo* and *Acacia catechu*, mixed with *Bombax ceiba* and *Streblus asper* (Dinerstein 1979a) and its understory is often densely vegetated. Thirdly, a moist riverine forest is present, an assemblage of *Mallotus phillippinensis* and *Syzigium cumini* (Jnawali and Wegge, 1993). Fourthly, a mixed hardwood forest is present, named the *Ficus glomerata-Mallotus philippinensis-Eugenia jambolana* association. It borders the floodplain, resembling a more common ‘West Gangetic Moist Mixed Deciduous Forest' that is present throughout the region. Moist soil conditions have buttressing as consequence. Of the four forests, this forest resembles a tropical evergreen forest the most (Dinerstein, 1979b).

Three main types of grasslands are present in the region. On floodplains tall grasses with the *Saccharum spontaneum* species are dominant (Dinerstein, 1979b; Lehmkuhl, 1989; Peet et al., 1999a). Other tall grass species mixed in are *Phragmites karka*, *Narenga porphyrocoma, Saccharum bengalensis* and shrubs like *Callicarpa macrophylla*. The grasses grow to approximately 3-4 meters, providing shelter to a number of endangered species and are able to withstand inundation. They are encountered in the floodplain and abandoned river channels. *Saccharum spontaneum* is described as a pioneer species. Its flowering is right after the monsoon, probably explaining their dominance in the advantage in the early successional stages of vegetation in wetter parts of the park (Dinerstein, 1979b). Located further from the floodplains *phantas* are present. These phantas are grasslands that previously have been used for agriculture and are considered to owe their existence to human interference (Dinerstein, 1979a; Pokheral, 1993), but this is not clear for every grassland. Nowadays they are vegetated with shorter grasses (< 2 meters) such as and *Imperator Cylindrica*, *Vitiveria zizanioides* and *Desmostachyia bipinnata* (Peet et al., 1999b) Also some tall grasses (> 2 m) such as *Narenga porphyrocoma* and *Erianthus ravennae* can be present. Several assemblages of these grasses have been described (Dinerstein, 1979b; Lehmkuhl, 1989, 1994; Jnawali and Wegge, 1993; Pokheral, 1993; Peet et al., 1999a).

Whether the grasslands are named phantas or wooded grasslands is attributed to their disturbance history. If the disturbances have been caused by humans, they are called phantas (Pokheral, 1993). For other grasslands the origin is unclear (Pokheral, 1993). The largest phantas present are Lamkauli, Baghaura and Khauraha (figure 2). Another difference between wooded grasslands and phantas is that wooded grasslands are more savannah type, with more trees present than in the phantas. Whether a grassland is a phanta or a wooded grassland can change because they are considered to lie on a continuum (Dinerstein, 1979b). According to literature, the phantas were cultivated and grazed in Bardia National Park from 1965 to 1975 (Brown, 1995). Since then, because of the establishment as national park, villages present on Baghaura Phanta and Lamkauli Phanta were relocated out of the reserve (Upreti, 1994). On top of that, from 1979 to 1984, 1572 families have been removed from the Babai valley in the eastern part of BNP (Brown, 1997).

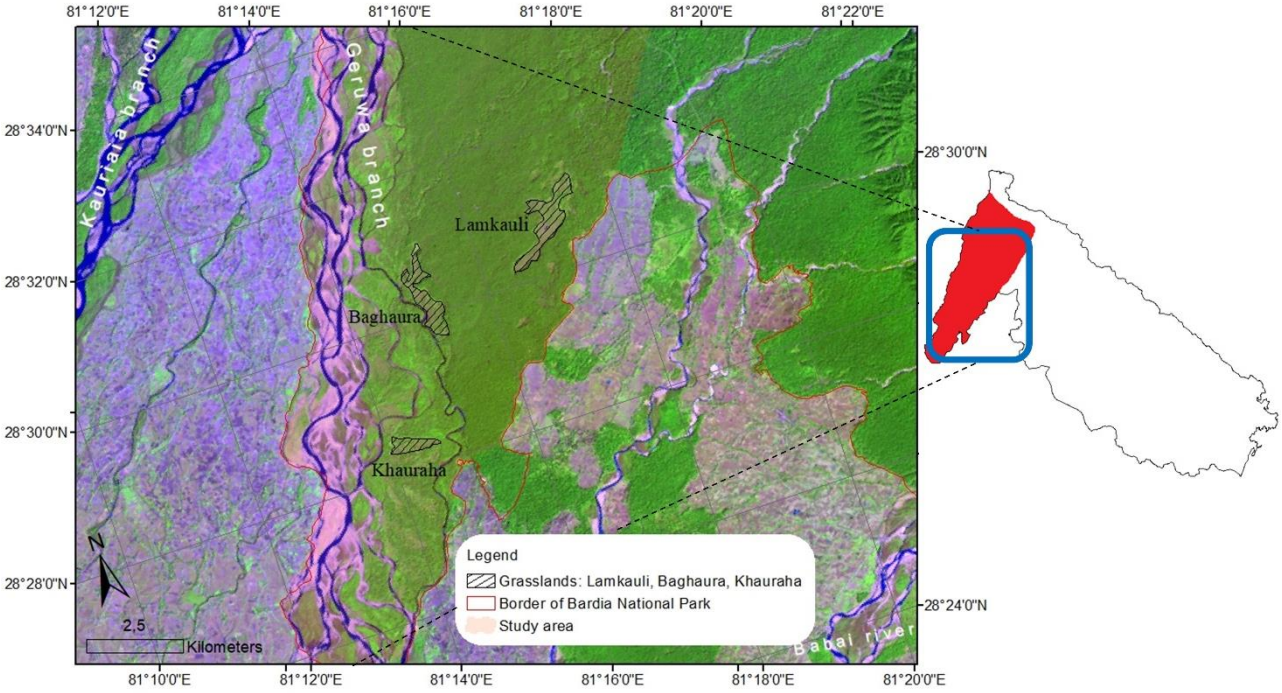

Figure 2: Zoomed in on the study area (lightly shaded red). The grasslands of Lamkauli, Baghaura and Khauraha are shown which are of scientific interest for tiger habitats. Favorable grasses for ungulates are investigated by Shyam Thapa to increase the prey base of tigers. This is a false color composite (RGB = 652 for Landsat 8 imagery, 2019)

2.1.2 Ecological function

The importance of the several present habitat types for ecology has been addressed by several studies and an overview is shown in Table 1 (Dinerstein, 1979). The table gives an overview for the species and displays the ecological importance of several habitat types and their successional stage. Missing in this table are the hispid hare and Bengal florican, which rely on the *Erianthus Ravennae-Imperata cylindrica* assemblage (Inskipp and Inskipp, 1983; Peet, 1997). Also missing are the introduced rhino populations (Jnawali and Wegge, 1993), that rely on tall floodplain grasses. Evident from this graph is that the deer, primary prey of tigers, rely heavily on the early and middle successional stages of habitat. For hog deer and rhino it is thought that the abundance and distribution of the animals is greatly affected if changes occur in the composition and area of tall riverine grassland (Peet, 1997; Odden et al., 2005).

Table 1: Habitat preference of large mammals present in Bardia National Park, after Dinerstein (1979a), names for habitats not adjusted to the names used further in this report. Adjusted names: Tall grass floodplain = wet tall grassland, open grassland = short grassland, savannah = dry tall grassland.

	Habitat type(s) preferred	**Successional stage of habitat type(s) preferred**	
			area %
Hog deer	Tall grass floodplain	Early	Less than 10
Indian hare	Tall grass floodplain	Early	Less than 10
Blackbuck*	Open grassland	Early-middle	10
Swamp deer	Open grassland	Early-middle	10
Chital	Savannah, riverine forest**	Middle	30
Nigal	Savannah, riverine forest	Middle	30
Wild boar	Savannah, riverine forest, Sal forest	Middle to late	90
Elephant	All	Early to late	100
Barking deer	Riverine forest, sal forest	Middle to late	90
Langur monkey	Riverine forest, sal forest	Middle to late	90
Rhesus monkey	Riverine forest, sal forest	Middle to late	90
Goral	Sal forest	Late	10
Sambar		Late	70

** Blackbuck became locally extinct about 1973 but still survives as a relict herd in a sanctuary 30 km from Karnali-Bardia.*

*** Riverine forest in this instance includes early riverine forest and the moist mixed riverine forest.*

**** The area considered in this table is the study area of Dinerstein in 1979, delineated in figure 4.*

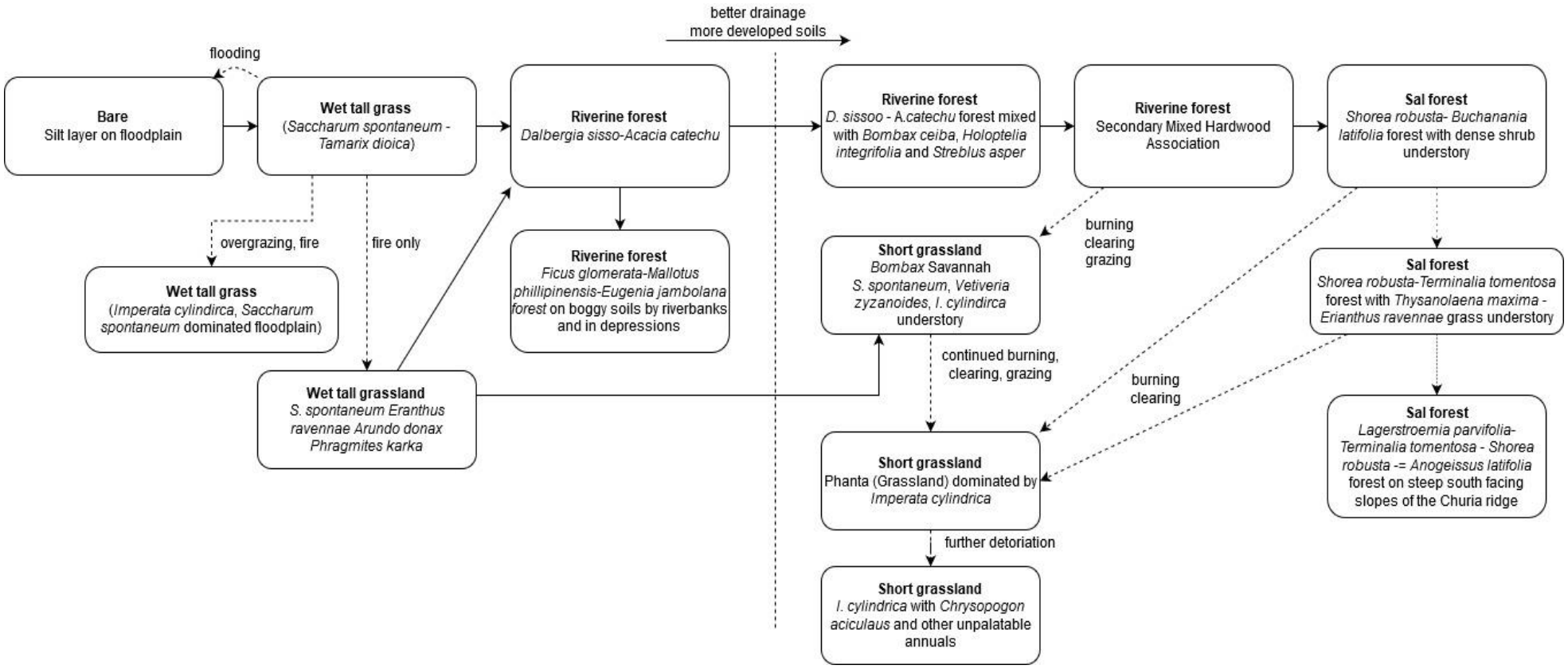

Figure 3: Succession of vegetation types in Bardia National Park according to Dinerstein (1979a). Solid lines represent pathways of succession, dashed lines illustrate disturbances and dotted lines (Sal forest) show other options for successional steps. The names of the vegetation types are adjusted to the labels used in the level 2 land cover maps used further in this report and are further explained in section 2.2. The original names are a more elaborate and can be found in Dinerstein (1979a) from which this figure is adopted.

2.1.3 Vegetation dynamics

As previously stated, of prime importance for presence of grassland are disturbances, which can be fluvial, anthropogenic (cutting, grazing), fires (natural and anthropogenic), and grazing (natural). Fluvial processes are considered to be the most rigorous. Most of the grasslands are present on gravel bars and in active and abandoned stream channels. A study by Ghimire et al. (2014) has been conducted on forest fires in Bardia park using remotely sensed MODIS data. Results are a hazard map, with largest occurrences of forest fires in Sal forest and near the borders of the park.

The forest fires are considered unable to completely set the vegetation back in succession, because of the fire resistant nature of tree species and the magnitude of the fires according to Lehmkuhl (1989). Grassland in the park is cut short by park staff and local people. Annual management practices by the staff includes cutting, burning and uprooting of shrubs and trees to maintain the presence of the grasslands. Next to the ecological importance of the grasslands, grasslands serve as thatching material for the houses of local people. Each year permits are given to local villagers for a restricted period in the year for harvesting resources (Lehmkuhl, 1994; Brown, 1997; Peet et al., 1999a).

With no disturbances present, the line of succession is from floodplain grasslands via riverine forest with *D. Sissoo* and *A. catechu* to other riverine forest types, based on development of soil and better drainage the *Ficus glomerata-Mallotus philippinensis-Eugenia jambolana* if the soil is boggy or eventually to climax Sal forest (figure 3). Proposed is that disturbances hinder this succession resulting in floodplain grasslands turning into wooded grasslands due to the presence of fire, and if disturbances as fire, grazing or cutting continue it leads to the open grasslands (phantas).

2.1.4 Mechanisms of vegetation-flood interaction

Riparian vegetation and river interactions have been extensively studied (e.g. by Hupp and Osterkamp, 1996; Lorenz et al., 1997; Vesipa et al., 2017). The three main elements of interaction are vegetation, sediment and the water stream. High discharges can have diminished survival rate of vegetation as consequence. Next to physical damage and uprooting, anoxia can occur due to prolonged inundation and burial by depositing fresh alluvium. Low discharge rates can have drought stress as consequence, adversely affecting adult vegetation and seedlings when the ground water table is too low. Flooding and associated clearance of vegetation together with deposition of fresh alluvium are observed in Bardia National Park (Dinerstein, 1979b; Lehmkuhl, 1994; Peet et al., 1999b).

2.2 Literature review of methodology

2.2.1 Remote sensing studies in Bardia

Several studies in similar ecosystems in the Terai Arc Landscape have successfully used satellite imagery to study space-time dynamics of land. An overview is given of their methodology, with focus on classification and sample collection, classified classes, and their accuracies. Also considered are the temporal components and incorporation of environmental disturbances. First an overview is given of the remote sensing studies on land cover of Bardia National Park and then an overview of similar ecosystems in- and outside of the Terai, followed by the use of annual land cover maps to map interannual vegetation transitions, providing insight in disturbance mechanisms.

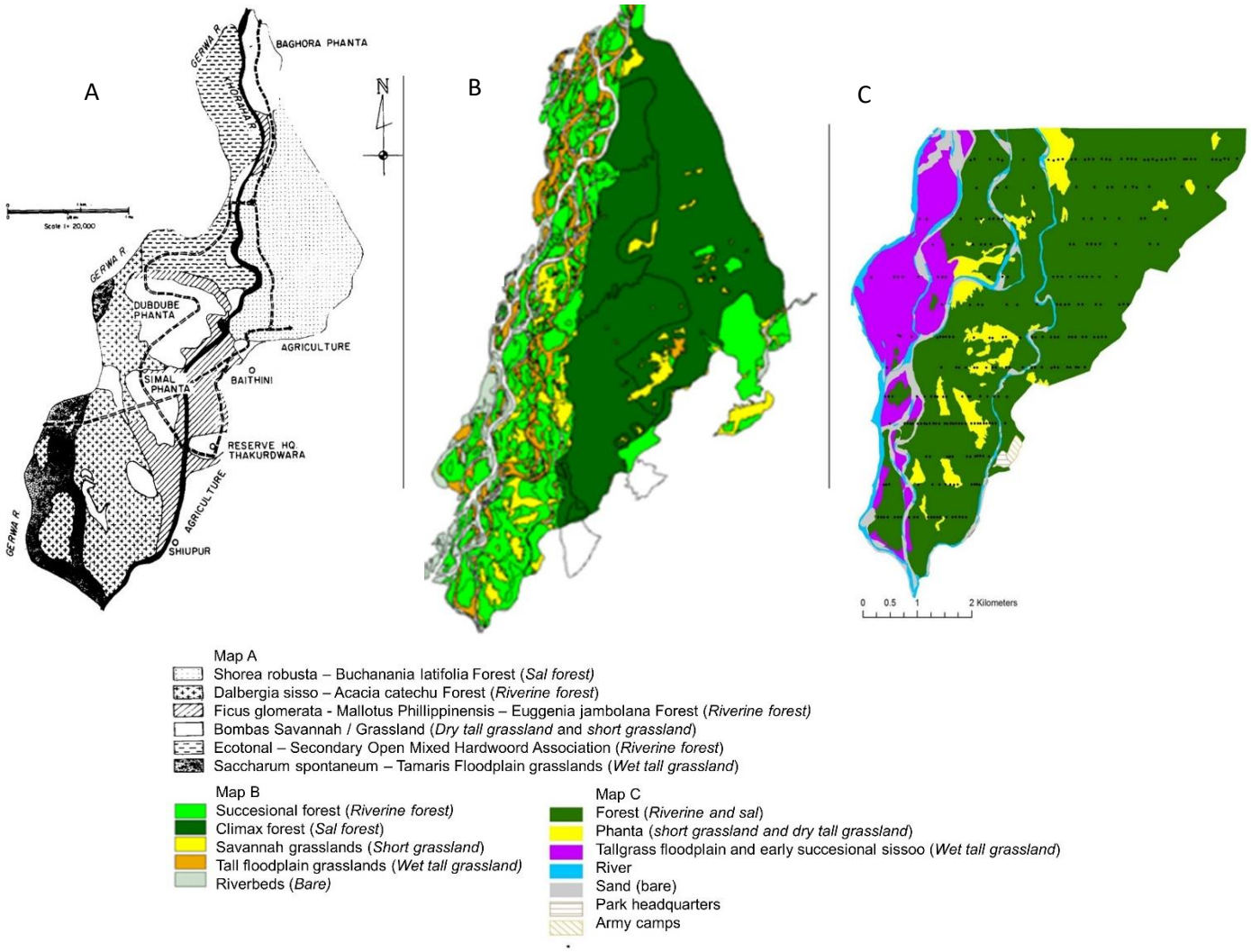

Figure 4: Land cover maps of the Karnali-floodplain of Bardia National Park (Dinerstein, 1979b; Sharma, 1999; Nagarkoti, 2012). Cursive vegetation types indicate the types used in this report (further explained in section 3.2).

In 1979, Dinerstein described and drew a map of the vegetation pattern in the Karnali-floodplain of Bardia National Park. An area of 11.8 km^2 which is part of the study area of this report is shown in figure

4A with the six vegetation types distinguished by Dinerstein described in the section on vegetation types (section 2.1.1). Later Sharma created a land cover map (1997/1999) of Bardia park (from Odden, 2007), displayed in figure 4B. He used the classes successional forest, climax forest, savannah grassland, tall floodplain grassland and riverbeds. No information on accuracy are present for these maps. In Odden (2007), the data of Dinerstein and Sharma were compared (table 2). In comparison, an increase of vegetation successional trajectory is observed, which is in line with statements of other studies (Peet et al., 1999b; Jnawali and Wegge, 2000). No comparison was made with the land cover measured by (Nagarkoti, 2012) which delineated forest, phantas, tall grass floodplain with early successional sissoo forest river and sand in the south of the Karnali floodplain, using topographic map and Google Earth imagery. It was used to investigate habitat preference of Chital deer.

Table 2: Land cover compared from maps shown in figure 4. Table from Odden (2007)

	1976 (Dinerstein)	1997 (Sharma)
Tall floodplain grasslands	8.5%	4.6%
Savannah grasslands (*imperata dominated)*	22.9%	18.8%
Successional forest	44.9%	51.6%
Sal forest	23.7%	25.0%

2.2.2 Land cover studies in the Terai

A more elaborate study on land cover has been conducted in Chitwan, for mapping habitat suitability of leopards (Thapa, 2011). Vegetation types in Chitwan are comparable to the types present in Bardia National Park. Field samples have been taken and used in a supervised classification with a Maximum Likelihood algorithm (ML). Vegetation classes that have been distinguished are sal forest, riverine forest and grasslands, subdivided in the assemblages lowland sal forest, sal mixed forest, hill sal forest, degraded sal forest, riverine forest (*Vellar* association), riverine forest (*Khair-Sissoo*), mixed riverine forest, floodplain grassland, tall grass land (swampy), tall grass land (dry), wooded grassland and short grassland. Half of the field samples have been used for classification and half for validation. The accuracy obtained was 84.5% and Kappa Index of Agreement was 0.83. Classes below 80% for user's and producer's accuracies are degraded Sal forest, riverine mixed forest, and tall grasslands. The study also used landscape metrics which are useful to measure spatial heterogeneity of the classes for categorical land cover. The metrics enable quantification of the spatial properties and geometrics patterns (McGarigal, 2002) that can link ecology to the spatial patterns.

In the TAL, the following studies used land cover maps to study changes of the landscape for which a more general delineation of classes is used to reduce errors in transitions between classes.

Acharya (2002) used three different change detection techniques for land cover change in Chitwan National Park. For the years 1988, 1992 and 2000, the study examines changes In land cover detected by

post classification comparison, image differencing and multitemporal composites. Supervised classification was done with Landsat TM imagery and a maximum likelihood classifier, whereas unsupervised classification was used for the multitemporal composite. 78% accuracy was achieved for the post classification. According to Acharya, the specific nature of changes is effectively studied with the post classification comparison if ground truth data is reliable. For post-classification comparison, errors can be accumulating in the comparisons of classifications due to misclassifications in the individual maps (Skidmore, 1999). Difficulties in obtaining sufficient accuracies in the classification can arise when classes have similar spectral signatures and when these signatures are inadequately selected (Li and Yeh, 1998).

For the buffer zone around Chitwan Park the land use change in the buffer zone has been studied by Baidya et al. (2009). Years considered are 1972, 1992 and 1999 using Landsat imagery, topographic and land utilization maps. Land cover was classified with a Maximum Likelihood Classifier and training samples obtained from a collection of sample data. Classes were agricultural land, forest, grassland, and water bodies, built up and shrub land. The overall accuracy was 79.0%, with for individual classes in descending order the user's accuracies: 97.7% for forest, then agriculture, grassland, waterbodies and at the lower end shrubland with a user's accuracy of 48,2%.

Furthermore, in Chitwan the extend of grasslands has been mapped in 2016 with handheld GPS and tracking the boundary of grassland and forest, resulting in accurate estimations of grassland coverage of the park (CNP, 2016).

In Northeast India, a comprehensive study by Biswas (2010) was conducted with focus on the Jaldapara Wildlife Sanctuary, considering the potential of remote sensing for grassland mapping and their temporal dynamics. Especially the Normalized Difference Vegetation Index (NDVI) and Normalized Difference Dry Index (NDDI) were considered useful for classification of distinct grassland assemblages based on their location, structure, and composition. At first unsupervised classification was used for creating land cover maps of satellite imagery (ASTER and Landsat) from 1978, 1990, 2001, 2004 and 2006. Field data collected with a random sampling design was used to associate the spectral clusters with ground vegetation, followed by change detection of the land cover maps. Level 1 consisted of grassland, woodland, forest, river and riverbed, and classes increased in detail in the level 3 classification: Short grassland, tall dense grassland, tall open riverine grassland, mosaic grassland, woodland, degraded forest and dense forest. Descriptions of these classes are available in (Biswas, 2010; Biswas et al., 2014). The vegetation types are similar to the vegetation observed in Bardia National Park. Temporal comparison of the level 2 and 3 classification provided more difficulties due to decreased accuracies between the years and thus making the comparison less reliable. An 80% overall accuracy was achieved for the land cover map of 2006. For separate classes it was >70% except for degraded forest and villages on the lower end (0.69% and 0.68%) respectively. Since no historic ground truth data was available the indices are compared of the historic land cover maps to the present land cover and enabled a degree of accuracy assessment, especially NDVI, NDMI and wetness were better than brightness and greenness, this assumes no changes within vegetation types. As a quantitative analysis of the vegetation pattern, landscape fragmentation metrics were used to evaluate the landscape pattern and enabled comparison of different areas with each other. Analysis of the temporal vegetation dynamics pointed out that the change of river course in 1968 had a large impact for the spatial pattern of grasslands, that experienced a shift towards later successional stages of vegetation.

Another remote sensing study with a temporal component was conducted in the Indian Terai done by Chitale and Behera (2014), who analyzed the vegetation and land cover dynamics between 1975, 2000 and 2010 in Katerniaghat wildlife sanctuary. This study area is located south of Bardia National Park and downstream of the hydrologically important Geruwa river. Satellite imagery used in this study is Landsat MSS (medium resolution), IKONOS and Quickbird (both high resolution satellite imagery) with accuracies of respectively 83.5%, 91.5%, and 95.2%. Accuracies were validated with field data and for the classification, decision tree classifiers were used. Geruwa river had significant impact in the form of flashfloods and sedimentation decreasing forest areas of the reserve. Especially during august 2009 heavy flooding was observed. During the timespan studied, the area of grasslands increased due to anthropogenic and natural disturbances.

In Manas National Park , Northeast India, Sarma et al. (2008) studied a shift in river course and its impact on the vegetation pattern in the park. The shift caused a change to dryer types of vegetation, that partly could have been prevented by more active management of the grasslands. Classes distinguished are alluvial grasslands, savannah grassland, shrub land (which includes forest), river and water bodies. Years studied are 1977, 1998 and 2006.

An example of a corridor investigated is the Kosi river wildlife corridor in Northeast India (Areendran et al., 2017) with an unsupervised classification and checked with field survey. Images compared are 2009 and 2014. A field survey was conducted for validation of the map that yielded an overall accuracy: 79.1% with a 0.77 Kappa Index. Next to analysis of the land cover changes in the past, a Land Change Modeler with Multi-Layer Perceptron (MLP) neural network is used for predictions. Using the current disturbance situation, Markov transition probabilities calculated the possible scenarios for the years 2020 and 2030.

2.2.3 Land cover studies outside of the Terai

Outside of the Terai, a study where the impact of hydrology on wetland vegetation is explicitly analyzed is conducted by Arieira et al. (2011) in the Pantanal, Brazil, where a driving factor for the pattern of vegetation communities are extreme hydrological scenarios. A promising approach was presented for mapping wetland vegetation combining geostatistics, field sampling and remote sensing (high resolution IKONOS imagery). The spatial pattern of the ecological important wetlands together with other vegetation communities is linked with the spatial pattern of inundation. The study shows the ability to classify vegetation communities by measuring structural and floristic characteristics of flora, combined with remotely sensed data and a DEM. Stratified random sampling or stratified systematic unaligned sampling is recommended by the study to prevent bias in the dataset (Lo and Watson, 1998)

On a larger scale, Hu and Hu (2019) considered interannual land cover changes and their driving factors in central Asia from 2001 to 2017. Landsat imagery was classified with a Random Forest classification algorithm, which is a decision tree classifier creating votes based on predictor values given to the model (Breiman, 2001). From this study, the dominant disturbance factors on a large scale are the amount of precipitation and degree of drought.

A sophisticated method for studying interannual land cover changes by disturbance mechanisms has been conducted in Canada (Hermosilla et al., 2018). The study looks into disturbance mechanisms such as fires and harvesting. A 29-year series of land cover maps was created based on a sophisticated algorithm incorporating image compositing and mosaicking by ‘best available pixel composites’ and post-classification processing including transition rules for land cover. The best available pixel selection is

based on White et al. (2014) and factors considered are the amount of days a pixel is off from the desired day of year. Presence of clouds and cloud shadows and the distance of these to the pixel is calculated. Together with sensor type a score for quality is given to a pixel in order to create the most reliable image composites for interannual comparison (Hermosilla et al., 2015a). Multicollinearity between predictors for the classifier (Random Forest) was calculated to find the best predictors and at the same time decrease the number of predictors needed and get rid of redundant information given to the classifier to reduce computation times. Useful combination of predictors to extract values for at each training pixels for developing the classification model were Landsat bands 4 and 7, EVI, TCG, elevation, slope and TRASP. Important to note in the study is that the classification model was considered portable through time (Gómez et al., 2016). One annual composite was used of which the spectral data at training sites was used to develop the classification model, and for other annual composites the pixels are labeled with the most voted class (Pal, 2005; Lawrence et al., 2006).

From the above-mentioned studies differences in methodology are observed, such as different temporal and spatial resolutions, different classifiers and methods for training (mostly MLC or RF for supervised classification). Also, the possible vegetation classes for classification and associated accuracies differ between studies. The possible vegetation types to classify is dependent on the spatial resolution of imagery, the classification and training sample and methodology and whether a temporal component is present. For temporal analysis, continuous land cover maps give more information on the nature and magnitude of disturbance, whereas the studies with change detection between a couple of years obtain a more generalized understanding of the vegetation dynamics during the studied timespan.

Part of the studies used supervised classification, where others use unsupervised classification. According to Hasmadi et al. (2009) as well as Ahmad and Quegan (2013), a supervised classification algorithm gives favorable results on accuracy classification compared to unsupervised. A priori knowledge is needed for supervised classification compared to unsupervised classification. The better performance of the MLC algorithm over the ISODATA algorithm (Ahmad and Quegan, 2013) is partly due to better separation of the spectral mean of the different classes. Several of the studies gathered the training samples in the field, where others gather them from high resolution data and only used field samples for validation.

3. Materials and Methods

The methodology includes how remote sensing and training data is collected and classified (section 3.1, 3.2 and 3.3) and how the land cover maps are analyzed, with the different work packages and steps visualized in figure 5. The basic data contains methodology on the imagery collection (section 3.1), the ground truth samples of vegetation in the field (section 3.2), classification and validation of the land cover maps (section 3.3) and datasets on hydrology and forest fires. After classification with a Random Forest classifier two timeseries of landcover maps are created, the first (level 1) with four classes with a timespan from 1993 to 2019 with an historic situation of 1964, and the second series (level 2) with 8 classes from 2013 to 2019. In section 3.4, the analysis of these timeseries is described to quantify coverage of vegetation classes, transition between classes in different spatial zones of the study area and development of landscape fragmentation metrics to assess habitat heterogeneity. To relate vegetational changes to the environment, indicators are calculated from four sources (section 3.5). The first two

datasets are a daily discharge and monthly precipitation dataset acquired by the Department of Hydrology and Meteorology (DHM) in Nepal, both measured at Chisapani weather station (figure 1). The third is a forest fire dataset detected with MODIS imagery (FIRMS - Active Fire Data).

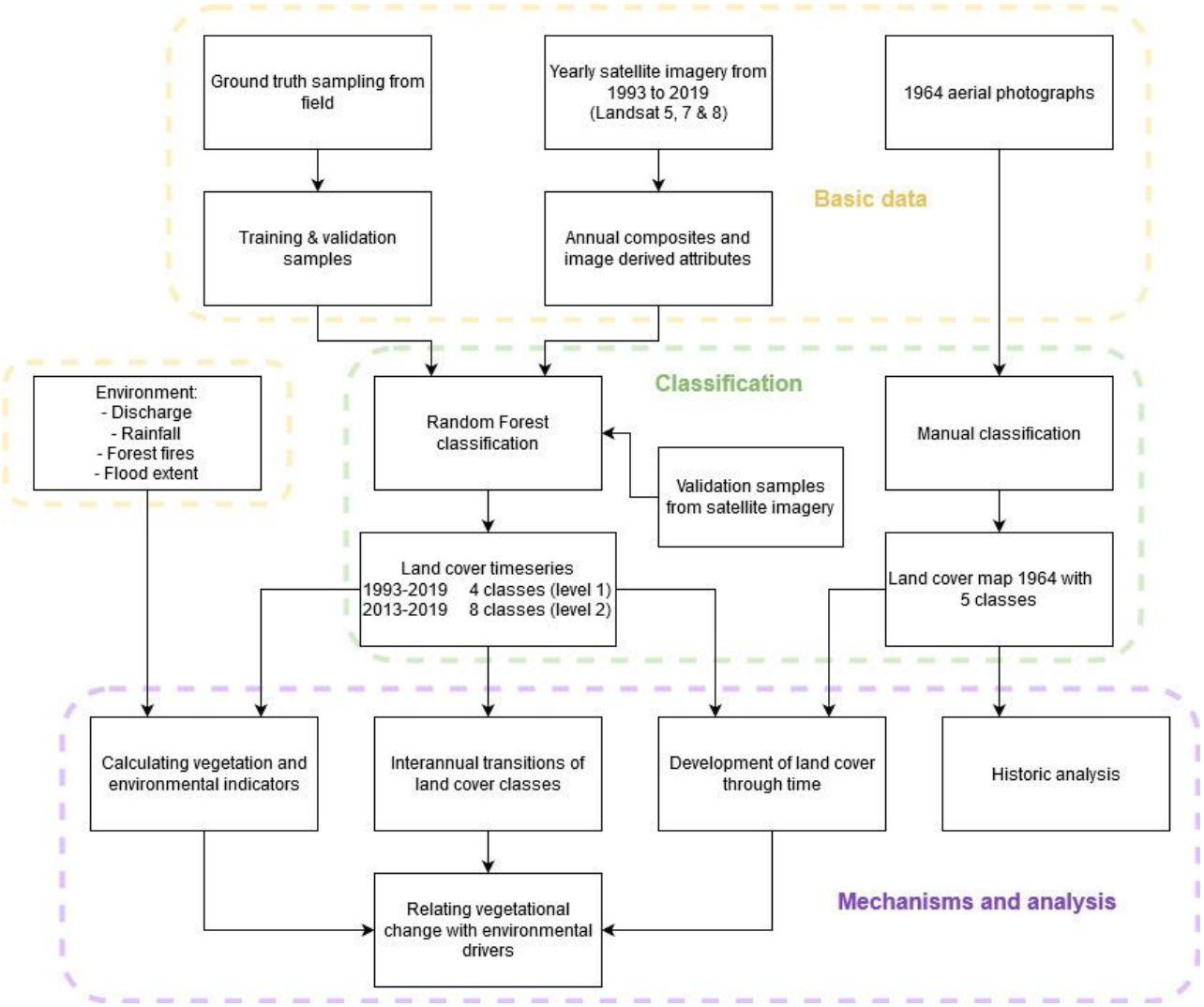

Figure 5: Flowchart from data sources to analysis steps.

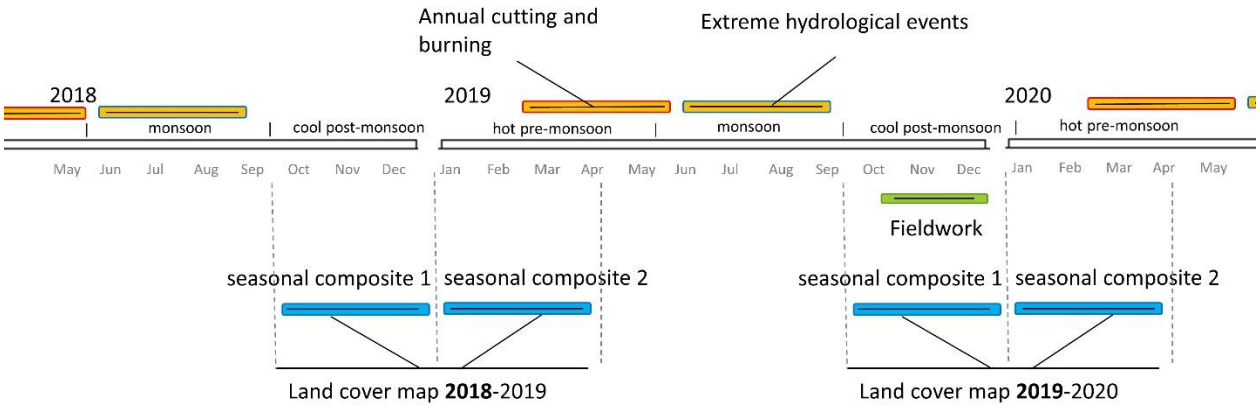

Figure 6: Timing of fieldwork, seasonal composites, land cover maps and disturbance factors of cutting, burning, and extreme hydrological events.

Figure 6 shows an overview of the timing of different aspects in this study. Disturbances from anthropogenic cutting and burning and nature forest fires typically happen at the end of the dry period, and disturbances caused by extreme hydrological events during the monsoon. The seasonal composites are explained in the following section on remote sensing (section 3.1.4). Important to note is that a land cover map is based on the last months of year 't' and the first months of year 't + 1' (figure 6). For clarity, the maps are given the name of t. This means that a land cover map containing satellite data from the dry period beginning in 2019 and ending in 2020 is labeled 'land cover map of 2019'. This is then also the same year as the disturbances happened. The disturbances happening in 2019 then have impact on the 2019(-2020) land cover map and changes could then be observed between the 2018 and 2019 land cover map.

3.1 Remote sensing data collection

Remote sensing is beneficial in a practical and economical point of view for studying space-time vegetation dynamics, especially over larger spatial and temporal scales (Langley et al., 2001; Nordberg and Evertson, 2005).

3.1.1 Landsat imagery

Landsat imagery is used in this study to address the spatial and temporal component. Its missions have been collecting moderate resolution imagery since 1972 until present. This range in time and the fact that it is satellite imagery with the highest resolution that is free since 2008 makes it the most adequate satellite imagery for this study. On board of the Landsat satellites are the sophisticated multispectral imaging sensors Thematic Mapper (TM), added on Landsat 4, and the Enhanced Thematic Mapper Plus (ETM+) in 1999 on Landsat 7. TM has a reflective resolution of 30m and 120m for the thermal band. ETM+ has a resolution of 30 meters for the multi spectral bands and 60 m for the thermal infrared band. See table 3 (*USGS, 2015*).

*Table 3: Landsat missions and spectral bands. Adapted from USGS (2015). Band numbers with wavelengths in micrometers. * LS 7 Thermal data was acquired with high and low gain settings, therefore two Band 6 files are delivered ** Data is recorded at a coarser pixel size and upsampled. Original pixel size of thermal data is 60 m (TM), 120 m (ETM+) and 100 m*

Landsat sensor	**LS 4 - 5 TM**	**LS 7 ETM+**	**LS 8 OLI/TIRS**	**Pixel size (m)**
Timespan	1982 - 1993 1984 - 2013	1999 - present	2013 - present	
Coastal aerosol			B1 (0.43 - 0.45)	30
Blue	B1 (0.45 - 0.52)	B1 (0.45 - 0.52)	B2 (0.45 - 0.51)	30
Green	B2 (0.52 - 060)	B2 (0.52 - 0.60)	B3 (0.53 - 0.59)	30
Red	B3 (0.63 - 0.69)	B3 (0.63 - 0.69)	B4 (0.64 - 0.67)	30
NIR	B4 (0.76 - 0.90)	B4 (0.77 - 0.90)	B5 (0.85 -0. 88)	30
SWIR 1	B5 (1.55 - 1.75)	B5 (1.55 - 1.75)	B6 (1.57 - 1.65)	30
SWIR 2	B7 (2.08 - 2.35)	B7 (2.09 - 2.35)	B7 (2.11 - 2.29)	30
Thermal	B6 (10.40 -12.50)	B6* (10.40 -12.50)	B10 (10.60 - 11.19) B11 (11.50 - 12.51)	30**
Panchromatic		B8 (0.52 -0.90)	B8 (0.50 - 0.68)	15
Cirrus			B9 (1.36 - 1.38)	30

The flyover time of the Landsat satellites is 16 days, so theoretically, in the period of two Landsat satellites in orbit 3-4 images will be taken in a month, and in the period with only 1 satellite in orbit (LS 5 TM from 1993 to 1999) 1-2 images per month. However, the study area has not been visited every month in the last decades. Figure 7 shows the Landsat images for the study area that are available for each land cover map.

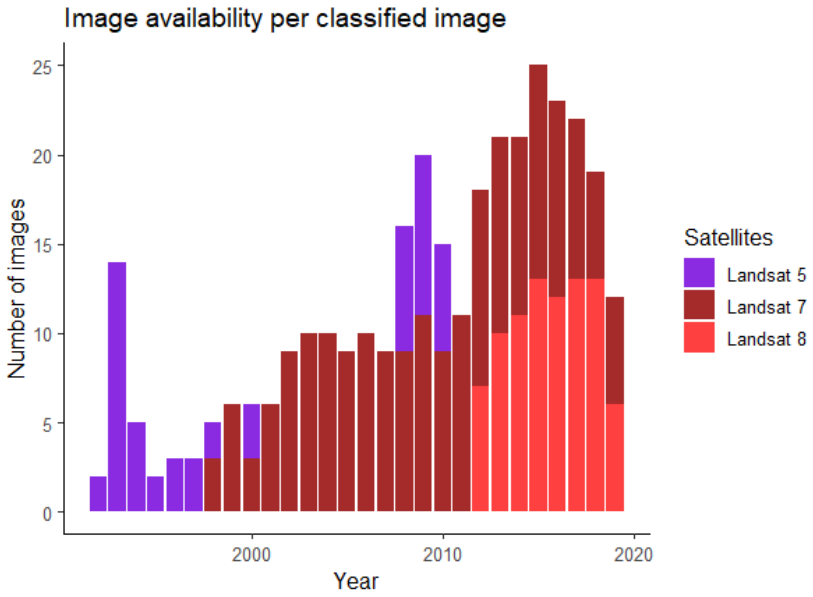

Figure 7: Available Landsat imagery for Bardia National Park. Note that the years shifted to one year earlier (Landsat was for example available from February 2013 and onwards). This was explained in figure 6.

The images taken by Landsat 5, 7 and 8 will be used in the timeseries. Some years have few images (figure 7), limiting the creation of land cover maps for these years. In figure 8 a flowchart of the process from image selection to land cover timeseries is shown. Data input is shown in orange.

3.1.2 Preparation of imagery

The important part for timeseries is that atmosphere, sensor, energy source and earth surface itself can cause unwanted disturbances to the image. Since the important component studied here is the changes in objects on the earth surface, this should be the changing variable. To be able to do this, the other three components must be corrected for.

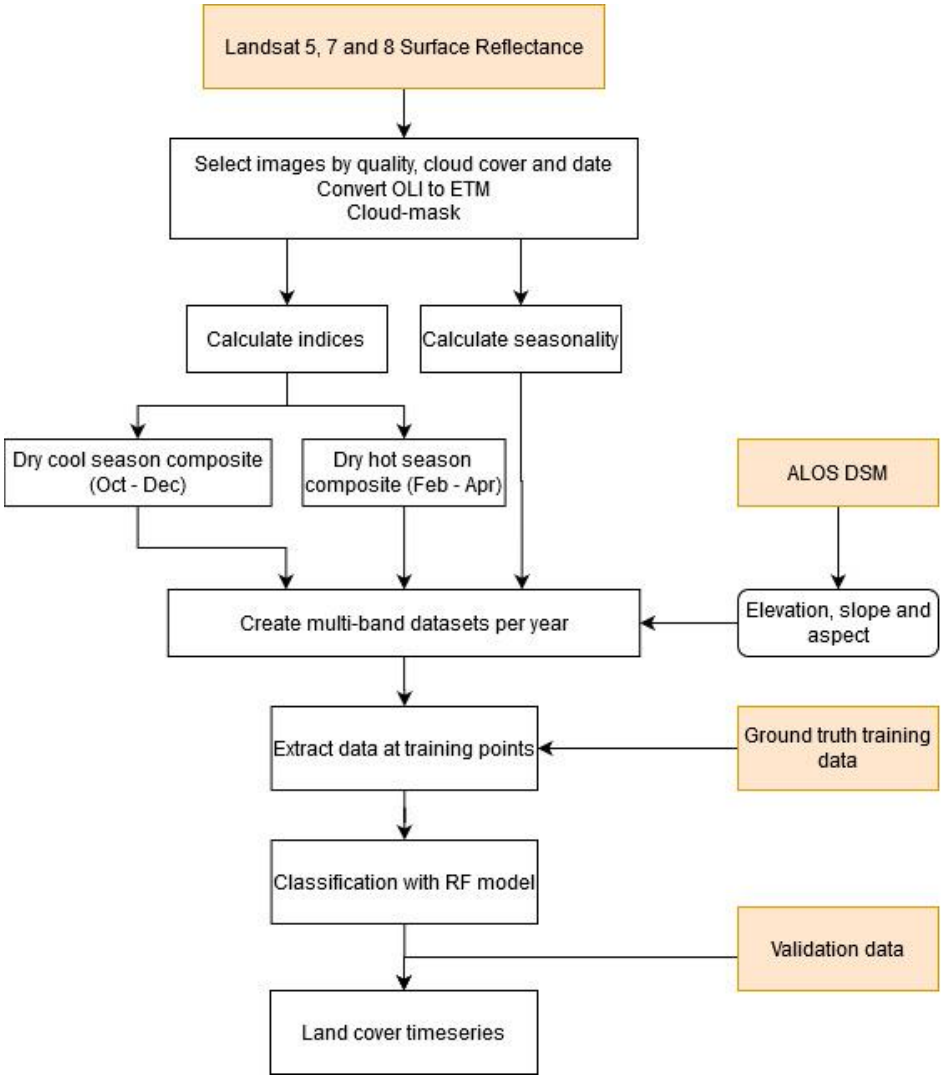

Figure 8: Flowchart with the process from image acquirement to the land cover timeseries.

To correct for variations of the energy source (e.g. sun angle) and atmosphere, the preprocessed Surface Reflectance (SR) dataset of Landsat is considered (Zanter, 2019). Although the atmospheric correction in surface reflectance imagery can come with additional errors (Schroeder et al.,), the Surface Reflectance

dataset of Landsat is chosen as advised by Young et al. (2017) because we are using multiple scenes for each time period. In the surface reflection there already has been corrected for the source, solar correction, and the atmosphere, limiting disturbances of these during classification. Further manual preprocessing such as radiometric correction, geometric correction and orthorectification are not needed since the dataset has already been preprocessed to 'Tier 1' quality (Zanter, 2019).

For sensors, it is important that the imagery is preprocessed for different sensors they are measured from, with the desired result as if the images are all taken with the same sensor (Hall et al., 1991). To provide continuity in data and since the OLI sensor has different specifications for the bands than TM and ETM+ sensors, the Landsat OLI images have been corrected to Landsat 7 ETM+ images using coefficients provided by Roy et al. (2016). Secondly, Landsat 7 endured a failure of the Scan Line Corrector from 2003 to present, resulting in gaps in the images. This is addressed by a gap filling algorithm using imagery right in front or right after the date and will introduce some errors in the classification to an acceptable margin.

Thirdly, clouds and cloud shadows can impede correct observations. Cloud masking has been done by selecting pixels that contain clouds or cloud shadows, and then updating the imagery so contamination pixels are not present anymore. The information on which pixels contain clouds or cloud shadows is available via metadata of the Tier 1 Surface Reflectance dataset of Landsat. The script *Fmask* (Zhu et al., 2015) has been used to create those cloud-masked images making use of the above mentioned algorithm. Lastly, the pixel values of several images per year created in the dry period have been combined and their median pixel value is taken to get rid of outliers.

In the past decades, the sensors have taken millions of images, which in recent developments of cloud platforms such as *Google Earth Engin*e (GEE) have become easier to handle. GEE is cloud platform software that contains open access imagery of several imaging sensors, such as Landsat, Sentinel and MODIS. This makes the creation of time series less time-consuming (Gorelick et al., 2017). Remote sensing algorithms for image enhancement, image classification and cloud masking are also available and can be edited (Gorelick et al 2017). Therefore, to create a time series on a yearly basis GEE is used.

3.1.3 Spectral metrics

To enhance the spectral information available, metrics are developed to increase the detection possibilities of the earth surface objects. Indices commonly use different bands together in a formula to enlarge differences or apply a transform to the bands. Vegetation reflects low in the red region and high in the near-infrared region compared to other objects, representing their photosynthecal activity. Indices based on this principle is NDVI, which is useful for vegetation type discrimination, being a measure for the chlorophyll and energy absorption of vegetation and enables biomass calculation (Rock et al., 1986; Myneni et al., 1995; Beeri et al., 2007). Other indices are the NDDI (Normalized Differenced Drought Index) that exploits the lower reflectance values of moist objects compared to dry objects (Rouse et al., 1973). Biswas 2010 uses NDDI successfully in Jaldapara National Park in India for discriminating between grasslands comparable in composition to grasslands encountered in Bardia. Next to that, remote sensing studies often use the Tasseled Cap Transformation, which filters useful spectral information from the bands of a sensor to calculate the spectral indicators Brightness, Greenness and Wetness of an image (Crist and Cicone, 1984). This transformation has proven to be useful in detecting disturbances in forest, different land cover types and different grassland types.

3.1.4 Seasonality

Adding seasonal spectral data reveals an improvement of the classification accuracy (Kelley et al., 2018), where for the mapping of coffee plantations the use of three seasonal composites in a year significantly increased accuracy of the classification with 7,8%-20,1% . To include seasonality two composites for each annual land cover map are created (illustrated in figure 6). The months per composite are October-November-December and February-March-April. The vegetation differs in phenology between these periods (Dinerstein, 1979a), which causes different reflectance values of the vegetation classes during different seasons and enhances the classification accuracy. Three-month periods are taken to make sure enough Landsat imagery is available.

3.2 Ground truth data collection

Field work has been done to have a clear idea of the vegetation types, and field samples have been taken for training the classification model and for validating the accuracy of the land cover maps. Ground truthing is an important aspect in land cover classification for both training the classification model and validation of the accuracy of the classified maps (FAO, 2016). During fieldwork, the following data was recorded: coordinates with a handheld Garmin GPS, vegetation type, height, cover and dominant species, further explained in this section.

3.2.1 Vegetation classes

For this study for the following vegetation types field samples will be collected to obtain the spectral signatures of the desired vegetation types for supervised classification. Choice for which vegetation types to classify has been done on the basis of literature on vegetation in Bardia National Park (Dinerstein, 1979a; Jnawali and Wegge, 1993; Peet et al., 1999a) and on remote sensing studies in similar environments (Sarma et al., 2008; Biswas, 2010; Arieira et al., 2011; Thapa, 2011; Biswas et al., 2014). The classification on level 2 detail use the following classes:

- Sal forest
- Riverine forest
- Shrublands
- Dry tall grasslands (savannah)
- Short grasslands (phantas)
- Wet tall grasslands (floodplain)
- Water
- Bare soil

For the level one classification the classes forest, grassland, bare and water are used. Including shrubland in the classification as intermediate step between grassland and forest did not have the desired accuracies during the first test runs.

This choice for classes has been made according to the description of vegetation species mentioned in section *2.1 Properties of ecosystem* and the classes used in other land cover studies with a temporal component as described in section *2.2 Literature review of methodology*. At an initial classification level, grasslands, forest and shrubland can be spectrally separated in the TAL (Biswas et al., 2014). For grasslands, Biswas et al. (2014) used NDVI and NDDI indices to distinguish riverine grassland from non-riverine grasslands. For short and tall grasslands, the moisture gradient proved important. The three subtypes of Sal forest have been combined to (climax) Sal forest, because of the similarity in composition and ecological function (Dinerstein, 1979b) and expected troubles with discriminating in spectral signatures, especially considering time-series analysis. Riverine forest has been chosen to classify separately from Sal forest due to its ecological function for ungulates (Dinerstein, 1980) The different types of riverine forests, *Dalbergia sissoo-Acacia catechu* (Khair-Sissoo forest) and the *Ficus glomerata-Mallotus philippinensis-Eugenia jambolana* forest association have been combined to the class "riverine forest". An extra class for shrubs is chosen to be able to classify the intermediate step between grass to Sal or riverine forest succession. Shrublands entails no distinct vegetation assemblage recorded by Dinerstein (1979b), Jnawali and Wegge (1993), but has been used in the Terai by Biswas (2010) and (Sarma et al., 2008) and provided interesting successional information on impact of disturbances in Canada (Hermosilla et al., 2015b). Discrimination between shrubland and other classes at the sample locations is based on height and cover of the shrubs and forests.

3.2.2 Classification of grassland types

For the classification classes, assemblages have been combined to more elementary classes named in Dinerstein (1979b) shown earlier in table 2 in the study area section 2.1 . Grasslands will be divided into wet tall grasslands (floodplain), short grasslands (phantas) and dry tall grasslands (savannah). These three grassland classes will contain the grassland assemblages as shown in table 3.

For the floodplain grasslands, the assemblages dominated by *Saccharum spontaneum*, *Pragmites karka* and *Saccharum arundinaceum* are combined. For the dry tall grasslands, assemblages dominated tall grasslands such as *Narenga porphyrocoma* and *Themeda arundinacea* will used, together with patches of *Imperata cylindrica* grasslands which are invaded by tall grasses such as and *Erianthus ravennae* and, again, *Narenga porphyrocoma.* For the short grasslands (phantas), the *Imperata cylindrica* assemblages where *Imperata* is dominant will be used. Other grass species commonly present on these open grasslands are *Vitiveria zizanioides* and *Desmostachyia bipinnata*.

Table 4: Vegetation assemblages present in Bardia National Park and its associated vegetation class as used in the level 2 classification model in this study. Grass assemblages from Peet et al. (1999a). Forest assemblages are from Dinerstein (1979a) and Jnawali (1993)

Assemblages	Vegetation class (level 2)
***Typha elephantina* assemblage**; permanently waterlogged sites	Wet tall grassland
***Phragmites karka-Saccharum spontaneum* assemblage**; seasonally inundated, heavily grazed	Wet tall grassland
***Phragmites karka-Saccharum spontaneum-Saccharum arundinaceum* assemblage**	Wet tall grassland
***Phragmites karka* assemblage**; Tall, dense riverine grassland, seasonal and permanent marsh	Wet tall grassland
***Saccharum spontaneum* assemblage**; Mixed *Saccharum spontaneum* phase, *Saccharum spontaneum* phase, *Saccharum spontaneum-Dalbergia sissoo* phase, floodplain grasslands, alluvial soils, often inundated	Wet tall grassland
***Imperata cylindrica-Narenga porphyrocoma* assemblage;** (1) *Saccharum spontaneum-Saccharum bengalense* phase, edges of wet sites, newer river terraces. (2) *Imperata cylindrica* phase, sites where tall grasses invading an *Imperata cylindirica* dominated sward.	Wet tall grassland/ Dry tall grassland
***Imperata cylindrica* assemblage;** *Imperata cylindrica* phase, *Erianthus ravennae* phase**;** *Imperata-Saccharum* phase; dry sites, well developed soils, previously cultivated	Short grasses/ Dry tall grassland
***Narenga porphyrocoma* assemblage**; Tall, dense grassland, older river terraces and wetter sites, influenced by fire	Dry tall grassland
***Themeda arundinacea* assemblage**; Tall, dense grassland, often at forest edge, well developed soils, influenced by fire	Dry tall grassland
Sal forest	Sal forest
Dry sal forest	Sal forest
Hill sal forest	Sal forest
Khair-Sissoo forest *(Dalbergia sissoo-Acacia catechu)*	Riverine forest
Mixed hardwood forest (*Ficus glomerata-Mallotus phillippinenis-Eugenia jambolana*	Riverine forest
Moist riverine forest (*Mallotus phillipinensis* and *Syzigium cumini*)	Riverine forest

3.2.3 Ground truth data

Characteristics of vegetation to be measured require to be of discriminating value such that the different vegetation types can be identified in the park. Vegetation cover and height have been proven to discriminate riverine grassland from non-riverine grasslands (Biswas et al., 2014). The recommendation from this study to focus the sampling of vegetation cover and height has been followed. Next to that, the dominant species of each vegetation type have been documented, enabling identification of them.

Height is important for distinguishing between the vegetation types (Edwards, 1983). The height of the 5 tallest trees at each sample location of 30x30 meters is averaged to indicate height of the top of the canopy. At places where the grasses have variable height, the 80% height was taken. To distinguish between the moist and dry grasslands height of the grasses is an important parameter. For example: *Phragmites karka* and *Saccarum spontaneum* which grow in moist conditions are high grasses, reaching

easily over 2 meters high. While on the contrary, *Imperata Cylindrica* does not reach over 2 meters and populates the dryer non-riverine grasslands.

Cover, here the projected crown cover, was expressed as a percentage (Edwards, 1983). The percentage indicates the area a crown covers compared to the whole plot. It indicates the density of the vegetation, enabling discrimination between assigning the vegetation type to the plot (Edwards, 1983). A photo was taken when the species is not recognized to enable identification afterwards. Important to be kept in mind is that the vegetation type is the most valuable data to record on the plots, it is used in the supervised classification for creating the vegetation map. The dominant species, cover and height have been used as discriminatory parameters to assign vegetation types to the plot.

Table 5: Dominant species per vegetation type used for assigning classes. Cover and height are used for further discrimination of classes.

Criteria	Dry tall grasslands	Wet tall grasslands	Short grasslands	Sal forest	Riverine forest	Shrubland
Dominant species	*Narenga porphyrocoma, Themeda arundinacea, Erianthus ravennae, Bombax ceiba*	*Saccharum spontaneum, Phragmites karka, Saccharum arundinaceum*	*Imperata cylindrica, Vitiveria zizanioides, Desmostachyia bipinnata.*	*Shorea robusta, Terminalia tomentosa*	*Dalbergia sissoo, Acacia catechu, Mallotus phillippinensis, Syzigium cumini, Bombax ceiba, Lantana Camara*	-
Cover	> 50 % grass	> 50 % grass	> 50 % short grass	> 50 % trees	> 50 % trees	> 50% shrubs
Height	> 2 m	> 2m	< 2m	> 5 m	> 5 m	< 5 m

In table 5 the rules and dominant species per vegetation type are shown. The range of height for shrub land is from 0 to 5 meters. The range of short grasslands of from 0 to 2 meters. Grasses higher than > 2 m are classified as tall grasses, being riverine or non-riverine dependent on which species were abundant. The < 2 m boundary is based on literature (Jnawali and Wegge, 1993; Peet et al., 1999a), although >3 m is named in Peet (1998) for tall grasses. For forest, the dominant species recorded at the sample locations are used for the riverine forest or Sal forest class.

3.2.4 Sample scheme

During fieldwork 359 samples have been taken. The area chosen for the sample plots is 30mx30m, associated with the Landsat pixel size. To obtain reliable data and results, a sample scheme was created containing the locations, number, and size of sample plots, together with the characteristics of the vegetation that would be measured. Eventually, the plan was adjusted due to safety issues. Tiger attacks have increased, probably due to larger tiger numbers and fewer prey. Sample locations therefore were taken during trips with staff of the National Trust for Nature Conservation (NTNC) located in Thakudwara, Nepal, that conducts and facilitates research on flora and fauna in Bardia National Park. The locations of the samples were dependent on the route of NTNC staff and on the accessibility by

roads. The downside of this strategy is lacking randomness and the increasing risk of bias in the dataset, which can result in a reduced accuracy of the vegetation map. On five locations with a view of the surrounding vegetation, the locations of vegetation types have been drawn to verify the vegetation type, and the exact location of the vegetation ground truths was recovered later via Planet satellite imagery (Planet Team, 2017). For these locations and other inaccessible places such as water or large fields of tall grasses, that were unable or unsafe to enter, the training data was collected from a distance or via visual interpretation of high-resolution satellite data. This imagery has a spatial resolution of 5 m and its acquirement date is the same moment as fieldwork time.

3.3 Classification & validation

3.3.1 Random Forest Classifier

The spectral information and predictor values of pixels at the 359 sample locations is extracted from the 2019 Landsat imagery. With the spectral information extracted from the 2019 image composite a classification model is trained and used to classify the annual image composites.

Several mature classifiers are available and used for vegetation mapping. A widely used classifier is the Maximum Likelihood algorithm, which rests on a statistical distribution pattern of the spectral data and is regarded as a classic supervised classification. However, in more complex areas where spectra of different vegetation types show marginal differences the results of the classification are often less satisfactory due to the Gaussian distribution as assumption for the data (Xie et al., 2008). In a study by Stuart (2006) the ML classifier was able to discriminate savannas, two types of forests and open water within 2 pixels (60 m), although subtypes within savannas, grassland, marshland and shrub land, where better discriminated with a continuous classification. In studies described in the Terai, described in section 2.2, Maximum Likelihood and Random Forest were used most abundantly.

A Random Forests classifier (Breiman, 2001) is an ensemble learning algorithm, producing multiple decision trees. For each pixel the model is applied to, votes are given by the different decision trees. It also uses a random subset of input predictors (Belgiu and Drăgu, 2016). A study of Shetty (2019) indicated the better performance of RF classifier than the CART and SVM classifiers. Shetty found that RF and Cart outperformed other classifiers on small sample sizes. Next to that, it was found that RF has a lower sensitivity to training sample quality (Xie et al., 2008).

In this study the Random Forest model is used, considering its earlier successful use (Xiong et al., 2017; Kelley et al., 2018; Shetty, 2019), lower sensitivity to training sample quality and most satisfactory results during initial tests. 70% of the field samples have been used for training and 30% of for validation. The Random Forest model for classification created for the image composite of 2019 is considered portable through time (Gómez et al., 2016). Pixels of the Landsat composites of earlier years (1992-2019) are labeled with the most voted class for these pixels (Pal, 2005; Lawrence et al., 2006).

For classification selection, several things have to be addressed regarding how the data is organized and what kind of information do the pixels contain (Xie et al., 2008). For Random Forest, the structure of the data is of importance. To prevent over classification of classes with a lower coverage, proportionally weighted sample distribution per class is advised (Xie et al., 2008). When balanced training sample amounts per class are used the underrepresentation of smaller classes is countered. The collected

ground truth dataset available contains approximately 50 samples per classification class, somewhat higher for the vegetation types tall grasslands and the more abundant Sal forest. Between 10*p* and 30*p* in number of data points are needed for each class, where *p* represents the number of spectral bands that are used in the classification (Xie et al., 2008). This puts the dataset of this study, according to this guideline, in the lower margins of the range that is suitable for RF classification. At the same time, the performance of Random Forest under lower datapoints is not to unsatisfactory compared to other classifiers (Shetty, 2019).

The Random Forest classifier is run with the following parameters: Number of trees is set to 100, resulting in workable computation time. Timeouts of the software were more common at higher number of trees. The number of variables per split is '0', the minimum size of the terminal node '1', fraction of input to bag per tree is '0.5', and out of bag mode is set to false.

3.3.2 Validation

For accuracy assessment the error matrix is constructed and the user's and producer's accuracy is calculated (FAO, 2016). For validation of the level 1 and level 2 classifications of year 2019 30% of the original dataset of ground truths is used and checked with the classification.

For the years prior to 2019, for which no ground truths are taken in the field, as a first step the reliability is visually interpreted to determine its suitability for analysis, and when satisfactory (for example no presence of water-classified pixels present due to clouds, shadow or the Landsat 7 scan-line failure at places where there is clearly forest). As a second step, error matrices are constructed using ground truths obtained from satellite imagery. This is only done for the level 1 classification since the imagery is not suitable for more detailed classification and only for the years 2000, 2010, 2011, 2018 because for these years adequate imagery of the study area is available for validation via Google Earth.

To obtain validation data via satellite imagery (1993-2018) a grid is created with an equal distance of 1200 meters between sample locations (figure 9). The location of these grid points primarily covers forest, so to have a better representation of the grassland, bare and water classes a second grid is overlain over the floodplain, displayed figure 9. Locations are assessed with Landsat imagery available via Google Earth and the vegetation class at the sample location (in total 106) is noted.

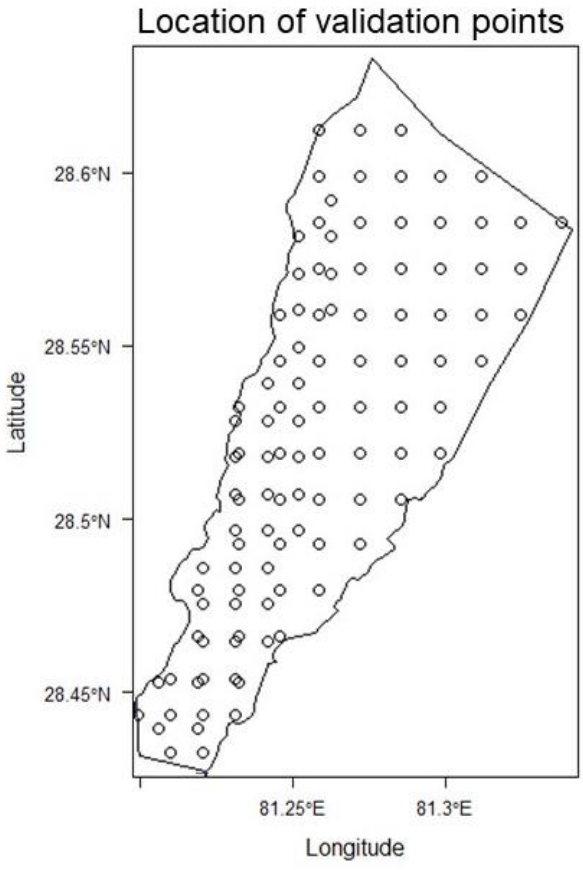

Figure 9: Locations of sample points for validation acquired via Landsat imagery

The validation points are compared to the classified land cover classes and an error matrix is constructed from which the user's and producer's accuracy is derived. Software used for the explained survey collection is CollectEarth (Bey et al., 2016), significantly improving workflow of sample collection via Google Earth.

3.3.3 1964 aerial photographs and historic topographic maps

Next to the 1993-2019 series, aerial imagery of 1964 is used that enables an increase of the timeframe studied for aerial change of the vegetation pattern and change in river morphology. In Kathmandu old aerial photographs have been obtained from 1964, prior to establishment of BNP. The resolution of the imagery is 2-3 meters, the extent covering the whole of Bardia National Park. The images are used for analyzing the landcover at that time and indicating places of former settlements together with a topographic map of 1927 providing general historical information of the park and surrounding area, among which the location of villages, roads and river channels. The imagery is manually classified for the vegetating types forest, grassland, bare soil, water and agriculture. The individual photographs, 400 for Bardia Park, are combined and a point cloud is generated, followed by an orthomosaic. This orthomosaic is georeferenced with satellite imagery using unchanged features on the orthomosaic such as crossroads. After classification, the resolution of the map is resampled to 30 meters to be able to compare the pattern to the Landsat imagery. The software used for point cloud building and orthomosaicking is Agisoft Photoscan ("AgiSoft PhotoScan Standard," 2016), georeferencing is done in ArcGIS Pro. Although object based image classification would be suitable for classifying the older black-white aerial photograph (Vogels et al., 2017), because the area studied is not extremely large and noise is present in the images due to the conversion from analog to digital information the chosen method is manual classification.

3.4 Analysis of land cover maps

In this section the methods for analyzing the land cover dynamics is presented. Also a description of which vegetational indicators are extracted, used for relating the environmental drivers to changes in the vegetation pattern. First, the method for the different spatial zones are explained, then the calculation of the landscape fragmentation metrics that assist in analyzing the development of the vegetation pattern and lastly the transition between classes is calculated.

3.4.1 Areal changes within different spatial zones

Spatial differences of areal change of land cover are considered two ways: firstly, the division between inside and outside the floodplain is made. The border between floodplain and not-floodplain is based on an ALOS DEM (Tadono et al., 2014) and flood extent maps of the Karnali river (Van Kooten, 2019). Secondly, to provide insight into the spatial distribution of land cover dynamics, the land cover distribution perpendicular to the Geruwa river is calculated. Along the center of active channel belt of the Geruwa river a line is drawn from north to south. Perpendicular to this line zones of 500 meters are defined and for each zone the land covers are calculated, the zones displayed in figure 10. This provides information on the areal changes within specific distances of the floodplain.

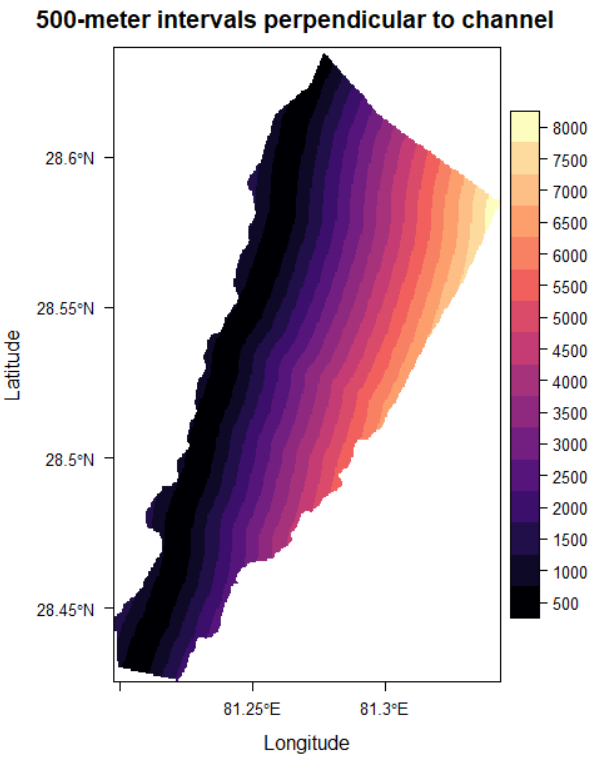

Figure 10: Spatial zones with intervals of 500 meter used for analysis of landcover perpendicular to the Geruwa river

3.4.2 Landscape pattern analysis

For analyzing the landscape pattern, quantification of characteristics of the landscape are needed to compare the landscape between years and gain information on the development.

In similar systems in the Terai, landscape metrics are used (Biswas, 2010; Thapa, 2011). Biswas (2010) used the metrics as a useful tool to quantify changes of the land cover maps and several metrics enabled comparison between other study areas in the TAL.

In Chitwan habitat heterogeneity was measured in the field along transects (Bhattarai and Kindlmann, 2012). The habitat heterogeneity index in this study was calculated by counting the habitat patches crossed along a transect and dividing the number by the length of the transect (Moe and Wegge, 1994). This index compares most with the landscape metric Patch Density used in this report. The finding in Chitwan was that the habitat heterogeneity is positively correlated to the abundance of prey for tiger (Bhattarai and Kindlmann, 2012). Especially fragmentation of the class is described by metrics such as number of patches, patch density, Euclidean Nearest Neighbor, SPLIT and Aggregation Index enable quantification of the fragmentation of the class (Sertel et al., 2018).

To quantify the development of the landscape pattern landscape fragmentation metrics are used. The landscape components and their spatial patterns can be defined by landscape metrics, which are capable of measuring and characterizing the spatial patterns through time (Da Gama Leitão and Stolfi, 2002). For the landscape pattern, multiple metrics are needed to cover the landscape pattern, but should be chosen well since some indices are highly related to each other (Turner and Gardner, 2015). To be able to analyze the landscape pattern objectively and quantitatively, indices are developed that effectively characterize the geometric and spatial properties of vegetation patterns (McGarigal, 2014). These

landscape metrics are based on the patch level, class level and landscape level. On the patch level the individual patches are considered, which are grouped per class in the class level. Landscape level metrics are the combination of the patch and class types in the area (McGarigal, 2014).

For this study it is chosen to focus on the development of the grassland class, the fragmentation of this class is calculated because of its ecological importance. The metrics indicate important elements for ecology such as the boundaries of classes that are of prime importance as these represent habitats for the tiger and its prey (Moe and Wegge, 1994).

Five metrics are considered to elucidate on the pattern of grassland in the park. These landscape metrics are described in table 5. The focus of these metrics is on the number of patches (PD), length of edges (ED), size of patches and aggregation of the patches (EMM_MN and AI). The metrics are calculated for each year of the level 1 classification between 1993-2019.

Table 6: Landscape fragmentation metrics used for quantification of the vegetation pattern (McGarigal, 199AD, 2002; Plexida et al., 2014). *Lower part of table from Sertel et al. (2018).*

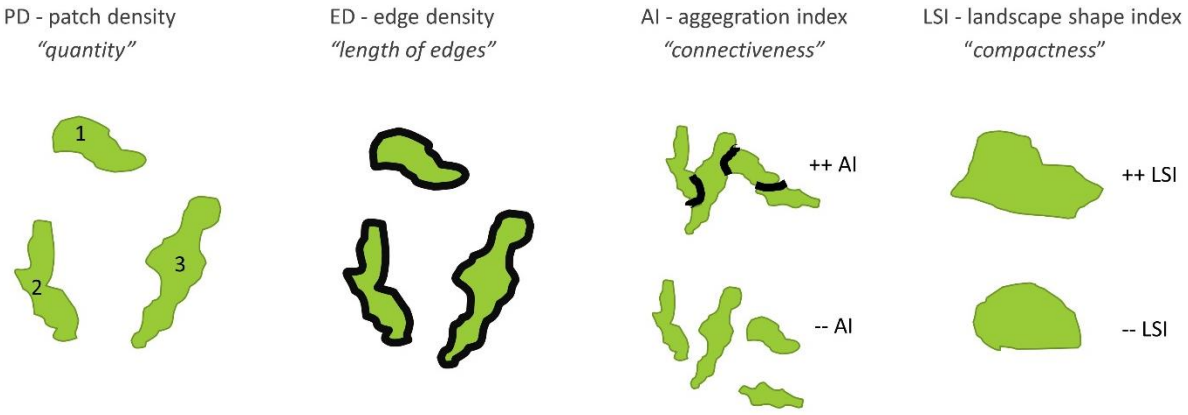

Metric	Description
Patch Density (PD)	Number of patches of corresponding patch type per unit area
Edge Density (ED)	The sum of the lengths (m) of all edge segments in the landscape, divided by the total landscape area (m^2)
Landscape Shape Index (LSI)	A standardized measure of patch compactness that adjusts for the size of the patch
Euclidean Nearest Neighbor Distance Mean (EMM_MN)	Shortest straight-line distance (m) between a focal path and its nearest neighbor of the same class
Aggregation Index (AI)	The ratio of the observed number of like adjacencies to the maximum possible number of like adjacencies given the proportion of the landscape compromised of each patch type, given as percentage

3.4.3 Transitions between classes

Transitions between classes are calculated on a pixel basis with a yearly timestamp (Mas and Vega, 2012). Per year a matrix is calculated containing the transitions between all the land cover classes. The transition matrices are calculated by taking the transition of a pixel of year *t* to year *t + 1.* For the level 1 classification 16 combinations are possible, for level 2 classification 64 combinations are possible. Although transitions from for example short grass to forest is not too common as intermediate stages of tall grassland and shrubland are expected, these transitions are not ruled out on forehand. There will be a focus on the level 1 classification series from 1993 to 2019, because the precipitation and discharge series are available for this timeframe (figure 11). Scripts already developed that assist with the explained calculations are *Intensity.analysis* (Pontius and Khallaghi, 2019) for crosstabulation and *raster* (Hijmans et al., 2011) packages in R (https://r- project.org, R Core Team 2016). The transitions between classes and the trend in these transitions is used as index for vegetational change in the study area.

3.5 Environmental indicators

To be able to relate vegetation dynamics to the environment several datasets are obtained, and indicators are calculated that provide insight in changes in the environment which can impact the land cover pattern. The coincidence of the datasets is shown in figure 11 and the environmental indicators are explained in this section.

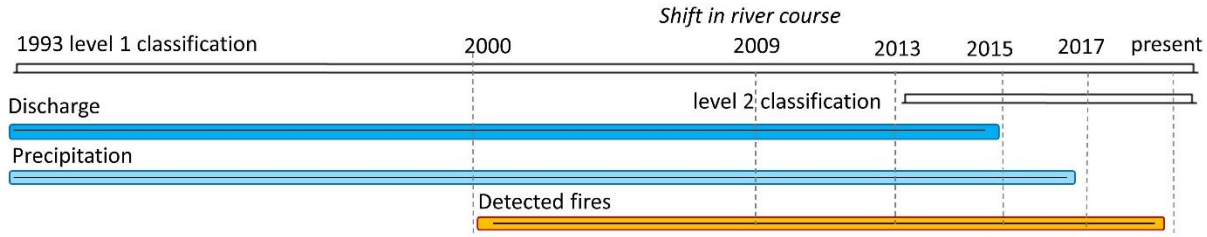

Figure 11: Coincidence of datasets.

3.5.1 Discharge and precipitation datasets

The available hydrologic data contains discharge and rainfall timeseries of Bardia National Park and is purchased from the Department of Hydrology office in Kathmandu. The discharge timeseries contains maximum monthly and daily discharges from 1962 to 2015, the precipitation amount is monthly from 1964 to 2017. Indicators used from these datasets are for each year the maximum monthly rainfall, maximum measured discharge, and duration of exceedance of a discharge threshold, with the threshold expressed in number of days per year. Extreme discharges and their recurrence times are calculated using the Gumble distribution based on the 54 year dataset. The timing of the extreme hydrologic events are compared to the areal change of the vegetation pattern. Another hydrologic indicator used is the switch of dominant discharge branch of the Karnali river (Sinclair et al., 2017; Van Kooten, 2019). The situation of the land cover before and after year 2009 is compared to assess the impact of the change from the fluvial perspective.

In literature is stated that mean average precipitation and average temperature has been increasing at Chisapani (Bajracharya, 2014), together with an increase in more intense but more sporadic precipitation

events (Karki et al., 2017). Cyclones are observed to be responsible for flooding in the Banke-Bardiya district by the Babia river (Chhetri et al., 2020). Dry spells are considered to be have become more frequent and longer in duration (Bajracharya, 2014; Karki et al., 2017), with probably increased water scarcity as a consequence.

3.5.2 Flood extent

Van Kooten (2019) modelled the flood extent of the Lower Karnali river for the situation of 2016-2018. This extent is calculated with a 2D HEC-RAS model for the recurrence times of floods of 1, 5 and 10 years. The land cover maps of years with extreme peak discharges are compared to the flood extent which provides insight on which part of the vegetation would be affected by a flood.

3.5.3 Forest fires

Next to hydrologic drivers, a forest fire dataset from 2000 to 2019 is obtained. The dataset flags MODIS pixels where fire has occurred, adding attributes such as the brightness, confidence of fire occurrence and time of day. The pixel of the MODIS imagery used is 1 kilometer in resolution, limiting information on the extent of the fire. From the dataset the number of pixels that during a year were flagged with presence of a forest fire is used as environmental indicator.

3.6 Relating vegetation to environmental indicators

For gaining insight in the driving factors of the vegetation pattern, the characteristics of the vegetation dynamics are related to the environmental indicators explained in the previous section. To study the relation plots are created with on the two axis the properties of land cover and environmental drivers (table 7). A statistical Pearson test is conducted to establish if the relation is statistical valid. This is done on a yearly basis, and years with extreme environmental events are labeled and compared to changes in the land cover and transitions between classes. No causal relation is established, but by additional knowledge of the system such as location and magnitude of changes, conclusions can be drawn on the outcome of the results.

Table 7: The information obtained from land cover maps and environmental drivers used in this study

Vegetation	**Environmental drivers**
Change in land cover area	Extreme discharge events
Change in transitions of classes	Extreme precipitation events
Landscape fragmentation metrics	Number of pixels that detected fires
	Duration of high discharge
	Change of dominant Karnali branch

4. Results

This section is organized in the following order: firstly, the spatial distribution and patterns of the two land cover classifications series are shown. Secondly, the coverage of the classes through time in multiple spatial zones and analysis of the vegetation pattern using landscape fragmentation metrics is presented. Section 4.3 contains the transitions between the land cover classes. In section 4.4, environmental indicators are calculated and in section 4.5 these are related to the vegetation pattern to gain insight in relation between the space-time dynamics of vegetation and environmental indicators. Lastly, in section 4.6 a short historical analysis is conducted and an overview of the classification model applied to segments of the Kauriala and Babai rivers is presented. In figure 12 the 352 locations of ground truth sampling are shown.

4.1 Spatial distribution of land cover

4.1.1 Level 2 classification

Figure 13 shows seven annual land cover maps from 2013 to 2019 created with the Level 2 classification. The landcover of year 2019 is characterized by patches of dry tall grasses and short grasslands within the riverine forest, located between the Sal forest in the east and river channel in the west. Almost all grassland patches are in the riverine forest, located within 2 kilometers from the active Geruwa channel, except for the Lamkauli grassland (figure 2) The riverine forest starts to appear south of 28.55°N, 81.25°E and broadens downstream (2488 ha). North of this location no riverine forest is present and a cliff of +- 7 meters in height divides the Sal forest and the floodplain (photo 1). No open grassland patches are present except close to the smaller rain fed streams in the eastern part of the study area. Sal forest dominates the eastern and northern part of the study area (6689 ha / 50.0%).

The patches of grass within the riverine forest consist of dry tall grassland (359 ha) and short grassland (433 ha). The area covered by water (690 ha) represents the situation during the dry period, since imagery of the dry period is used. The main channel diverts at 28.59°N to the Kauriala branch of the Karnali river. In and near the active river channel the wet tall grasses (1185 ha) dominate the channel bars, and on most bars shrubland (242 ha), dry tall grasslands and riverine forest are present. On the western side of the Geruwa river, close to the built-up area, some bars are covered with short grassland.

Photograph 1: Sal forest on top and grasses below. This marks the spatial extent of fluvial disturbances of the Karnali river. More southwards this boundary is lower in height.

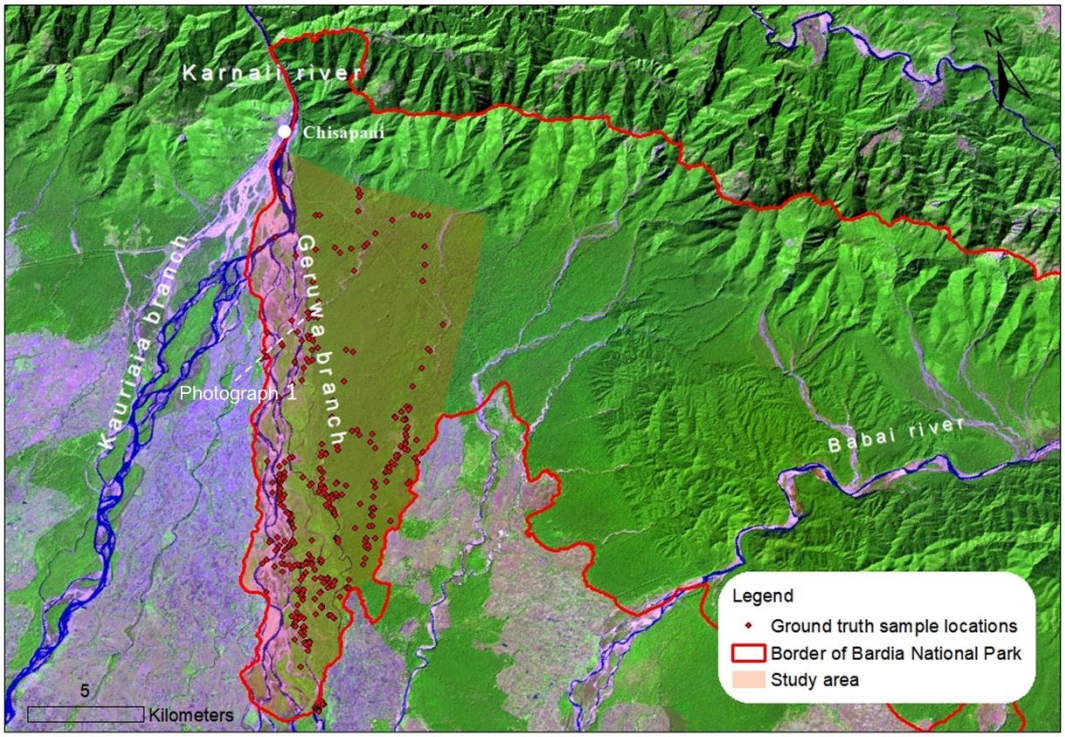

Figure 12: Sample locations in the study area

Figure 13: Maps of the level 2 land cover classification of the study area from 2013 to 2019

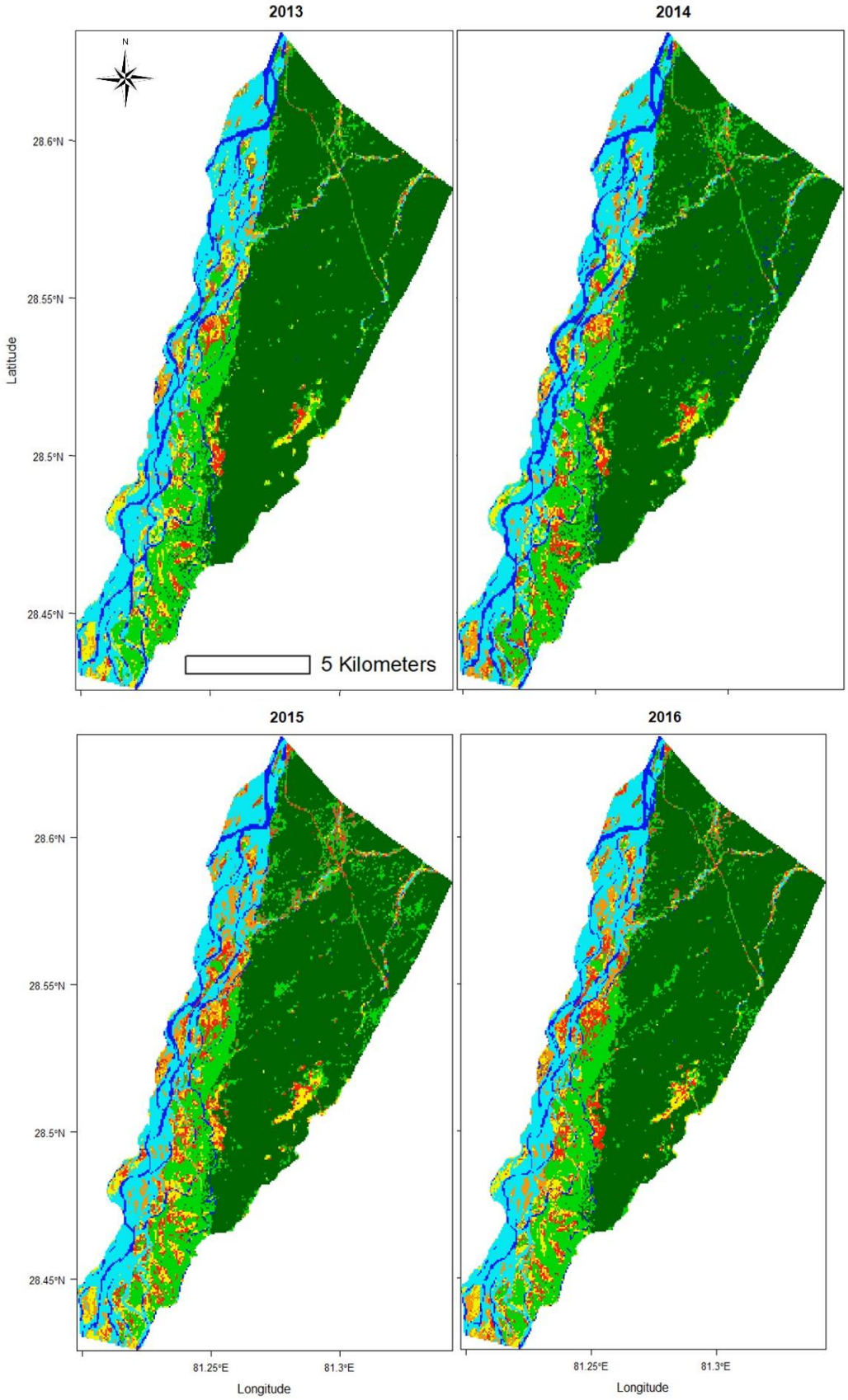

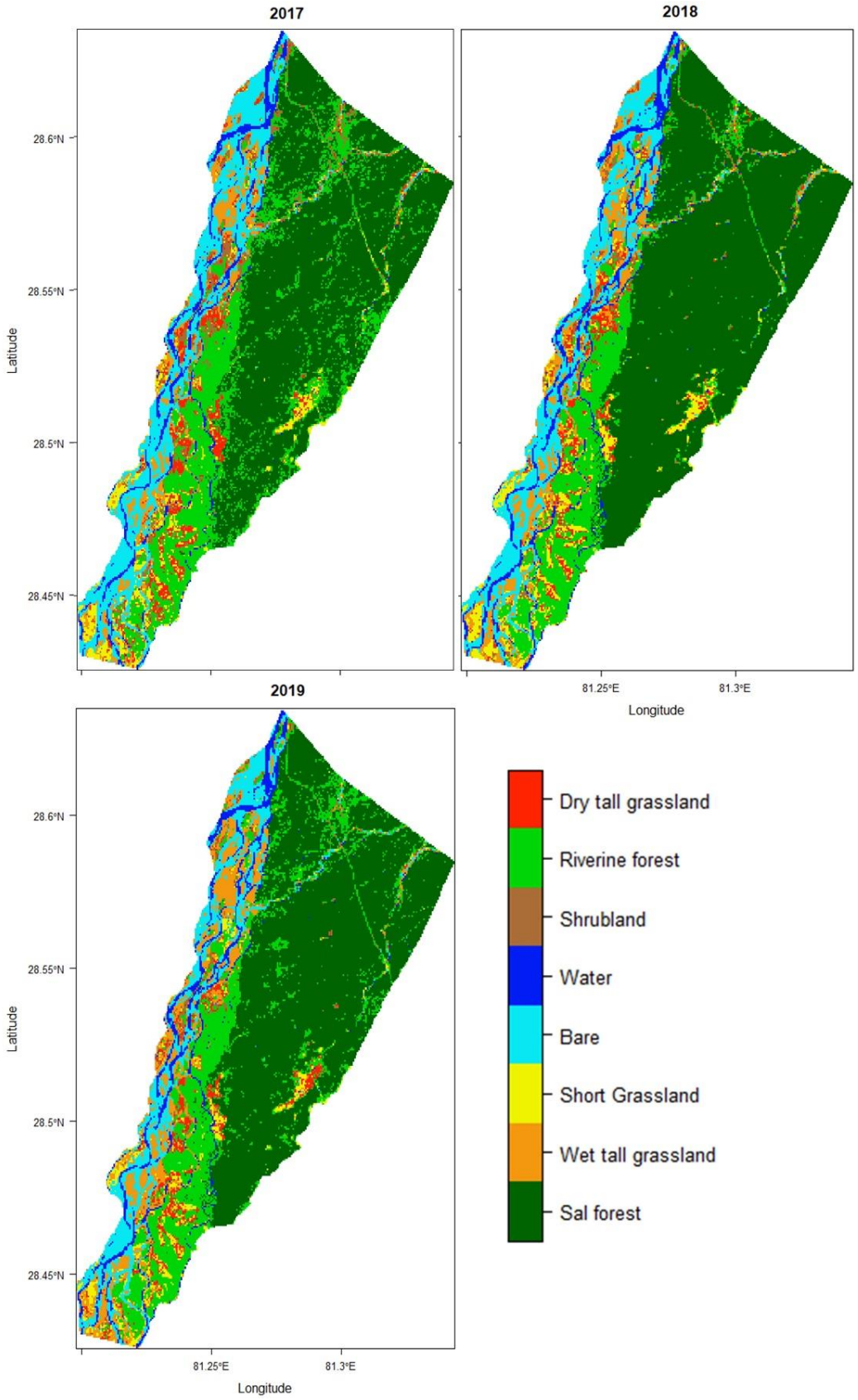
2017
2018
2019
28.6°N
28.55°N
28.5°N
28.45°N
Latitude
81.25°E
81.3°E
Longitude
Dry tall grassland
Riverine forest
Shrubland
Water
Bare
Short Grassland
Wet tall grassland
Sal forest

4.1.2 Level 1 classification

For the level 1 classification, the spatial distribution of land cover with a five-year interval is shown in figure 15. At the bifurcation, the avulsion of the main channel from the Geruwa to the Kauriala branch is visible in between year 2005 and 2010. This avulsion happened in 2009 (Sinclair et al., 2017). The dynamic nature of the stream channel is visible in the relocating, appearing, and disappearing of the channels and bars. For vegetation, trends visible are opening up of grasslands when the situation in the years 1993 and 2000 are compared, and encroachment hereafter.

Apart from the 1993-2019 series land use in 1964 is manually classified, and the land cover is shown in figure 14. In comparison to 1993, in 1964 the channel belt is located more to the east and grassland covers a larger area. In the eastern part of the study area more patches of grassland are present, especially close to the smaller streams originating in the Siwalik hills and close to the Lamkauli grassland. Interpretation has to be done with care between the 1964 and the other classified maps because the classification methods differs.

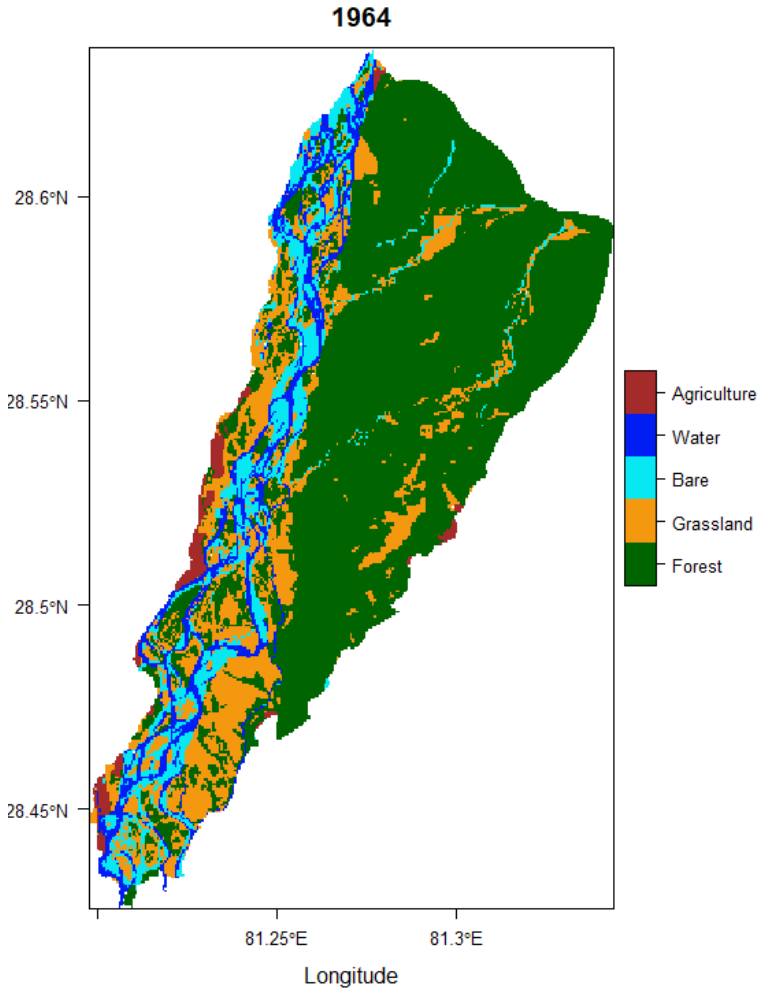

Figure 14: Land cover of 1964 based on aerial imagery

Figure 15: Land cover maps with +- 5 year in between of the level 1 classification. The complete collection of maps is in appendix A

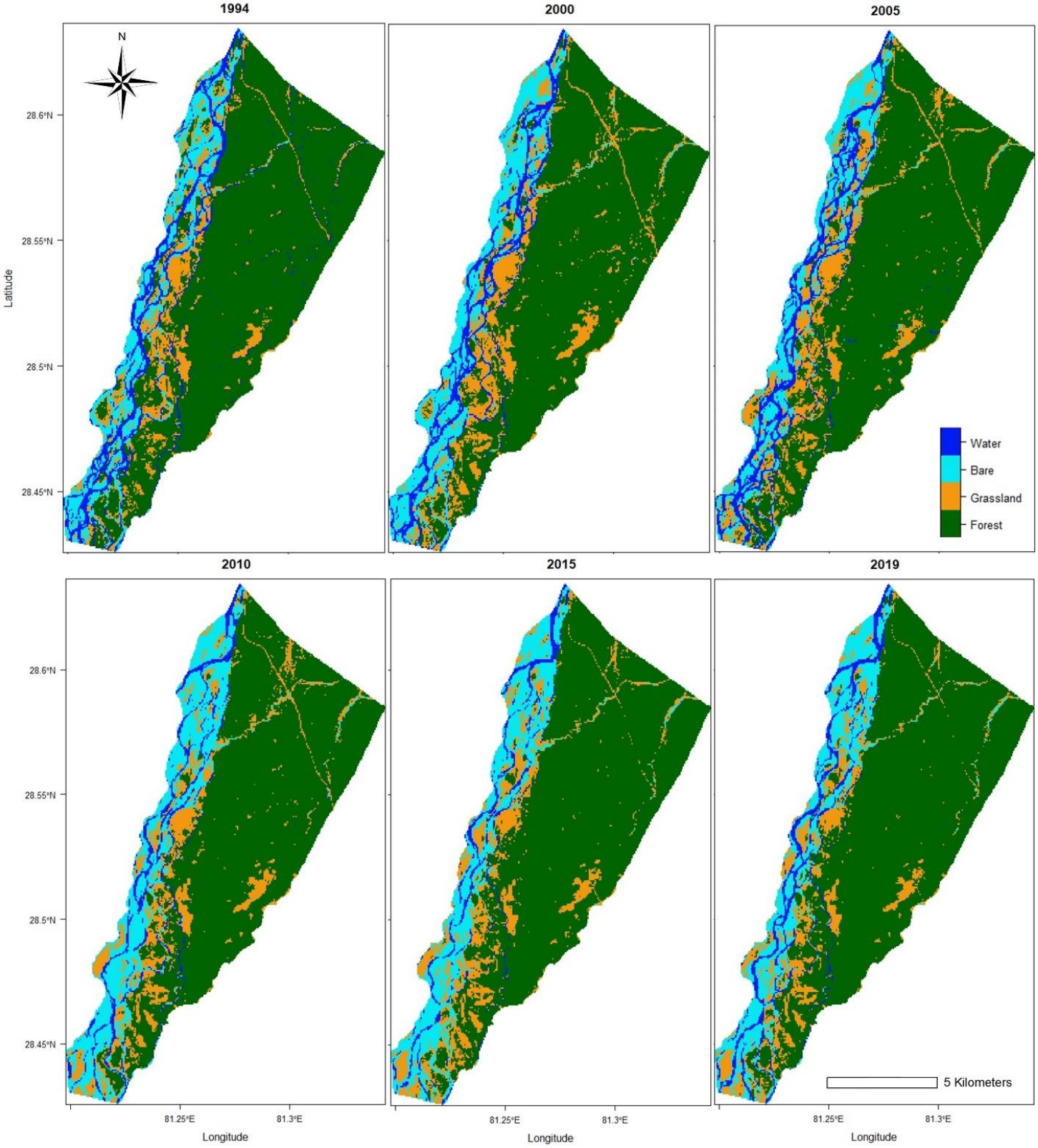

The 1964 map contains information of the landscape that is still remnant in the series from 1993 to 2019. The almost completely abandoned river channel visible in figure 16 has been vegetated with grassland and then forest.

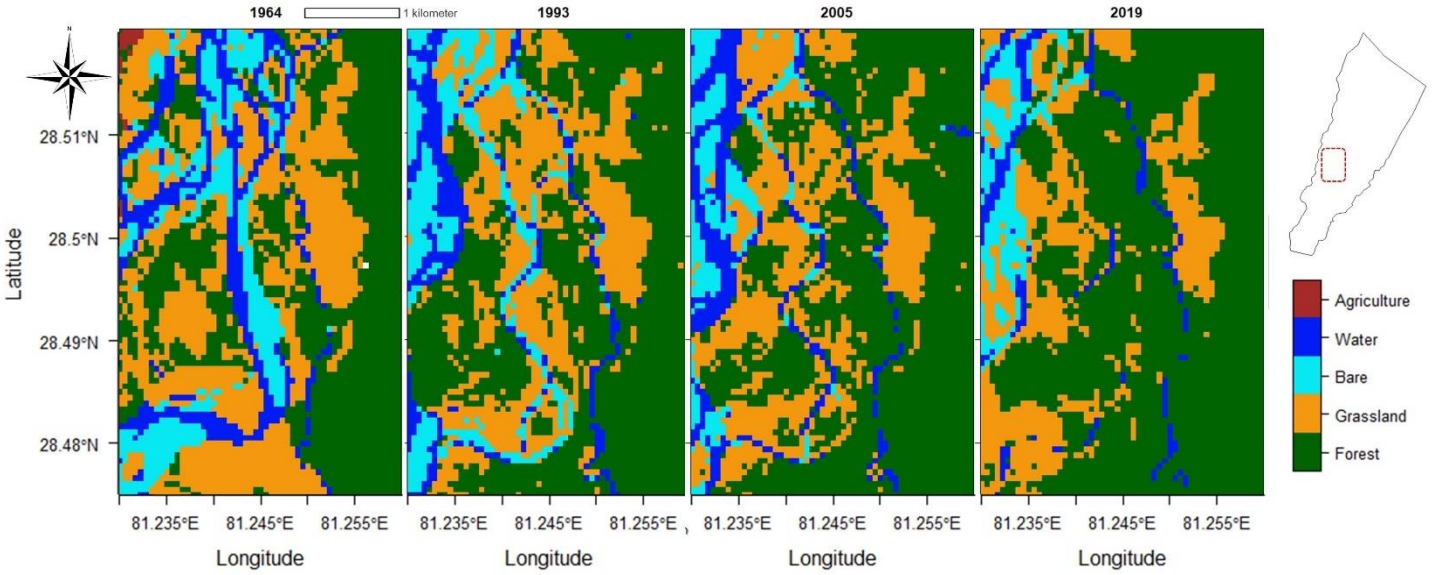

Figure 16: Land cover of abandoned river channel near the Baghaura grassland.

Over time, significant changes are observed in the grasslands north, west and south of the Baghaura grassland (28.50N°, 81.25E°). The situation is shown for 4 moments in time (1964, 1993, 2007, and 2019). A stream channel that is present in 1964, is completely covered by grass in 1993 and forest in 2019. The area west of this channel experienced a transition from grassland to forest between 1964 and 1993, and from 1993 to 2005 grasslands increased again. In figure 17 the general development in the southern part of the study area is displayed, where also the Khauraha grassland is situated (28.47N°, 81.24E°). For the grasslands south in the study area the trend in transition of grass to forest is different than near the

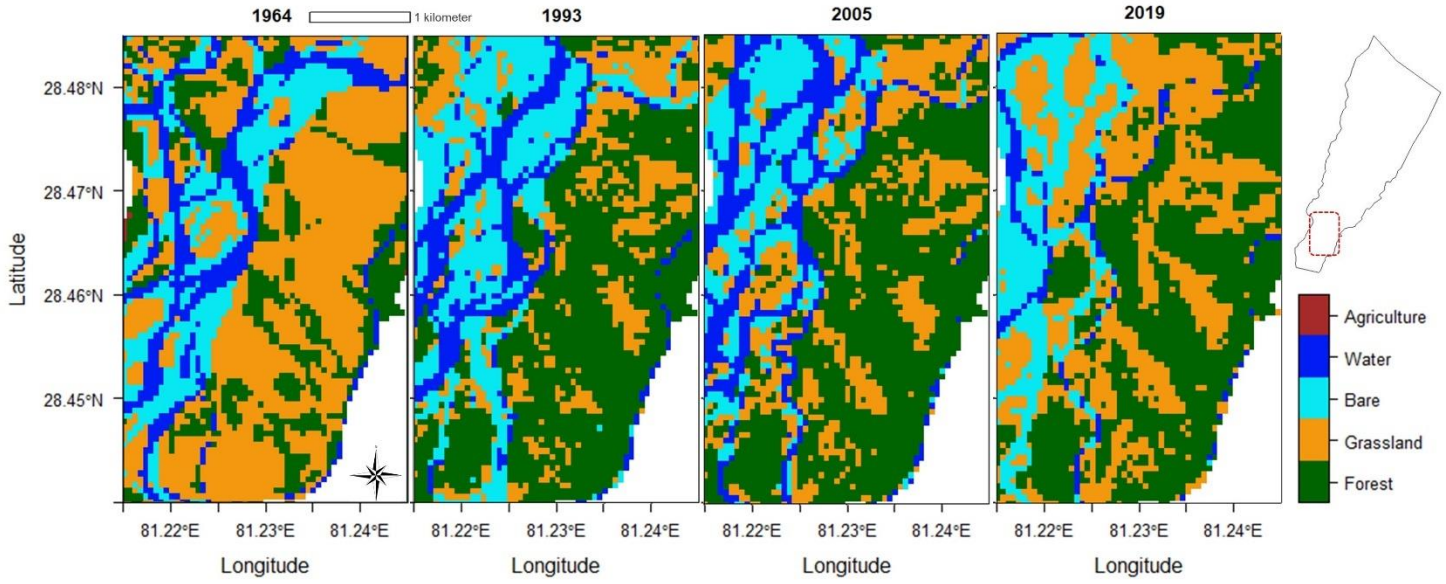

Figure 17: Land cover in the southern part of the study area.

Baghaura grassland. From 1964 to 1993, a large transition of grassland to forest happened. From 1993 to 2005 a slight increase of the grasslands is observed and in 2019 more grasslands are present in the channel belt and the grasslands within the forest increased in extent.

4.1.3 Location and total duration of classes (level 1)

In figure 18, the area that has been covered by water or grass at a certain moment in time from 1993 to 2019 is shown. For water, the presence is calculated based on the dry period (October – April), so no flooding is taken into account here. It shows all channels that have been active (figure 18A). The grasslands have been present in and near the channel belt and near smaller rain fed streams of the Siwalik hills (figure 18B). The amount of years water has been present is largest in the smaller streams and some central channels. For other channel water has been present for 5 to 10 years. Some grasslands have been present for the last 27 years, visualized in dark green (figure 18D).

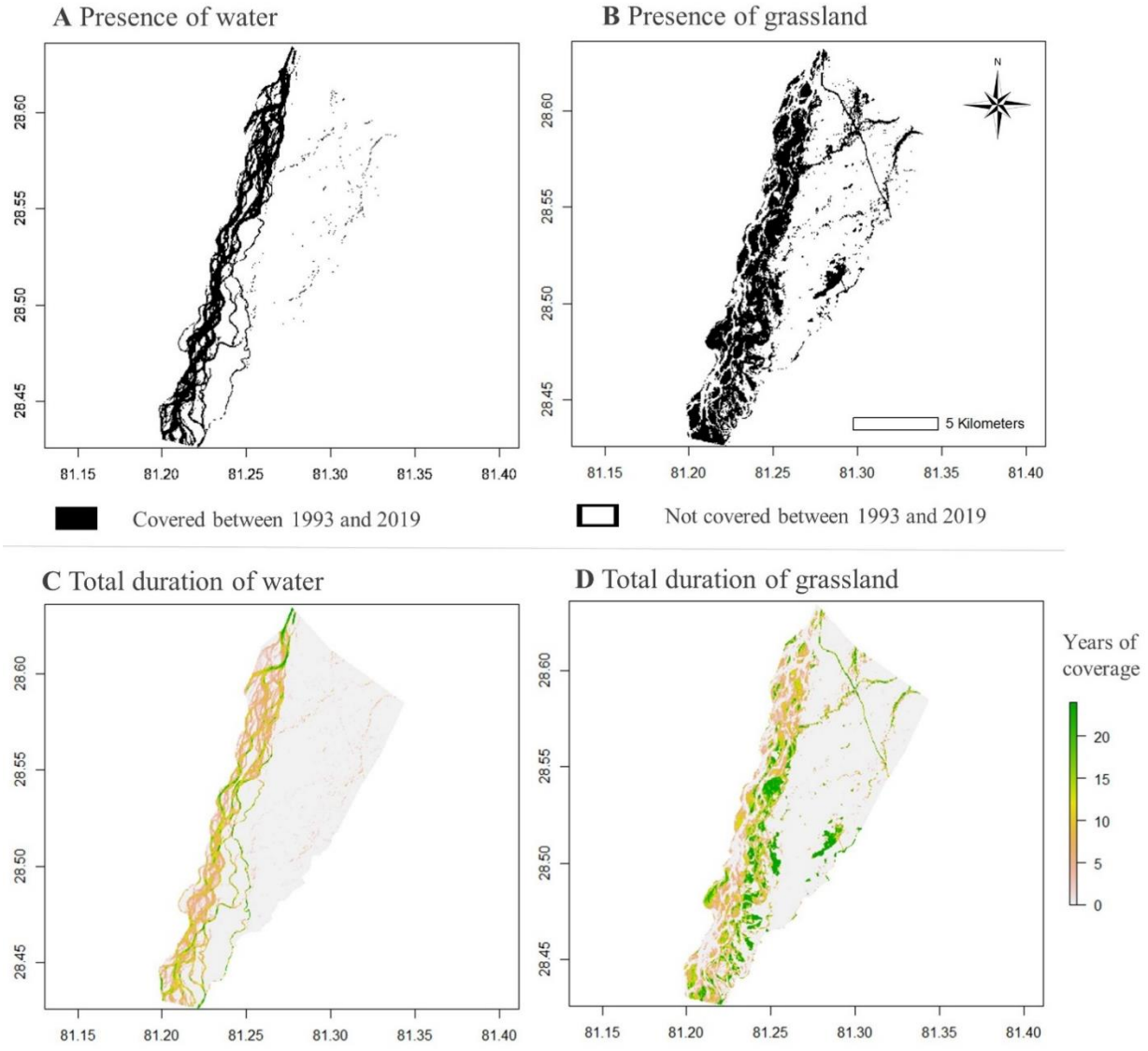

Figure 18: For 1993-2019, shows where water and grassland have been present (A,B) and for how many years (C,D) based on the land cover timeseries.

4.1.4 Accuracy of classifications

Firstly, the maps discarded because of visual inspection are discussed. Secondly, the accuracies of the classifications are presented (all error matrices can be found in appendix C). Thirdly, unrealistic class transitions are shown and lastly the two levels of classification are compared.

Decided is to not use 1995 and 2006 in the analysis of land cover dynamics due to unrealistically large portions of water and bare observed in the forest because of clouds and the Landsat 7 Scan-line error (only for the land cover map of 2006).

The proportion of the ground truths correctly classified (overall accuracy) for the level 1 and level 2 classification of year 2019 is 84.7% and 71.9%, respectively (table 8). For the level 2 classification of year 2019 two additional validation runs are performed and added in appendix C (69.5% and 75.7% overall accuracies). Next to the overall accuracy, the user's (UA) and producer's accuracies (PA) are considered. The user's accuracy is how often the class on the map will actually be present on the ground. The producer's accuracy is the proportion of ground truths of the reference data that is also a class in the classification map. For the level 1 classification, UA is highest for grassland (91.9%) and lowest for bare (60%) followed close by water (62.5%). PA is higher for forest (90.5%) and lowest for grassland (77.3%).

Table 8: Confusion matrices of the level 1 and level 2 classification for year 2019, created with 30% of the ground truth data.

2019 level 1	**Forest**	**Grassland**	**Bare**	**Water**	**Sum**	**UA**
Forest	38	5	0	0	43	88.4
Grassland	3	34	0	0	37	91.9
Bare	0	4	6	0	10	60.0
Water	1	1	1	5	8	62.5
Sum	42	44	7	5	98	
PA	90.5	77.3	85.7	100.0		**84.7**

2019 level 2	**Sal forest**	**Wet tall grassland**	**Short grassland**	**Bare**	**Water**	**Shrub land**	**Riverine forest**	**Dry tall grassland**	**Sum**	**UA**
Sal forest	23	0	0	0	0	0	0	0	23	100.0
Wet tall grassland	0	5	2	1	0	0	0	1	9	55.6
Short grassland	0	1	19	1	0	2	0	2	25	76.0
Bare	0	1	1	8	0	0	0	0	10	80.0
Water	0	0	0	0	8	0	0	1	9	88.9
Shrubland	0	1	2	0	0	3	2	1	9	33.3
Riverine forest	1	1	1	0	0	0	10	0	13	76.9
Dry tall grassland	0	1	4	0	0	3	2	6	16	37.5
Sum	24	10	29	10	8	8	14	11	114	
PA	95.8	50.0	65.5	80.0	100.0	37.5	71.4	54.5		**71.93**

For the 2019 level 2 classification, the lowest user's accuracies are observed for Shrubland (33.3 %), followed by 37.5% for dry tall grassland. The highest user's accuracies are found for Sal forest (100% followed by water (88.9%). For the producer's accuracy the values are lowest for shrubland, wet tall grassland and dry tall grassland (37.5%,50% and 54.5% resp.) and highest for Water (100%) followed by Sal forest (95.8%).

The very low values for shrubland is because few samples used for accuracy estimation are shrubland. The classification is probably higher than displayed in the error matrices. For better overview of accuracies of the maps more sample locations should be used, preferably more evenly distributed over the classes.

For the years 2000, 2010, 2011 and 2018 for which validation points are collected via satellite imagery the highest overall accuracy is observed in descending order of achieved accuracies: 2010 (86.8%), 2011 (84.9%), 2018 (78.3%) and 2000 (75.5%). Classes typically underperforming in accuracy is bare for user's accuracy and water and grassland for the producer's accuracy. For water, the explanation can be found in the large seasonal differences in water coverage, and not all available satellite imagery was from the same date as the Landsat imagery for classification.

Overall, the classifications of level 1 are considered useful for detecting long term trends. For interannual fluctuations caution should be taken with drawing conclusions. To solve this, the observed changes could be accompanied with visual inspection of satellite imagery to validate observed changes.

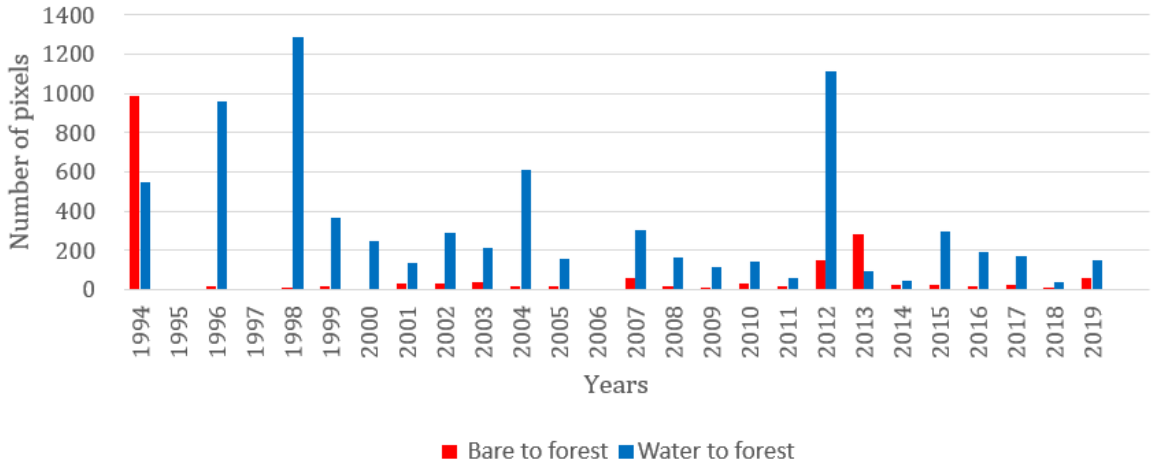

Figure 19: Unrealistic transitions from bare and water to forest indicates less reliable maps. Either map with timestep t has too much water or bare classified in the forest (most likely) or map t+1 has forest classified where in reality is bare and water. The total number of pixels is 171391

Figure 19 shows unrealistic pixel transitions. Shadow present in forest and along forest edges can be classified as water and especially in the classifications of 1994, 1996, 1998, 2004 and 2012 large portions of water turned to forest, indicating that in the year before portions of forest were classified as water (see appendix A). Furthermore, unrealistic transitions from bare to forest happened from 1993 to 1994 and from 2012 to 2013, meaning that more noise in the satellite images is present in these years and probably the overall classification of these years is less accurate.

When comparing the level 2 classification with the level 1 classification, the situations are not completely similar. More grasslands within the channel belt are observed in the level 2 classification, being more sensitive for grasses with a lower density. The level 1 classification has a higher threshold for recognizing grasslands and therefore shows only more densely populated grasslands. On top of that, the level 2 classification classifies at multiple places riverine forest where the level 1 classification classifies grassland. Summarized, compared to the level 2 classification, pixels in the level 1 classification that are mixed with bare and grass have a lower threshold for classifying bare compared to grassland, and for the boundary between grassland and riverine forest, the level 1 classification classifies more pixels as grassland than riverine forest.

4.2 Temporal development of land cover

In this section the results of the temporal dynamics of land cover area of the level 1 and level 2 classifications are shown in more detail and in different spatial zones. Next to that, the landscape fragmentation metrics are used to quantify changes of the grassland class in the level 1 classification.

4.2.1 Coverage of the level 2 classification through time

Considering the timeframe from 2013 to 2019, the most significant trends are a decrease in bare area and an increase in wet tall grassland (figure 20). In figure 20, the y-axis in panel C stops at 25% for visualization purposes. The other 75% of the of the area outside of the floodplain is Sal forest.

The bare area decreases from 2192 to 1373 ha, which is a decline of 37.4%. The area classified as bare in 2013 is predominantly vegetated with wet tall grasslands in 2019. During these seven years, wet tall grassland experienced a growth of 280 ha to 1185 ha (an increase of 323%). Next to an increase in wet tall grassland, also an increase of dry tall grassland, shrubland and riverine forest on the channel bars is observed. In the study area, Sal forest covered 6997 ha in 2013, 6689 ha in 2019 and experienced fluctuations in area especially in 2015 and 2017. When considering Sal and riverine forest together, a decrease is observed between 2014 and 2015 and an increase from 2015 to 2019. The total area covered for shrubland is 239 ha in 2013, a maximum of 588 ha in 2017 and in 2019 the cover was 241 ha. Riverine forest covered 1718 ha in 2013 and 2488 ha in 2019. For some classes, the fluctuations between the years of coverage are high, indicating that error is present in the classification. This is the case for the year 2017, where a much larger area of riverine forest is present than in 2016 and 2018. Short grassland is stable, except in the year 2019. Of dry grassland in total 1.6% (218 ha) is present in 2013, increasing to 4.4% (587 ha) in 2015, and then gradually decreasing to 2.7 % (359 ha) in 2019.

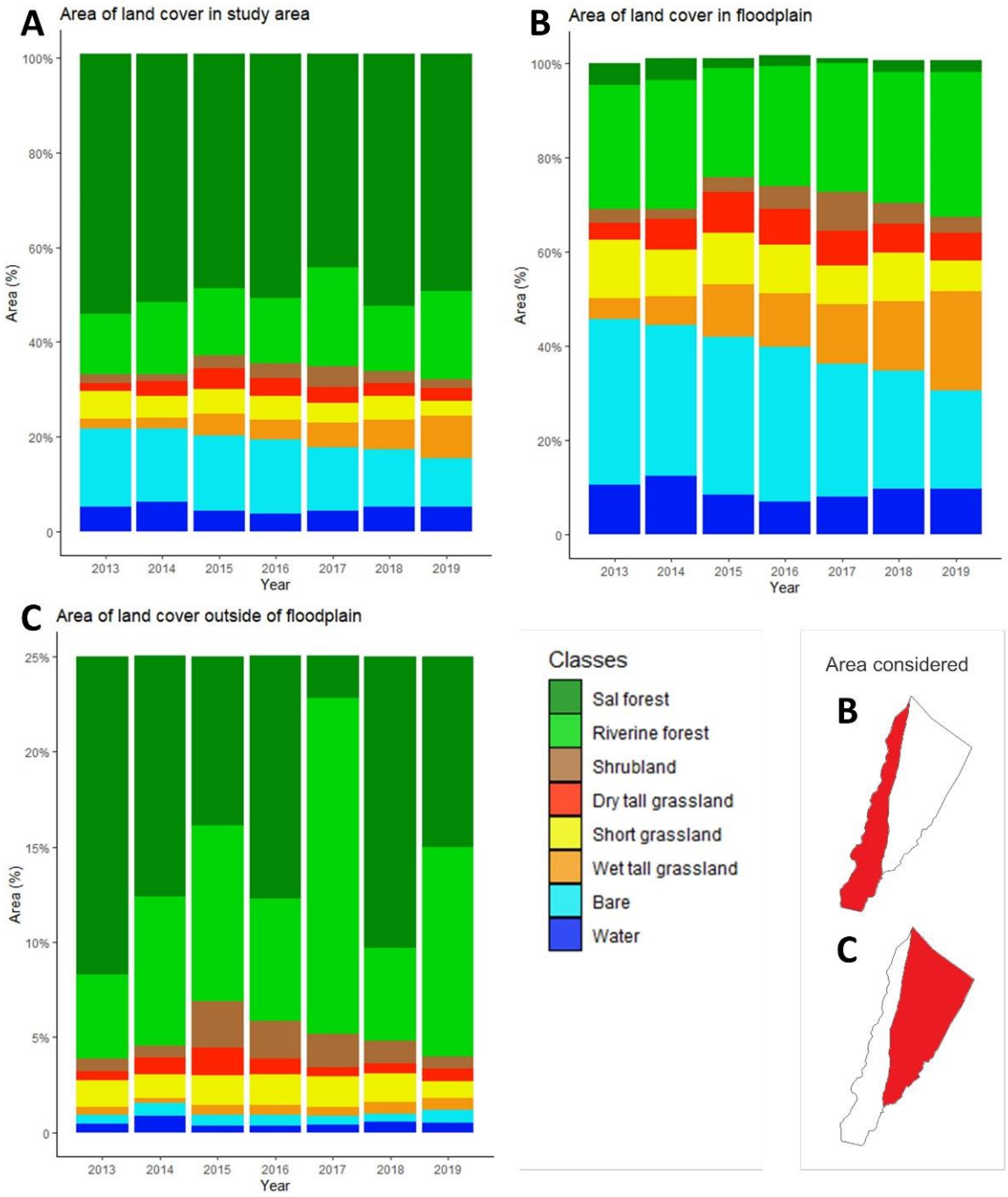

*Figure 20: The coverage of the level 2 classification plotted against time. **A** represents the whole study area, **B** the floodplain and **C** outside the floodplain. Y-axis values have different meanings: For **A**, 100% area is the total study area (13459 ha), for **B**, 100% the area of the floodplain (5248 ha) and for **C** 25% of the area outside the floodplain has been chosen to increase for visualisation purposes. The remaining 75% of the area outside the floodplain consists solely of Sal forest.*

In the floodplain (Figure 20B), the most significant trend is the decline in bare area and the increase of wet tall grassland and riverine forest. From 2014 to 2015 riverine forest did decrease with 209 ha from 1364 (26.0%) to 1155 ha (22.0%) in the floodplain and experienced from 2015 to 2019 a mean net increase of its area with 95 ha/year. Another significant element is from 2015 and onwards: between

2014 and 2015 grasses experienced an increase and the two classified forest types a decrease, and since 2015 forests increased again and especially shrubland and dry tall grassland experienced a decrease in aerial cover. The large fluctuations between riverine forest in 2015 and 2017 are likely due to errors in the classification.

Outside of the floodplain, the most significant observation is the decrease between 2014 and 2015 coinciding with a large increase of shrubland. Shrubland change occurs partly close to the perennial streams and the national highway that crosses the park from Chisapani to the eastern border of the study area.

4.2.2 Coverage of the level 1 classification through time

In figure 21 the percentage of area covered by the level 1 classification is plotted against time. The most relevant changes are a decrease of water class and an increase of bare class in 2008 and 2009. The two largest increases for bare is from 2679 ha (1999) to 3056 ha (2000) and from 2836 ha (2007) to 3051 ha the following year (2008) and 3354 ha the year thereafter (2009). Hereafter, the coverage of bare and water experienced a steady decline from 3354 ha in 2009 to 2044 ha in 2019 for the study area. This decline is also observed earlier in the level 2 classification series as discussed in the previous section. In 2000 another increase in bare is observed from 1185 ha (1999) to 1584 ha (2000), coinciding with a decrease of 216 ha grassland and 116 ha of forest. Outside of the floodplain an increase of grass is observed of 152 ha during this period.

The trend of forest can be divided in three periods and two events. The following three periods can be distinguished: a stable period from 1993 to 1998, a decreasing trend from 2001 to 2010 and an increasing trend from 2010 to 2019. Two events break the trend: in 1999 and 2000 a fast decrease of forest is observed to 8408 ha, which increases again in 2001 (8951 ha) to roughly the same coverage area of forest before 1999. In 2015 another decrease is observed to 8798 ha from 8974 in 2014, hereafter following the increasing trend again from and 2015 onwards to 9276 ha in 2019.

The coverage of grassland experienced different trends. From 1993 to 1998 an increasing trend of 1536 ha to 1788 ha is observed. In the years 1999, and 2000 grassland has a much higher coverage (resp. 2097 ha and 1995 ha), followed by four more variable years. In 2001 the coverage is 1502 ha, in 2002 1747 ha, in 2003 it is 1517 ha and in 2004 1909 ha. From 2004 to 2007 a steady increase is observed. In 2008 and 2009 large decreases are seen, and then an increasing trend from 2010 to 2019 to a larger coverage than earlier has been observed during the studied timespan.

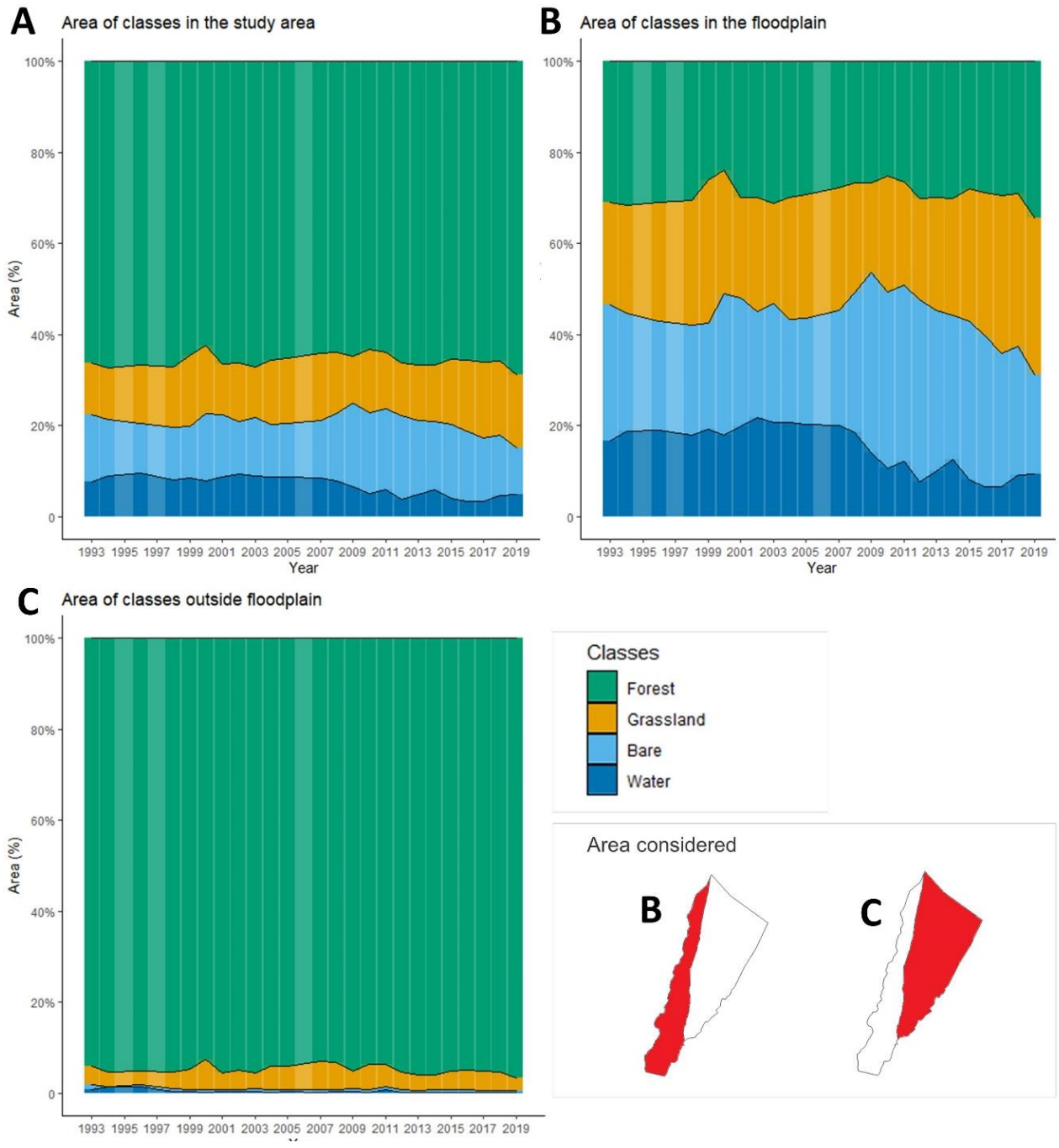

*Figure 21: The coverage of the level 1 classification plotted against time. **A** represents the whole study area, **B** the floodplain and **C** outside the floodplain. Light shaded columns are years with no data. Water area can be interpreted as average water cover during the dry season.*

4.2.3 Location of disturbances

Figure 22 shows the land cover distribution perpendicular to the Geruwa river. Years displayed are during the large observed decreases of grasslands in the years 2008 and 2009. Between 2007 and 2009, most changes happened within an interval of 0-1500 meters of the channel. In the first interval of 500 meters both grass and riverine forest decreased in area, and bare increased significantly. This highlights the dynamic nature of the grasslands close to and within the channel belt of the Geruwa river.

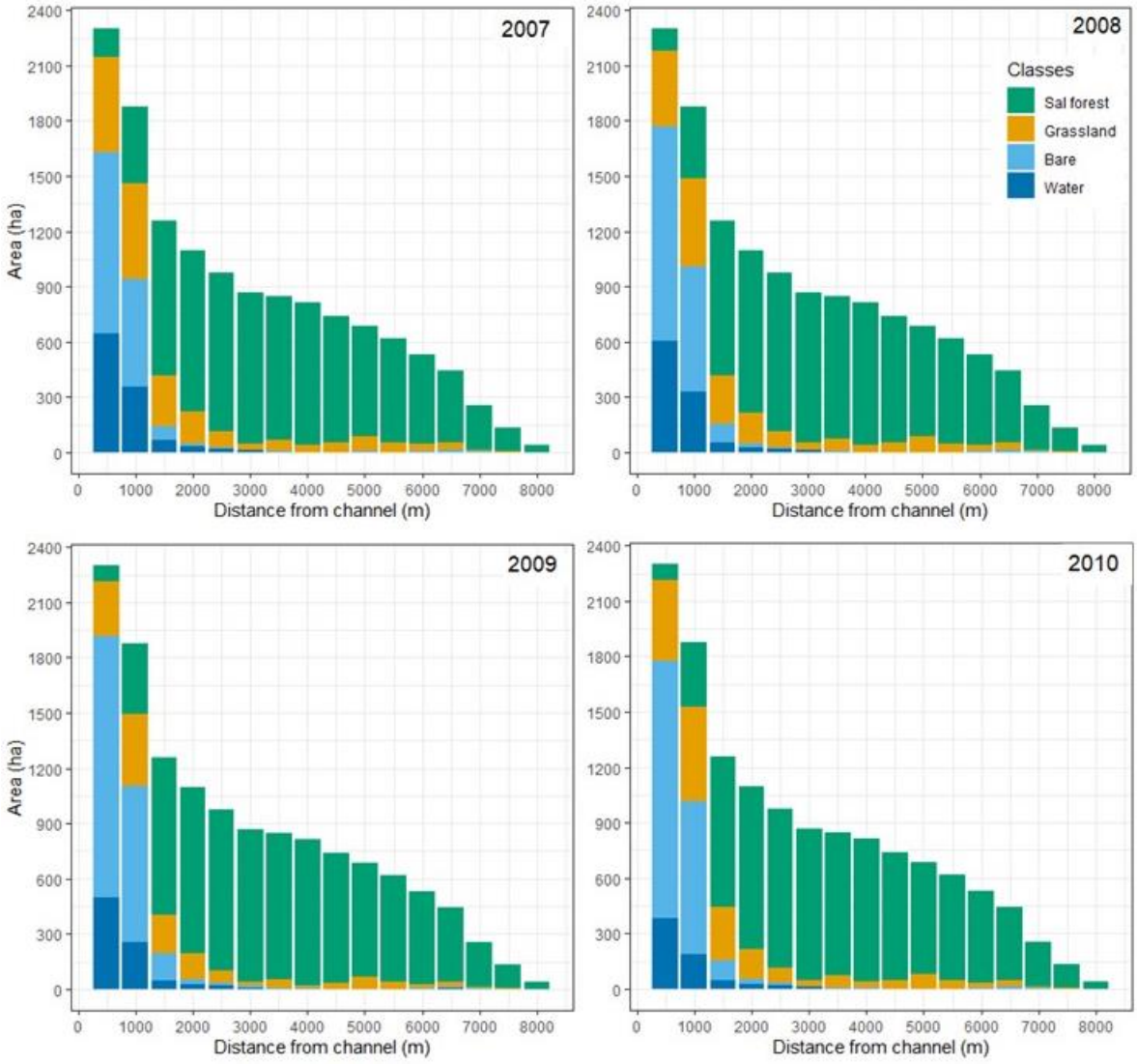

Figure 22: The coverage of the level 1 classification plotted perpendicular to the floodplain with intervals of 500 meter.

4.2.4 Analysis of vegetation pattern

Figure 23 shows the landscape metrics calculated for the grassland class of the level 1 classification. Over the last three decades, Patch Density, Edge Density and Landscape Shape Index experience a decrease, whereas AI showed an increase and ENN no particular trend. The declining trend in patch density and edge density indicates a decrease in patches in the study area. High values are encountered in 1993, 1994 and 1995, 1997, 2007 and 2011. Especially the values of 2007 and 2011 are much higher than the values of the years before and after. Patch density for 2009 is low compared to the years before and after.

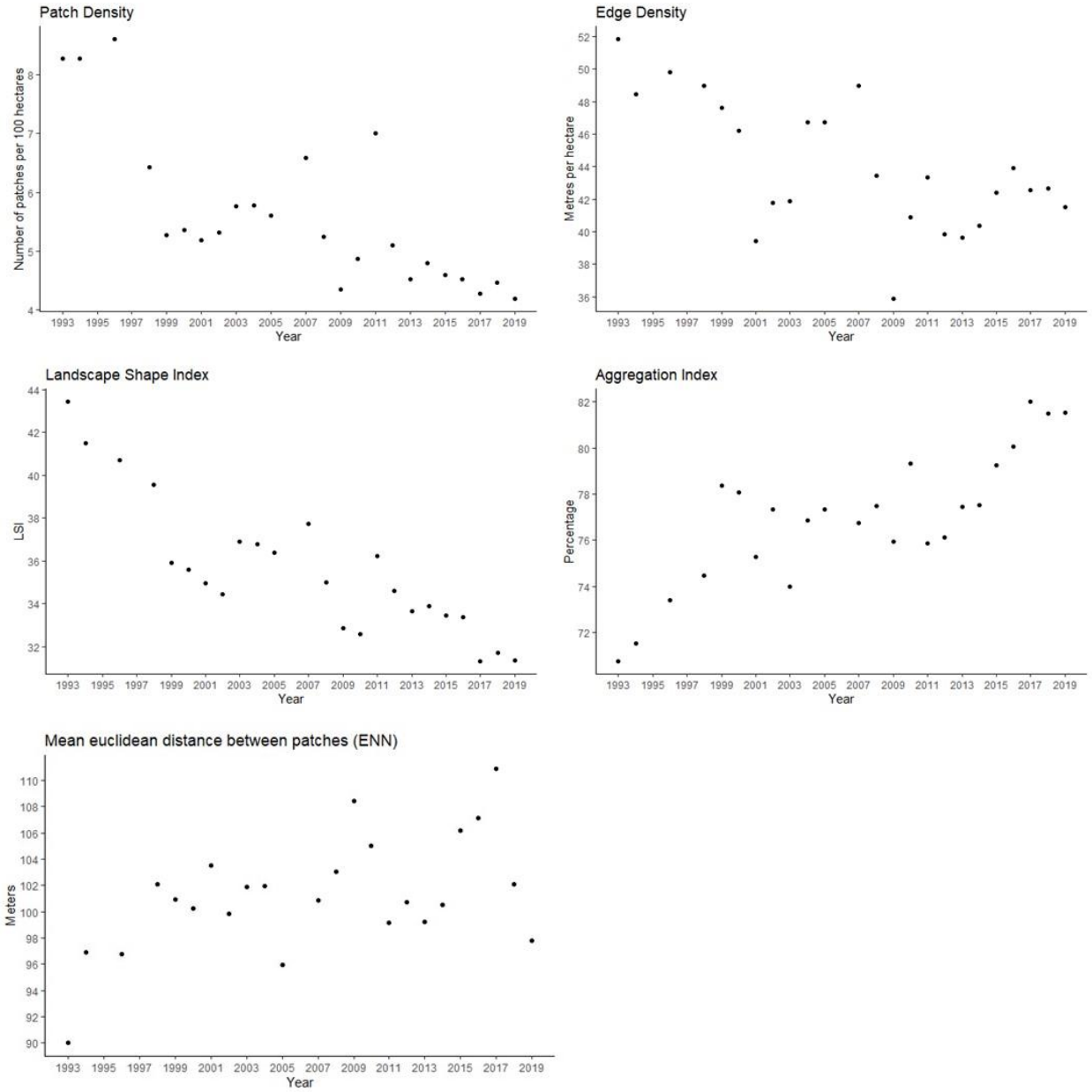

Figure 23: Landscape fragmentation metrics through time for the grassland class.

The metrics Patch Density and Edge Density do not follow the exact same trend. From 1998 to 2002 Patch density has lower values than expected when following a linear decline. This means that more patches are found in the classified maps from 2003 to 2007 than from 1997 to 2002. Noise of the satellite images can interfere here, as Landsat 7 has a line scan error (from 2003 till present) which likely introduces some wrongly classified lines that can contribute to an increase in patch density.

LSI shows a decrease with the same jump from 2002 to 2003 as observed for patch density and edge density, but the decline in trend is still present. Year 2007 and 2011 are high outliers, and lowest values are observed in 2017-2019. The patches have become more compacted over the last three decades. The aggregation index shows an increase, meaning an increased isolation of grassland patches.

The results for the fragmentation of grassland patches can be summed up as follows: Patch Density shows an decrease in the number of patches, the length of the edges of the class grass with other classes decreased, the patches of grass have become more compact, the patches have become more connected to eachother and the distance between patches did not follow a clear trend.

4.3 Transitions

In this section the transitions between classes is shown in a Sankey plot (figure 24) which gives an overview of the class dynamics and their trends during the studied timespan.

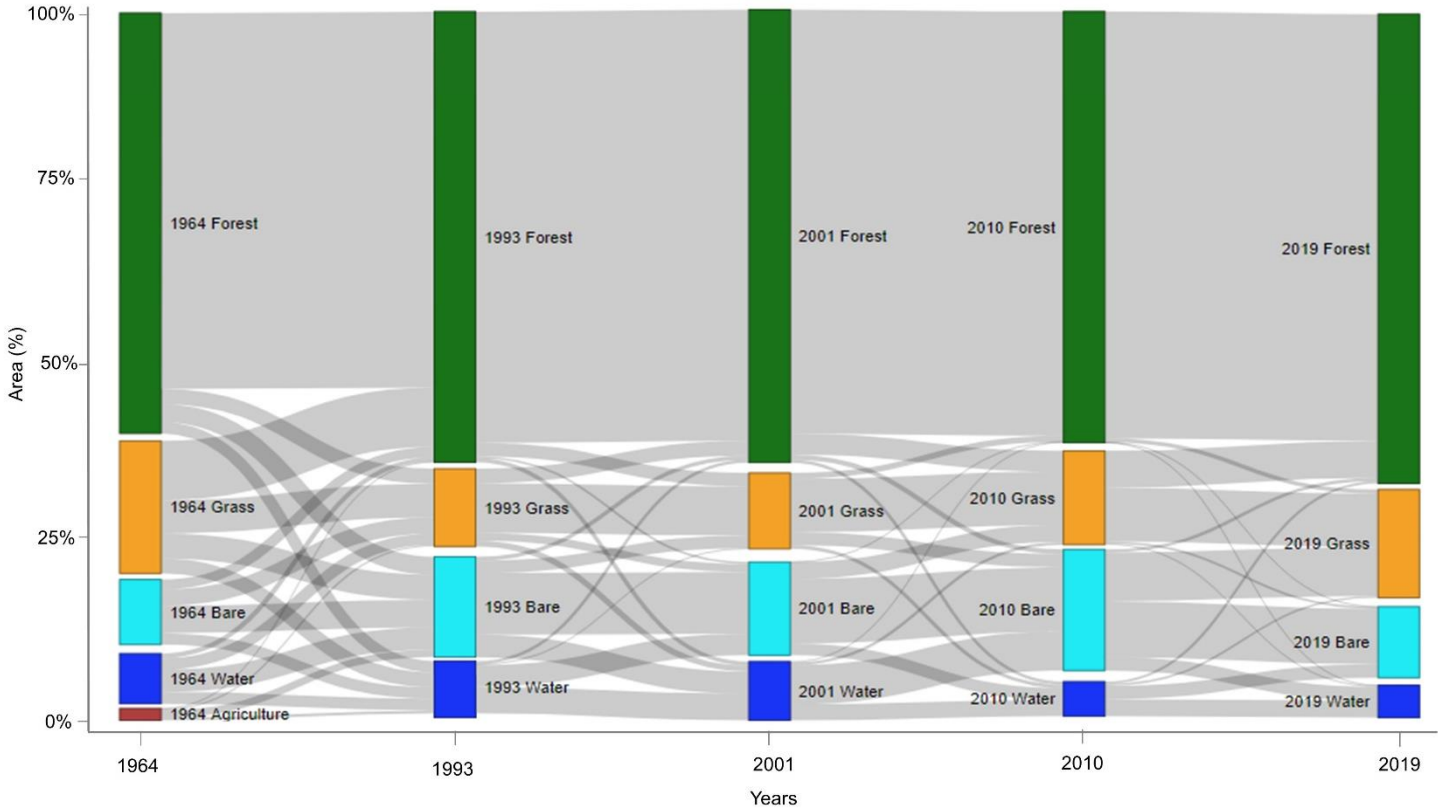

Figure 24: Sankey plot with transitions between classes of the level 1 classification. Thickness of connecting grey bars indicate size of area transitioned.

Figure 24 shows the transitions between each class for the years 1964, 1993, 2001, 2010 and 2019. It gives an overview of the transitions of classes between certain classification years. Furthermore, it includes the classification of year 1964, so instead of an 8- or 9-year timestep a 29-year timestep is taken between 1964 and 1993.

For the comparison between 1964 and 1993, almost half (1167 ha) of the grass area at that time present turned into forest 29 years later. Of the other half, 660 ha stayed grassland and 791 ha turned in either bare or water. Agriculture turned into bare and water. The area covered as water in 1964 is almost completely transitioned in other classes, and the water class in 1993 consists of all classes covered in 1964 evenly.

The area covered by bare and water in 1964 is comparable to the area covered in 2019, whereas the area covered by bare and water in 1993, 2001 and 2010 is larger. The area of grass in 1964 was larger than any other year, while bare and water were comparable in area to the 2019 situation. The successional transition from grass to forest from 2010-2019 was larger than for the comparisons of 1993-2001 and 2001-2010.

The transitions between classes for 1993-2001 is evenly balanced. Transitions between grass and forest together with transitions between water and bare are most dynamic. For 2001-2010 the largest transitions are seen in forest to grass and in water to bare. Comparing the situation of 2010 to 2019 shows a large portion of bare turned into grassland, grassland turned into forest and almost no transitions to bare and water are present, a more static nature than observed in earlier years.

4.4 Environmental Indicators

In this section the possible driving factors are shown, with first the hydrological indicators based on discharge and precipitation, followed by a forest fire dataset.

4.4.1 Discharge

Extreme discharges of the Karnali river can be two- or threefold of the yearly average peak discharge, as observed in the years 2000, 2008, 2009, 2013 and 2014 (figure 25). The amount of the five largest discharges is equal or greater than 12500 m^3/s, which is a recurrence time equal or greater than five years (figure 25). These five years with discharges that exceed a recurrence time of 5 years will be labeled as ‘extreme discharge years’ and compared to land cover transitions in the following section. The 5 year recurrence interval has been chosen because it has been postulated that discharges with these intervals have major changes in the river courses in the Ganga Plains (Thorne et al., 1993).

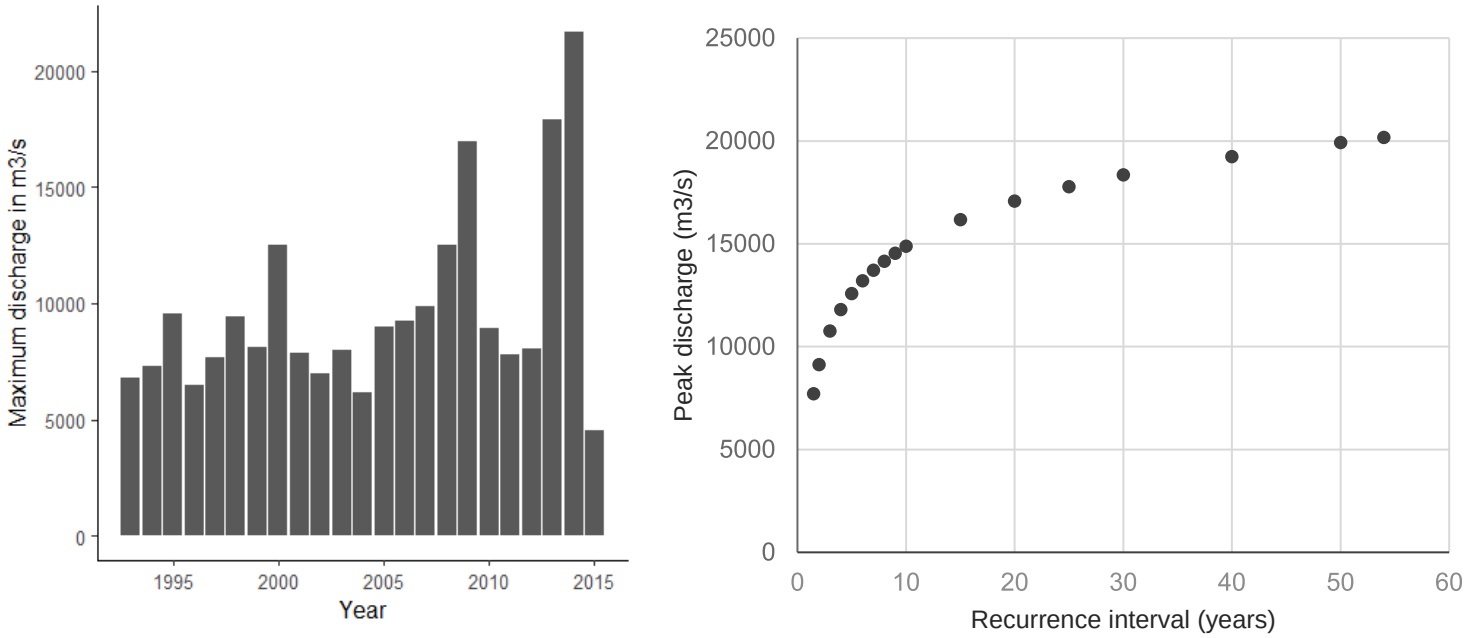

Figure 25: Dataset of peak discharges with the maximum discharge per month on an annual basis (left panel). Recurrence of extreme discharges at Chisapani (right panel). No data available after 2015 (Department of Hydrology and Meteorology, no date).

The next hydrological indicator is the number of days in the year that a discharge of 5000 m^3/s is exceeded (figure 26). The years of 1998, 2000, 2008 are considered as the most extreme years for duration of high discharge and used in the following section for relating hydrology to land cover changes.

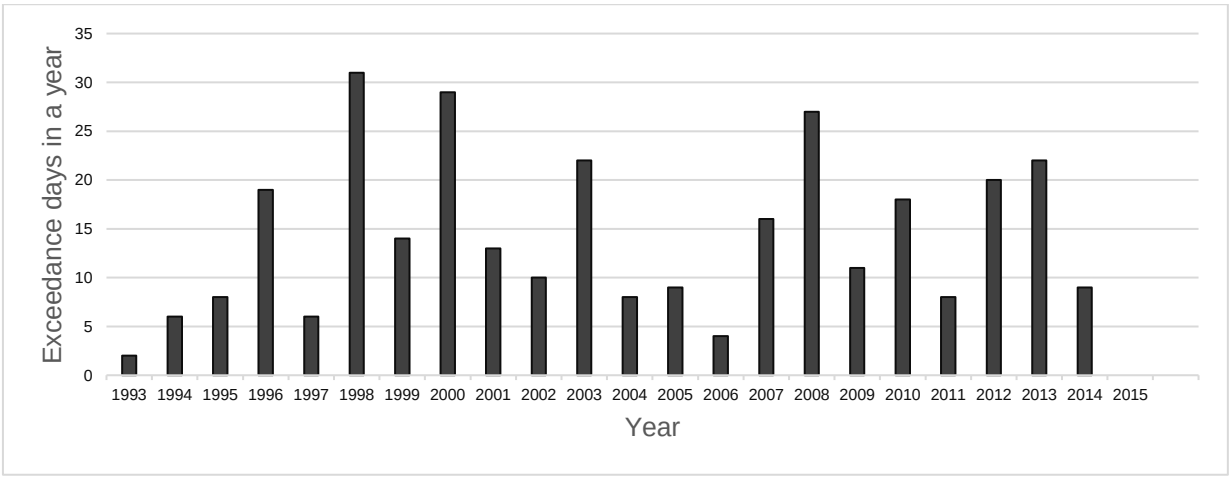

Figure 26: Based on daily discharge dataset (Department of Hydrology and Meteorology, no date) the number of days in a year are summed to calculate the duration of high discharges greater than 5000 m^3/s. Not accounted for multiple events in a year.

4.4.2 Rainfall

From the monthly rainfall series the maximum monthly rainfall per year is taken and its recurrence time calculated (figure 27). Year 2007 and 2014 have the highest amount of rainfall in a year of 15600 mm and 16731 mm respectively. These two years together with the years of high discharge are chosen as hydrologic disturbance years next to the extreme discharge years.

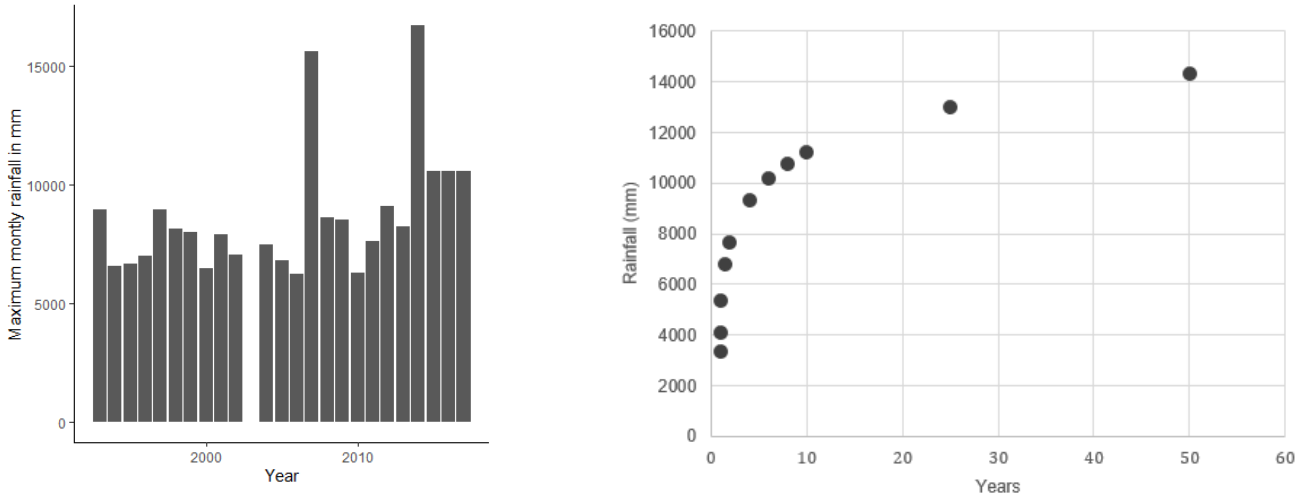

Figure 27: Left panel; Dataset of maximum monthly precipitation amounts per year. Right panel; recurrence rainfall time of peak discharges calculated with a Gumble distribution and based on a 57-year daily discharge dataset. The discharges are measured at Chisapani weather station and are viable for the Karnali river. The precise discharges for the Geruwa and Kauriala river are unknown. (Department of Hydrology and Meteorology, no date).

Forest fires have been most abundant in the years 2012, 2014, 2016 and 2019, based on the number of MODIS satellite pixels that detected a forest fire. These years are used as disturbance factor and these years are flagged as high disturbance years for forest fires (figure 28).

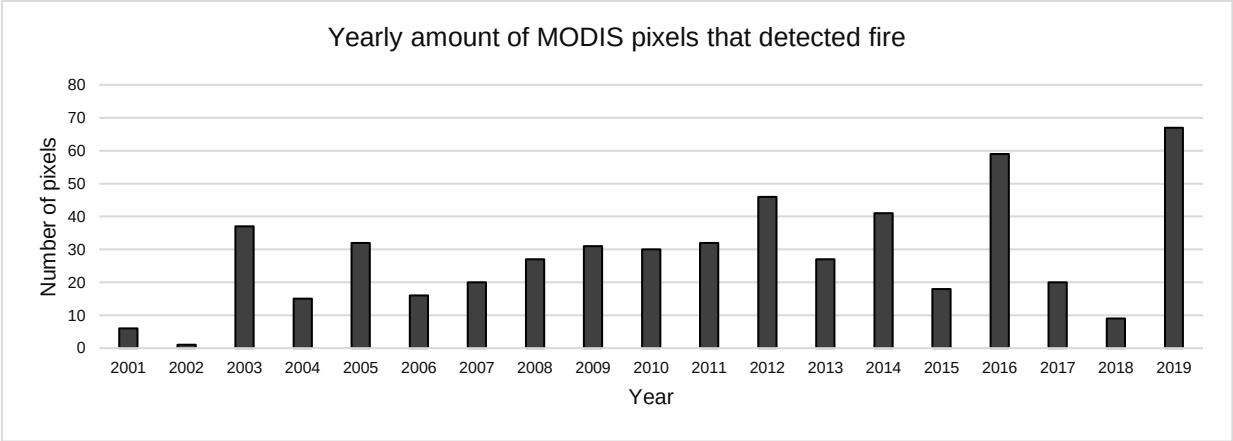

Figure 28: Based on 20-year forest fire dataset the number of pixels is counted that detected a forest fire. Pixel size is 1 kilometre and satellite is MODIS (FIRMS - Active Fire Data)

4.5 Relation between land cover dynamics and environment

In this section the changes in land cover are related to the environmental drivers derived from discharge, precipitation, and forest fires.

4.5.1 Grassland to Bare transitions

Figure 29 shows the number of hectares of grassland that converted to bare area per year for three distinct areas. In the study area, large numbers of hectares grassland that transitioned into bare coincides with the hydrologically wet years (figure 29A). Inside the floodplain, the largest transitions of grass to bare are observed during 2000, 2008 and 2009, coinciding with high discharge in that year. This contrasts with the years after the change in river course of the Karnali river: during 2013 and 2014 the grass to bare transitions have not been larger during the extreme discharges (figure 29B). Outside the floodplain, the transitions of grass to bare coincide with high precipitation years in 2007, 2009 and 2014, but not to all high discharge years (figure 29C). The magnitude of change for grassland is 20 times higher inside the floodplain compared to outside the floodplain.

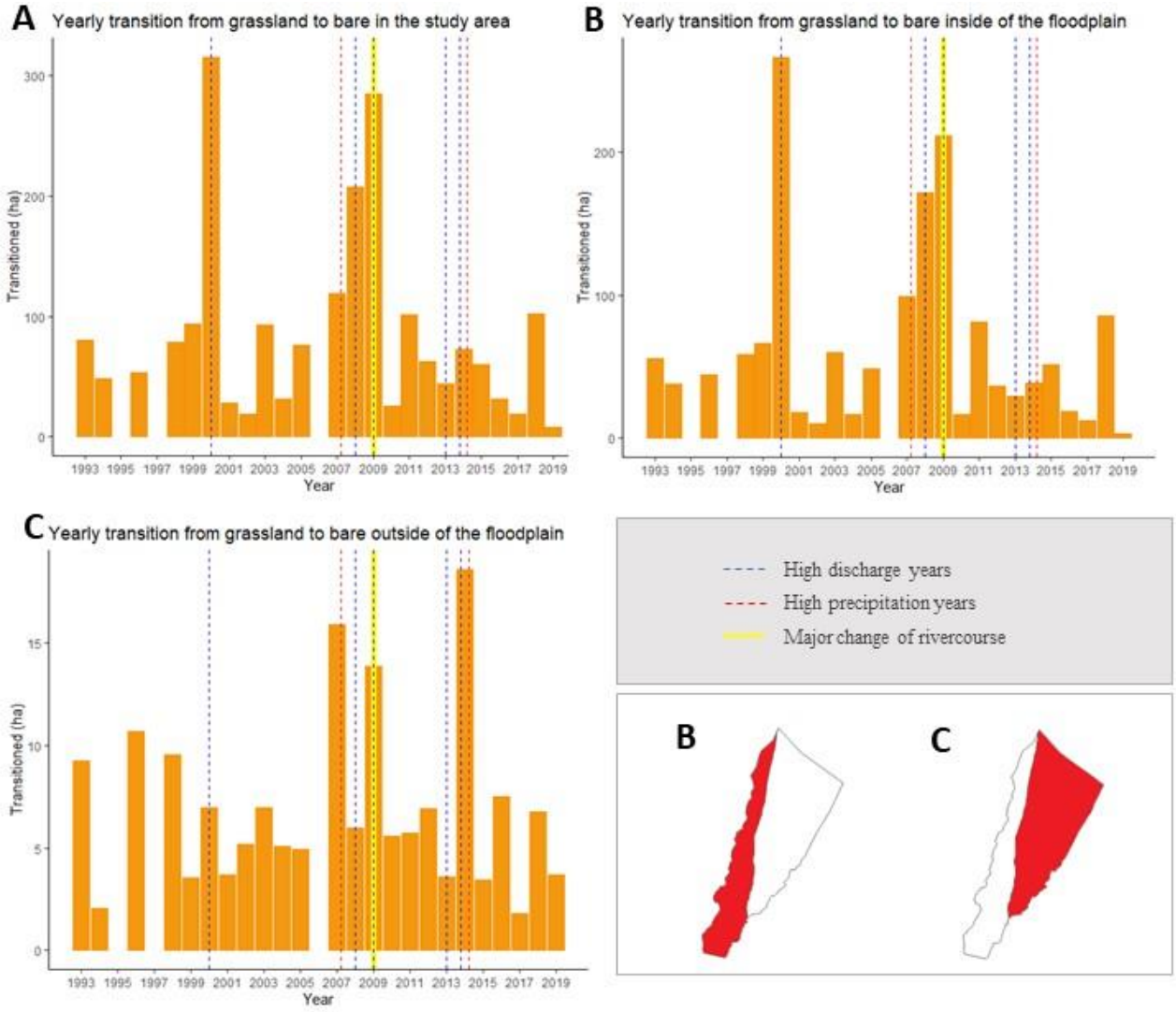

Figure 29: Transition from grassland to bare shown with extreme hydrological events as vertical lines. In the panel at the right-bottom the investigated areas for B and C are displayed.

4.5.2 Net changes of forest and bare

For forests, the net change is visualized in figure 30. Loss of forest is observed in 1999 and 2000, gained again in 2001. This large gain of forest and large decreases of the previous year incites some questions for the reliability of the transitions recorded. It is possible that due to errors less forest was classified in 1999 and 2000 and in 2001 this loss is compensated for in the classification. During extreme discharges and precipitation events no large transitions are observed, and for the extreme discharge year of 2009 even a gain in forest is observed. For the net change of bare large increases of bare coincide with extreme discharge years before the shift in river course. After 2009, this is not observed, and even large increases are seen.

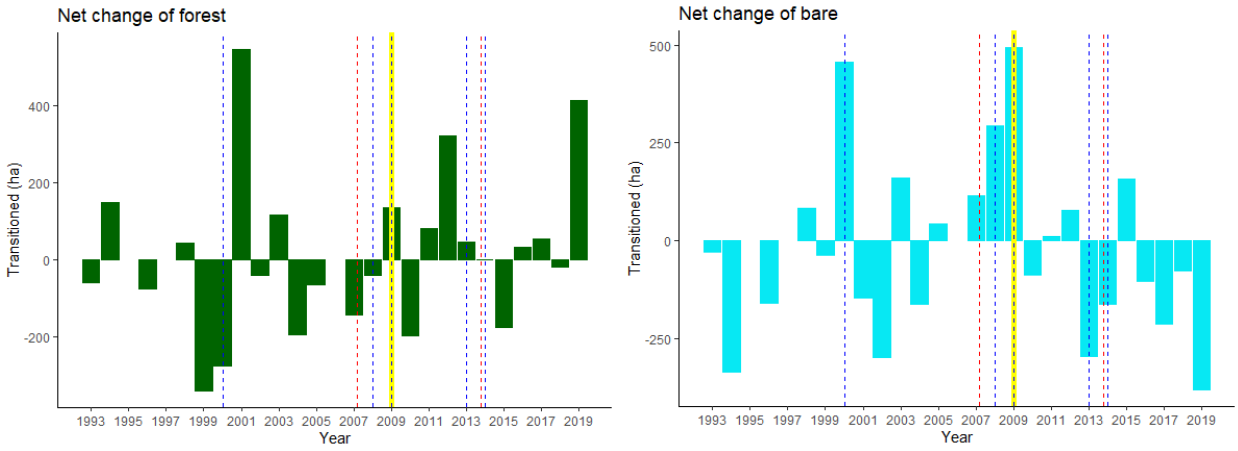

Figure 30: Net change of forest and bare classes

Figure 31 shows the nature of transitions for grassland on yearly basis. Transitions of grassland to water significantly declined after 2009. Large transitions of grassland to forest are observed for 2001 and 2019, which seem unrealistically high. Largest transitions of grassland to bare are in 2000, 2007, 2008 and 2009.

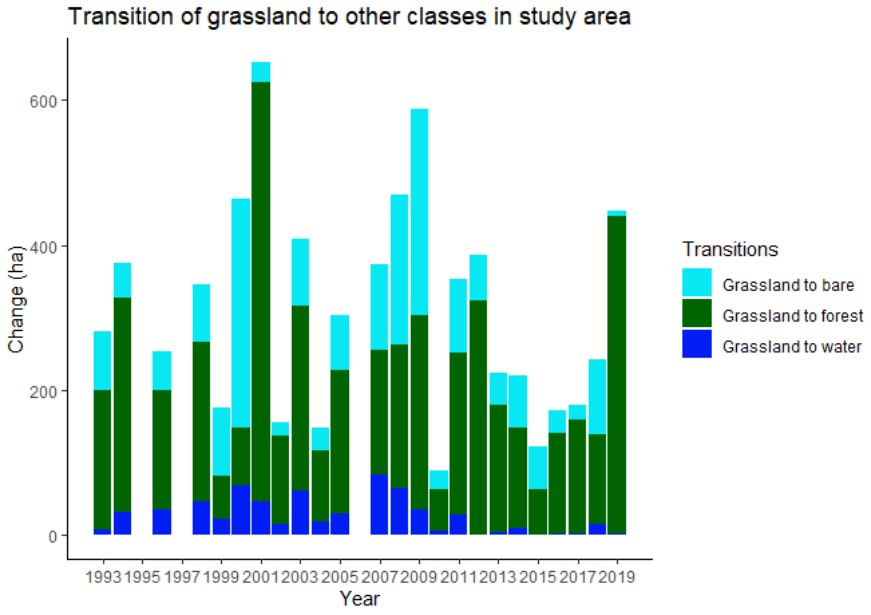

Figure 31: Transitions of grassland to bare, forest and water

4.5.3 Correlations of environmental indicators and land cover

Environmental indicators and yearly transition magnitudes are plotted and checked for statistical correlation with Pearson's test. For extreme discharges, a correlation is present between the maxium discharge in a year and the amount of grassland to bare for the period between 1993 -2009. This is not the case for 2010-2019, where the high peak discharges of 2013 and 2014 experience no larger transitions from grassland to bare than years with average peak discharges (figure 32).

Outside of the floodplain, extreme rainfall events and grassland to bare transitions show correlation, where the high values of 2007 and 2014 are the years with the highest precipitation events recorded and coinciding with highest transitions from grassland to bare. Solely observing gain for the bare class, the extreme discharges of 2013 and 2014 are outliers.

For forest fires, no relation could be detected for number of MODIS flagged forest fires and the amount of forest that was lost (figure 32). This was also checked for the level 2 classification and transitions between classes did not show a correlation with the variation in the used forest fire dataset.

Figure 32: Correlation tests for environmental drivers and land cover class dynamics, calculated for the floodplain area.

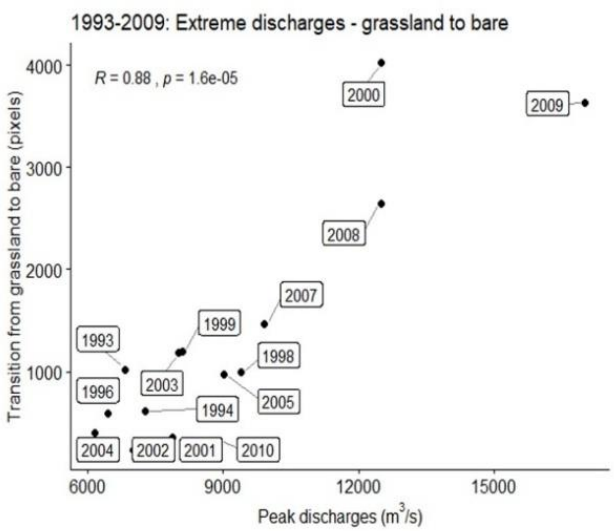

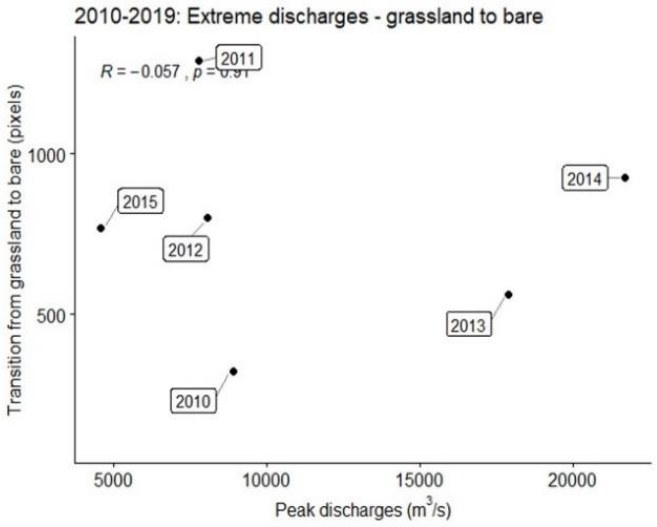

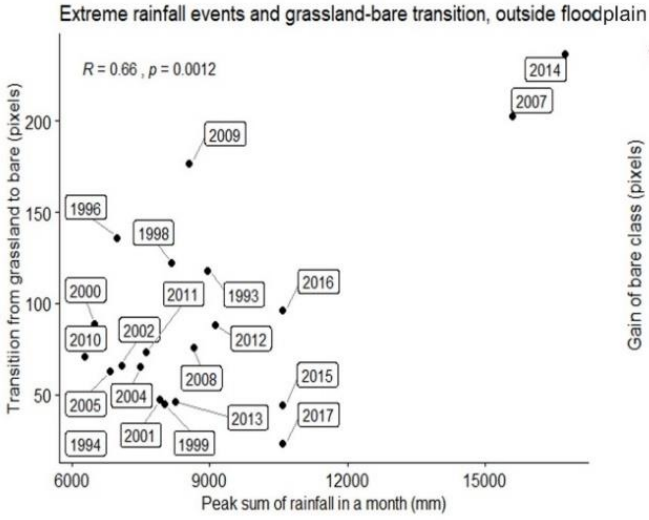

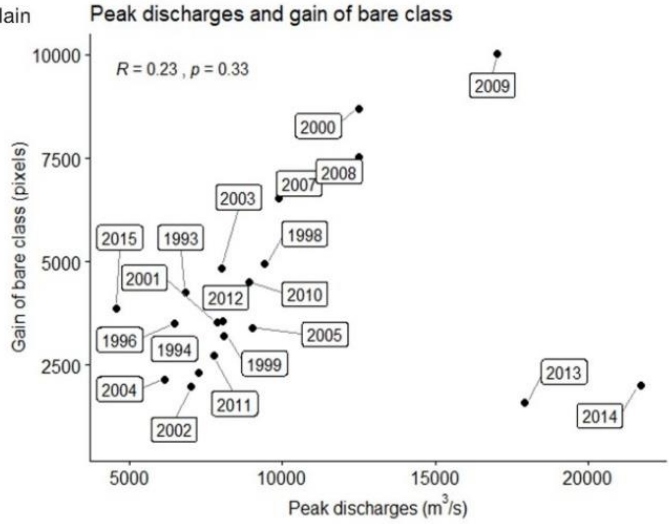

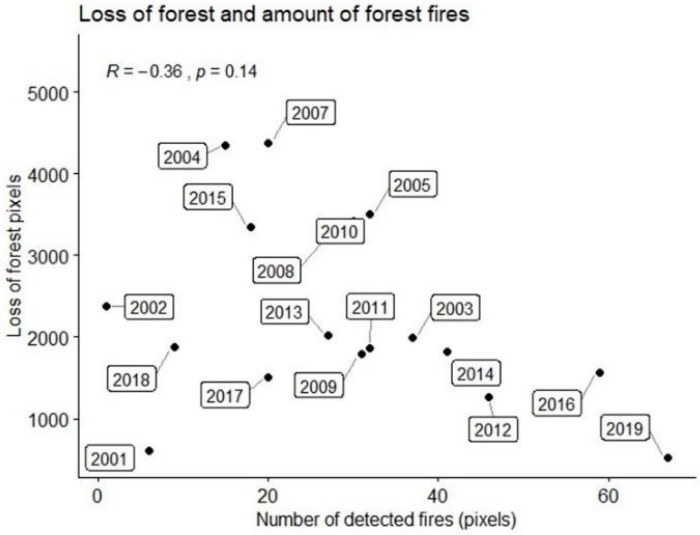

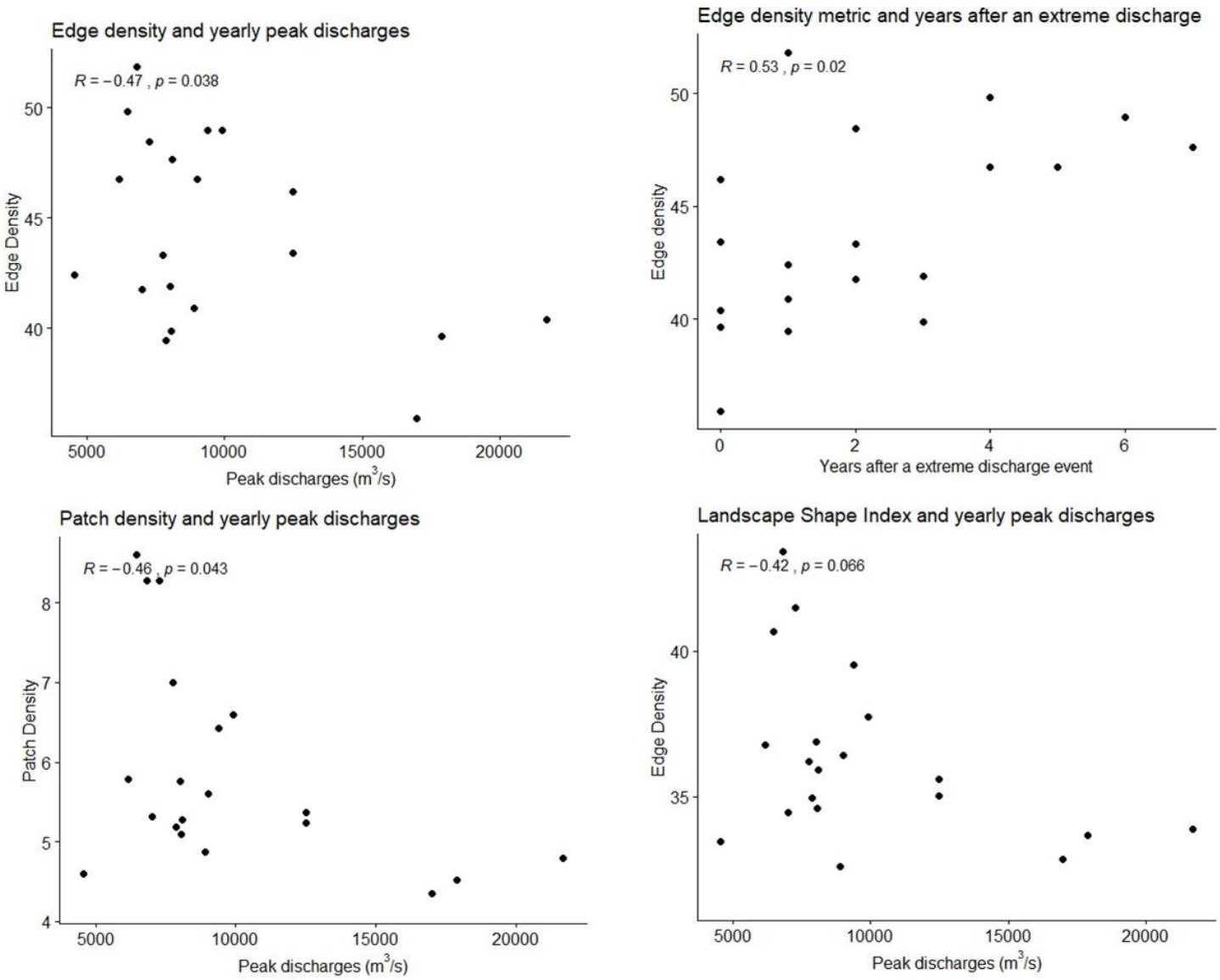

Figure 33: Correlation test for landscape fragmentation metrics and environmental drivers, plotted for the whole study area.

Comparison between landscape metrics and hydrological indicators (figure 33) for the whole study area show correlation between peak discharges and edge density, patch density and edge density and years after an extreme discharge. For LSI compared to peak discharges the statistical hypothesis is just rejected. For the Aggregation index and Mean Euclidean distance no correlation was observed.

4.5.4 Flood extent

Figure 34 shows the results for the land cover within areas defined by flood recurrence time. This is done for three recurrence times of flooding: 1 year, 5 year and 10 year with flood extents of respectively 2184 ha, 3185 hectares and 3326 hectares for the study area of this report. The inner circle represents a recurrence time of 1 year, the second circle of 5 years and the outer circle a 10-year recurrence time. The difference between a 5- and 10-year recurrence time flood is marginal. And for these recurrence

times the number of forest hectares affected are significantly higher than for the 1-year recurrence discharges. From the level 2 classification can be derived that the forest type is solely riverine forest. If a flooding with a 5-year recurrence time would occur, 851 ha of wet tall grassland would be affected in 2019, which is 71.8% of the total coverage of wet tall grassland in the study area.

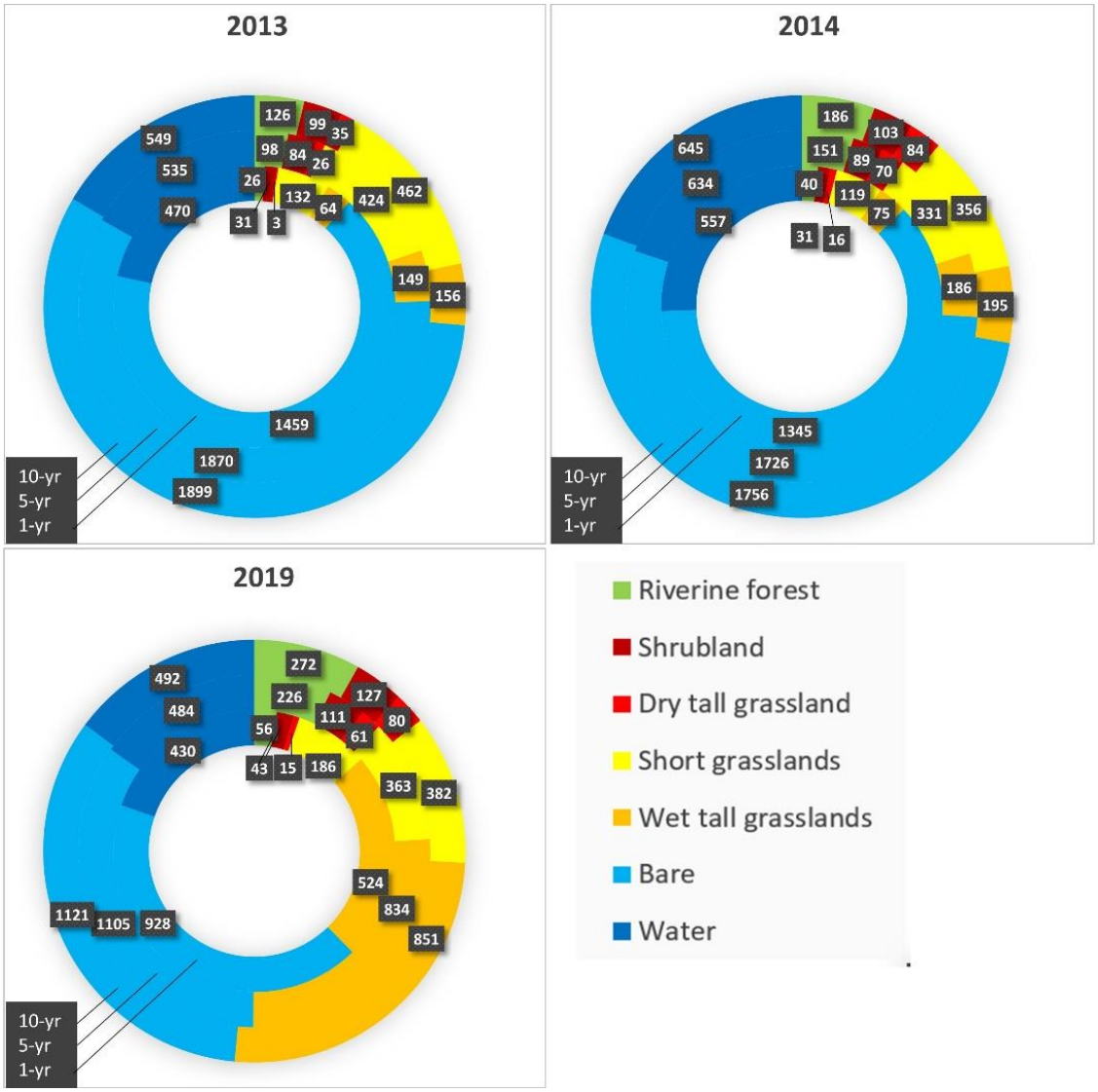

Figure 34: Comparison of land cover in areas defined by flood recurrence time, i.e. 1-year (inner circle), 5-year (middle circle) and 10-year (outer circle) recurrence intervals as modelled by Van Kooten (2019). Numbers are in hectares.

4.6 Historical and regional analysis

In this section the land cover in the study area is analyzed from an historical and regional perspective to gain insight in their origin.

4.6.1 Historic perspective

Several grasslands patches found in the land cover maps of 1993 - 2019 can be traced back to the 1964 map (figure 35). Their location is outside the active channel belt and consist of short grassland and dry tall grassland mainly. The grasslands Baghaura, Lamkauli and Khauraha belong to these grasslands (earlier described in figure 2). Grassland present on the channel bars is barely persistent from 1964 to 2019, and together with their residence time of 5-10 years (computed in section 4.1.3, figure 18) it highlights their dynamic nature.

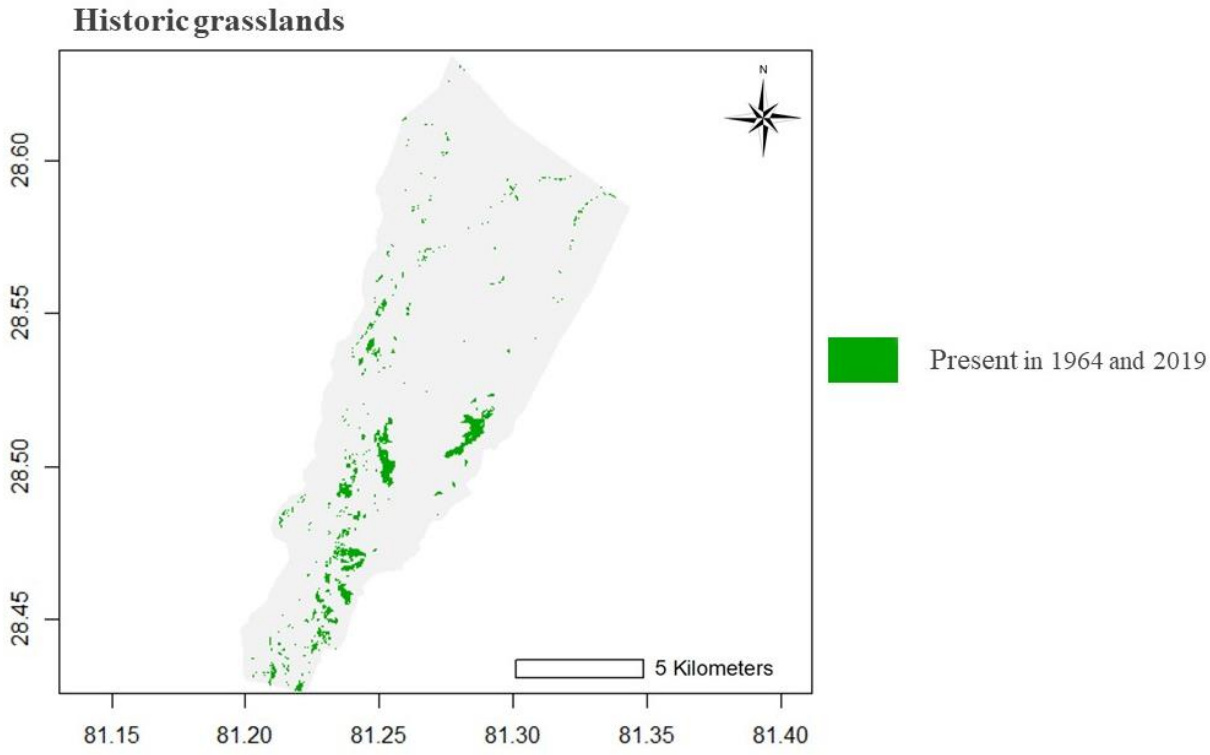

Figure 35: Historic analysis of grasslands. The 1964 map is compared to grasslands present in 2010-2019

In maps classified by the topographic survey of Nepal (figure 36), the Lamkauli grassland can be traced back to 1927, consisting of the village Lathwa, underlining the anthropological origin of this grassland. A significant change in land cover is the deforestation, for example clearly visible between the Geruwa and Kauriala river.

A 1926/1927

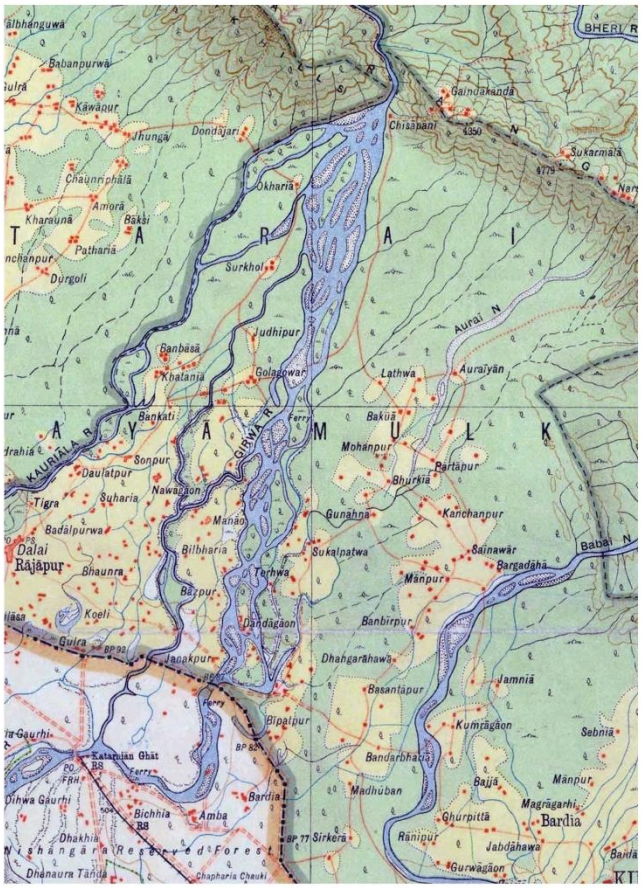

B 1984

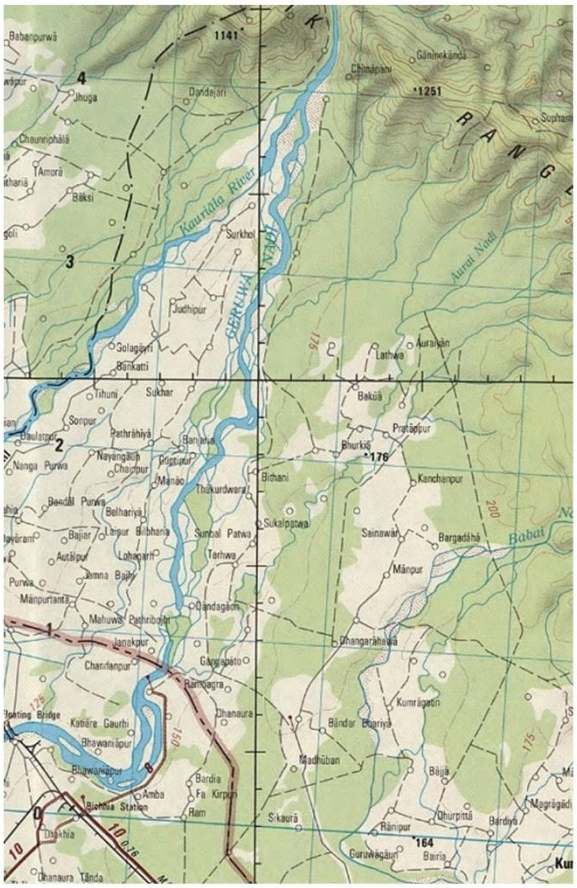

Figure 36: Topographic maps from the topographic survey department in Nepal, based on aerial photographs (complete maps in appendix E).

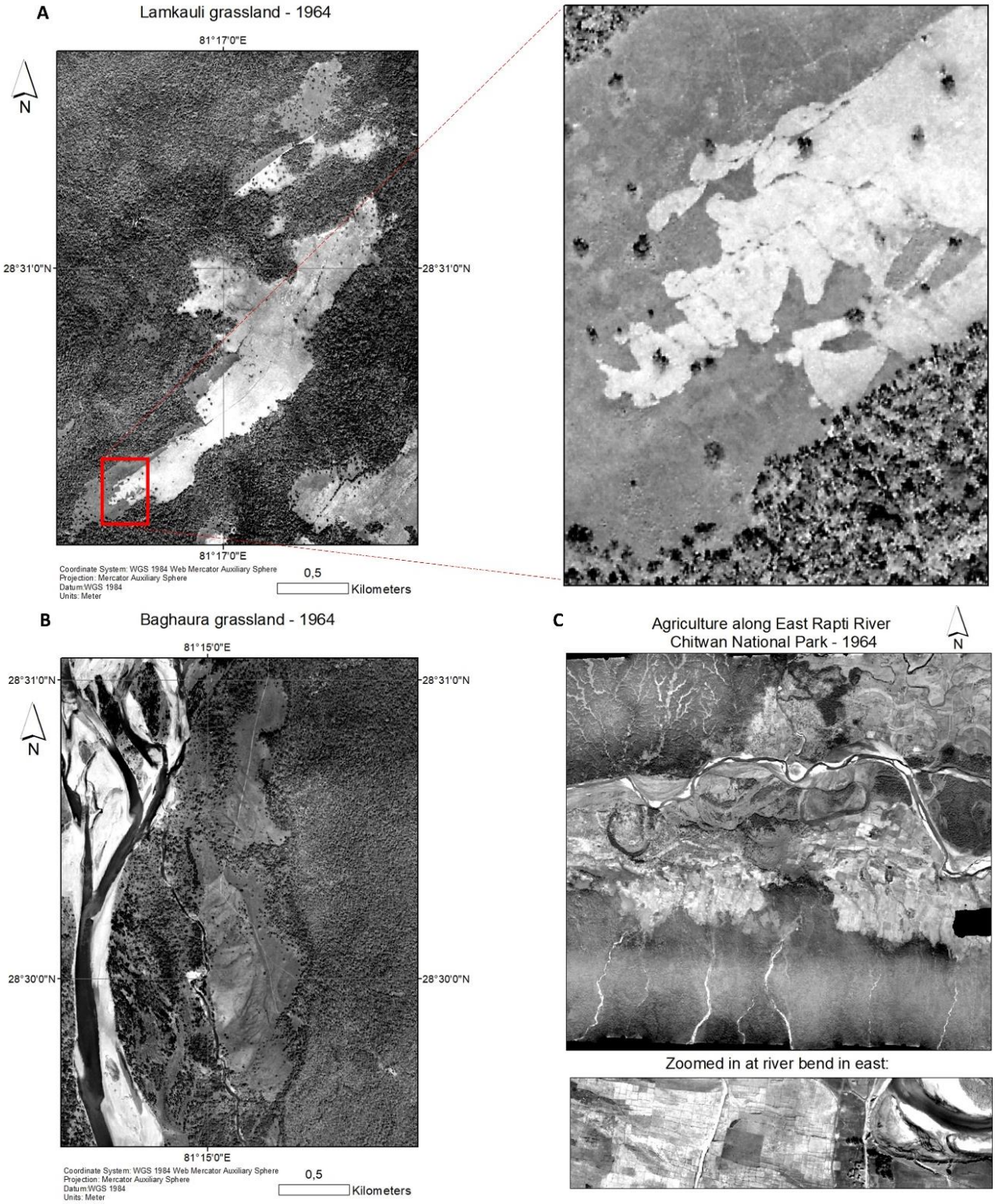

Figure 37: 1964 aerial photographs. ***A****; the Lamkauli phanta with supposedly anthropogenic cutting practices. Darker shaded grass is tall grass, light grey is short grassland.* ***B****; Baghaura grassland.* ***C;*** *a comparison with Chitwan National Park, where agriculture was present in what is now the core area of the Park.*

Figure 37 shows the situation of the Lamkauli and Baghaura grassland on aerial photographs from 1964. On 37A cutting patterns are visible, highlighting the impact of antropogenic activities for Lamkauli. On 37B is visible that the grasslands west of Baghaura are more savannah type, with trees more dispersed than at present in that area. No signs of a village or agriculture in Bardia is oberved. This is the case in Chitwan, where clearly squares for agriculutral fields are vsibile on the nowadays phantas.

4.6.2 Regional perspective

To gain additional insight into the land cover dynamics of the study area, two neighboring areas are classified with the trained models as well. To put the impact of peak discharges on vegetated area in the Geruwa branch in perspective, it is compared to the Kauriala branch to the west and the Babai river to the east (figure 38). The Kauriala river is the main branch of the Karnali river since 2009. The Babai river lies to the east, is mainly rainfed, and has a high hydrologic impact on the eastern side of Bardia National Park (Adhakari, 2013).

A comparison of area versus time is made to (1) see whether hydrologic events are also visible in the other two areas and (2) to detect some artifacts in the classification, since the classifications are made with the same satellite images but a different mask for the study area. No ground truths are taken for the Kauriala river and the Babai river, but the same vegetation types are present. The results are not checked for accuracy.

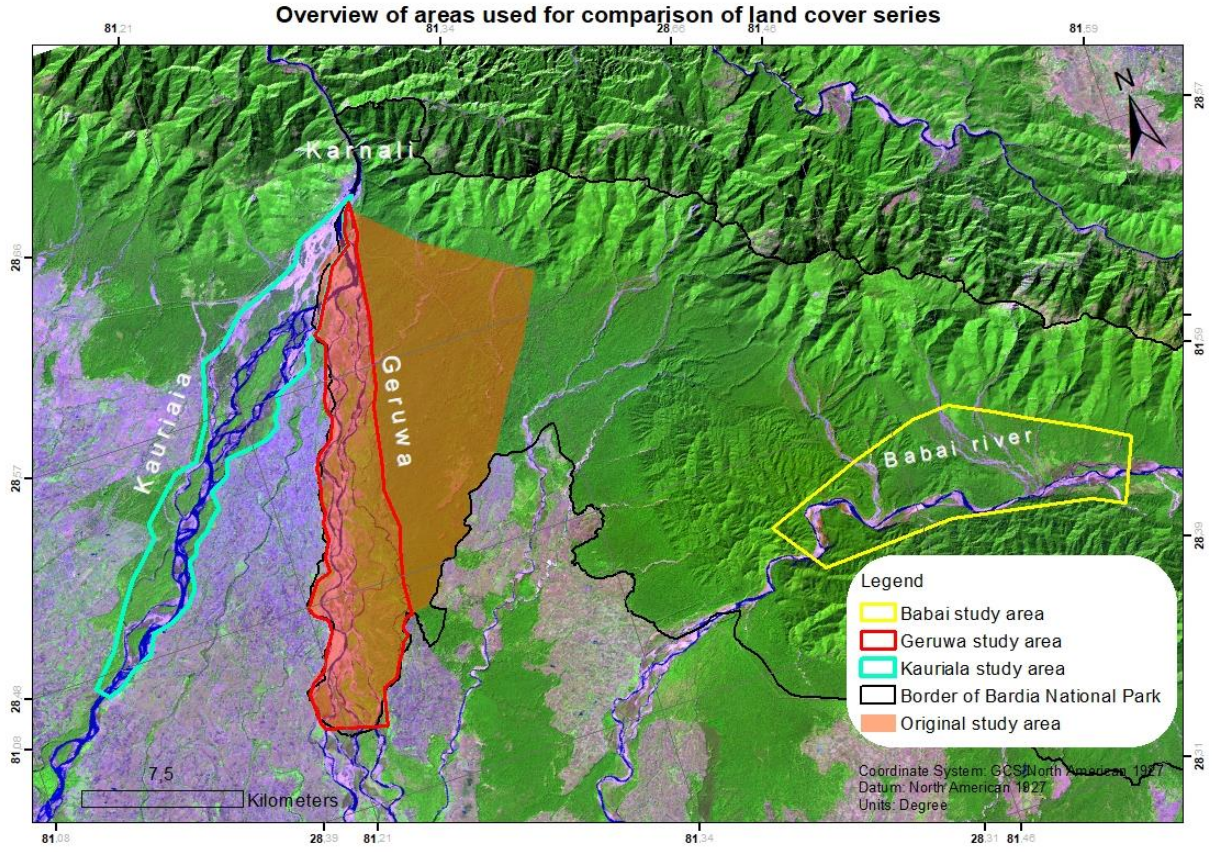

Figure 38: The three rivers shown for which the land cover near the floodplain is compared and linked with extreme hydrologic events

Firstly, the Kauriala and Geruwa river are compared with the level 1 classification. For the water class, the change of dominant channel from Geruwa to Kauriala is clearly observed. Whereas the area of grass increases in the floodplain of the Geruwa river, the floodplain of the Kauriala river experienced a decrease of grassland and increase of bare area since the avulsion in 2009, as shown in figure 39.

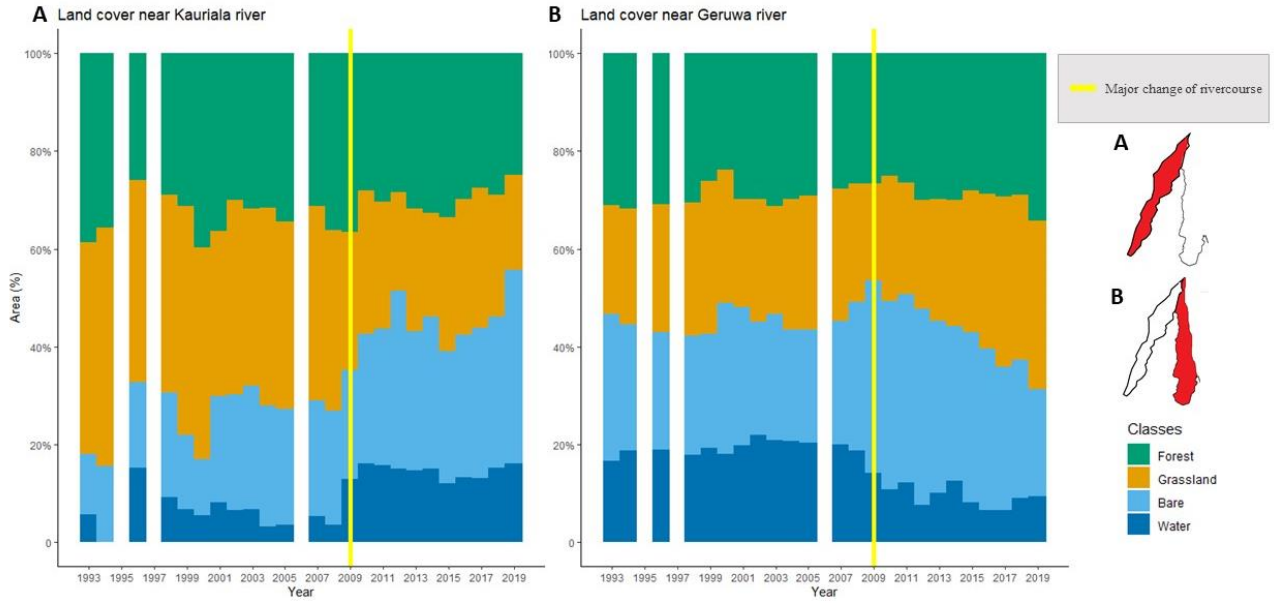

Figure 39: Comparison of land cover (level 2) near Kauriala river and Geruwa river with the change of dominant channel shown as yellow vertical line. White vertical columns mean that the years (1995, 1997 and 2006) have no data.

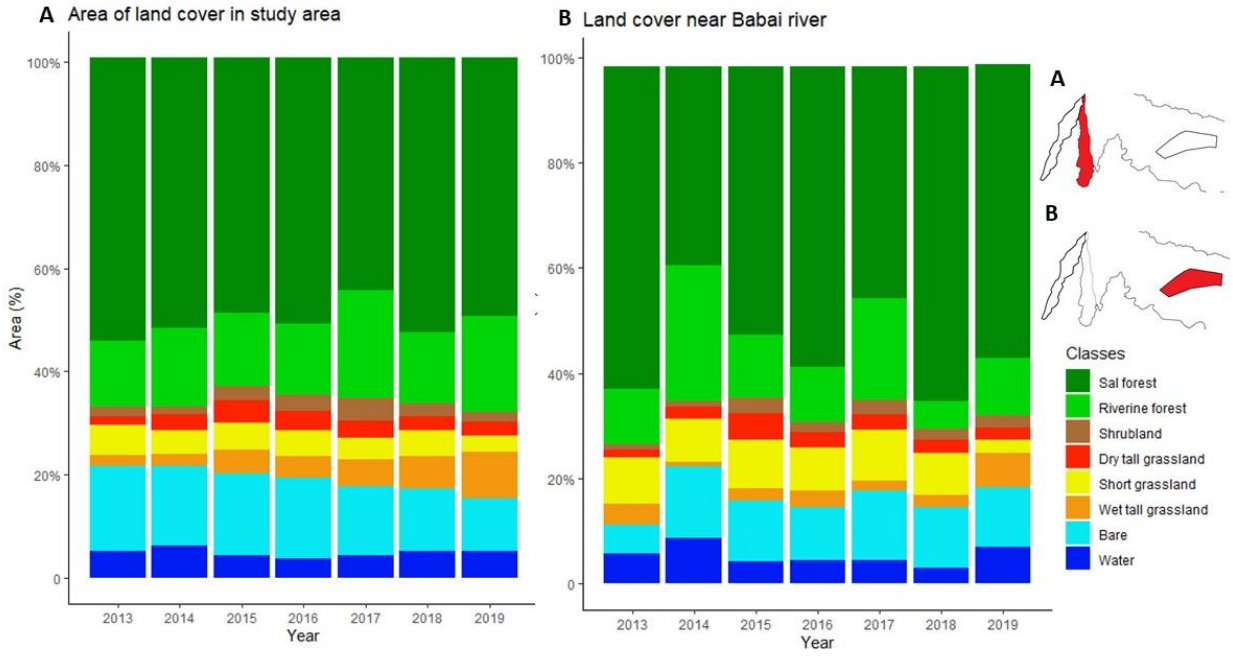

Figure 40: Comparison of land cover (level 2) near Geruwa river and Babai river with the change of dominant channel shown as yellow vertical line. White bars represent missing data.

Comparison of the land cover area near the Geruwa river and the Babai river shows the following (figure 40): during the 2014 extreme precipitation amounts, bare area near the Babai river increased significantly and forest and wet tall grassland decreased, whereas this is not observed for the land cover near the Geruwa river. Furthermore, the coverage of bare increased during 2017, when flooding was recorded downstream of the Babai river (ICIMOD, 2017).

From these comparisons the following is the main result: the active channel of the lower Karnali (so Geruwa or Kauriala) has a smaller grassland coverage than the other channel. For the Babai river the extreme rainfall in 2014 measured at Chisapani coincides with a successional setback in grass and forest cover.

5. Discussion

In this research two land cover time series of the Karnali floodplain in Bardiya National Park are presented, along with analysis of their spatial and temporal dynamics and the impact of environmental drivers. The classification of the land cover series is supported by field data of vegetation collected in 2019. For the analysis of the land cover time series the following elements are considered in space and time: the areal change of land cover classes, the spatial change perpendicular to the stream channel, landscape fragmentation metrics that quantify the pattern of grassland, transitions between land cover classes, environmental drivers derived from discharge, precipitation and forest fire datasets and lastly the relation in space and time between the environmental drivers and the land cover dynamics. This last part is predominantly done for the level 1 classification series due to the timespan of the datasets.

The land cover time series and its derived results can only be evaluated in combination with the possible uncertainty of the data. The first section in this chapter will cover this. In the second section the answers to the research questions are given considering the results of this study, in the third section the results will be put in context with literature and lastly research questions and recommendations for future research will be provided.

5.1 Uncertainties

Uncertainties in the results can originate from the classification model, its input data (field samples and satellite image composites) and validation data (collected in the field and with Google Earth). Errors could also be introduced via uncertainties in the datasets of the environmental drivers.

Firstly, errors in the input data for land cover map creation can be introduced via inaccuracies in satellite imagery composites and in field samples of vegetation types. Errors in the annual composites can originate from satellite artifacts (Landsat 7 scan-line error, presence of clouds, difference in acquirement date) and differences in sensor characteristics between the Landsat satellites. Recent years have more images available for creating the image composites, and the higher the number of images available per composite, the better the composite is thought to be. Furthermore, a more extended ‘best available pixel’ algorithm (White et al., 2014) for the satellite composites and post classification processing such as incorporation of logical transition rules done by Hermosilla et al. (2018) would increase reliability of the results. Introduction of bias in the dataset could be a source for errors, especially since an optimal

random clustered stratified sampling design for collecting field samples was not possible and the number of samples is somewhat low for optimal supervised classification. Also, misclassification in the field and collection of validation data with Google Earth can introduce errors. Misclassification in the field is not considered as a large source of error. Validation data gives insight into which degree the reference data is mapped correctly. Collection of validation data for land cover before 2019 was suboptimal, and with this also the assessment of accuracy itself for these maps. The imagery accessed via Google Earth for validation was not complete in coverage of the whole study area for some years and seasonal variation in water coverage makes validation more difficult as limited free imagery is accessible. For the level 2 classification, too few samples for shrubland were available to accurately assess accuracy for this class. For older imagery it is hard to distinguish the separate classes of the level 2 classifications accurately, limiting validation of the classification maps before 2019.

Uncertainties in the interpretation can originate from the following sources. Years with disturbance events may coincide with erroneous transitions in land cover introduced by the above-mentioned reasons. Also, the lack of a precise dataset of anthropogenic disturbances, such as where and when cutting and uprooting took place, how many permits were given for locals to enter the park and where active management with fire was executed. Since its expected large impact on the dynamics of vegetation, lack of information on this part hinders a more detailed analysis.

Although these factors pose limitations to optimal classification accuracies, the series of land cover maps are of sufficient accuracy (+- 85% for level 1, +- 72% for level 2) to draw general conclusions on the development of the land cover pattern.

5.2 Possible drivers of land cover change

The outcome of the study is discussed by answering the research questions.

I. What is the development of the land cover pattern in the past decades in the study area?

The land cover pattern experienced considerable changes since 1993, especially close to the Geruwa river. At two moments in time large transitions from grassland to bare are observed, after which revegetation occurs. In 2000, the forest and grassland cover recovered to the extent observed prior to the disturbance, whereas for the 2009 event, the increase in grassland and forest is still ongoing in 2019. In 2019, the largest coverage of grassland and forest is observed for the studied timespan, while areal coverages for bare and water was lowest. The trend observed in the level 2 classification is in line with the longer timeseries of the level 1 classification and shows the land cover dynamics in more detail. Furthermore, it shows that the increase in the area covered by grasslands mainly involves expansion of the wet tall grassland class. Successional growth is observed annually in the level 2 classification, except for 2014 to 2015 where a setback in forest is observed coinciding with an increase in shrubland.

Landscape metrics were used to describe the pattern of the grassland class in the level 1 classification From 1993 to 2019, the metrics indicated a decrease in the size and heterogeneity of the grassland class. These results indicate that the number of patches of grassland decreased, the length of contact of the grassland to other classes decreased, the grassland patches became more connected to each other and the shape of the patches of grassland has become more compact. Since these metrics are calculated for

the whole study area both the grasslands present in the stream channel and grassland present in the forest are considered. The signal could mainly be affected by variation in the distribution of the more dynamic wet tall grasslands, but also a decrease of small patches within the riverine and Sal forest is observed.

II. What is the variation in the environmental drivers in Bardia National Park?

The discharge dataset shows extreme discharges with a greater than 5-year recurrence time in 2000, 2008, 2009, 2013 and 2014. The rainfall dataset shows extreme rainfall events in 2007 and 2014. In 2014 the extreme precipitation and extreme discharge coincide. Droughts are not considered in this report.

For 2012, 2014, 2016 and 2018 most MODIS pixels were flagged for presence of forest fires. In the first 10 years of the dataset, the number of pixels where fire was detected is more stable, whereas for the years from 2011 to 2019, the variation between years is much larger. Whether this has a connection with the decreased discharge in the Geruwa branch, increased anthropogenic burning or changing climate is not understood.

Ghimire et al. (2014) created a fire hazard zonation map of BNP and found that more forest fires are present after 2008. They attribute this increase to possibly changing climatic conditions. On the other hand, the timing also coincides with the shift in the river course and if investigated further, the link to decreased discharge of the Geruwa river or increased anthropogenic management by fire could be an alternative explanation.

III. When and where did successional resets happen and what caused these resets?

At several moments in time successional resets happened. The first is from 1999 to 2000, when the coverage of bare increased heavily and forest experienced a large decrease. The observed coincidence of the increase in coverage of bare and the extreme discharge indicates flooding as the driving factor for this event. Most of the transition happened close to the river (Appendix B) obtained from the spatial analysis of land cover. The decrease in bare and increase of grass from 2000 to 2004 indicates regrowth of vegetation. Not explainable is the large transition from forest to grass observed one year earlier in 1999. Interpretation of the result and magnitude of transitions of grassland back to forest in the following year suggests an erroneous classification.

The second successional setback is observed in three separate but consecutive years. In 2007, during a high rainfall event, 15 ha of grassland to bare is transitioned in the east of the park close to perennial streams. In 2008 and 2009, large amounts of grassland are converted to bare area, coinciding with extreme discharges measured at Chisapani. During the extreme discharges in 2009 the main branch of the Lower Karnali system changed to the Kauriala river (Sinclair et al., 2017; Van Kooten, 2019). The 2008 transitions are observed close to the Geruwa river, whereas the 2009 transitions are also observed further away from the floodplain.

The third event is observed in the level two classification in 2015, where forest experienced a decrease and increases are observed for shrubland and the three types of grassland. The shift to earlier levels of successional vegetation does not coincide with either the forest fires or the hydrologic indicators.

Whether it can be attributed to another environmental indicator or increased uprooting and removal of trees in the area is unknown since detailed information on annual park management and variation therein is not available. After the successional reset in 2015, forest steadily increases from 2015 to 2019.

The location of the successional resets is close to the Geruwa river in 2000, 2008 and 2009, whereas in 2007 and 2014 the transition from grass to bare was mostly outside the floodplain. Within the floodplain, the forest is not older than around 27 years, since almost the complete area within the floodplain has been grass covered at a certain moment in time between 1993 and 2019.

The events of 2000, 2008 and 2009 coincide with extreme discharge events of the Karnali river. This, together with the location of these resets close to the Geruwa river strongly indicates high discharge as disturbing factor. Furthermore, the duration of discharge was assessed, but the statistical relation to grass-bare transitions was stronger for the magnitude of high discharges. The higher rates of grass-bare transitions measured outside the floodplain in 2007 and 2014 coincide with heavy rainfall measured at Chisapani and disturbing factors are the perennial streams originating in the Siwalik hills.

After the extreme discharges in 2009, dynamics of the water class greatly reduced. The area of water greatly declined, which entails that the average area of the river in the dry period did decrease. Decreased transitions from forest to water indicate that a smaller area of forest is eroded annually. During peak discharges of 2013 and 2014, no large successional transitions were observed in the floodplain, indicating that the reduced level of discharges in the Geruwa branch reduced impact on the vegetation pattern.

IV. How do environmental drivers relate to changes in the vegetation pattern in Bardia National Park?

The possible environmental drivers such as impact of magnitude of discharge, duration of discharge, magnitude of rainfall and shift in river course were plotted against each other and coincidence of discharge events and large transition events are assessed. The drivers were checked for statistical validity (correlation) against properties of the development of the vegetation pattern, such as change in coverage of a land cover class or transitions between classes.

The shift in the river course is thought to have had a profound effect on the relation between environmental drivers and the vegetation pattern. Until 2009, the annual number of hectares transitioned from grassland to bare has a statistical correlation with the magnitude of discharge or the magnitude of the extreme precipitation event, dependent on the location observed (respectively floodplain and non-floodplain). This was not the case after 2009.

For the years 2013, 2014 and 2019 the land cover in areas defined by flood recurrence time is assessed. Part of the vegetation would have been affected by floods in 2013 and 2014 according to the modelled flood extent, but no successional setbacks were observed. From 2015 and onwards, successional growth is observed and after colonization of grasses on bare soil, the vegetation types shrubland and forest increased in area. In 2019, almost half of the area that would be affected by a flood with a 5- or 10-year recurrence time was vegetated. Due to this increased coverage of vegetation in the floodplain, hydraulic roughness of the stream channel is greatly increased in Bardia National Park and downstream of the park. If a new shift in river course would occur and the Geruwa branch would become dominant again,

the increased hydraulic roughness could lead to severe flooding with loss of property and lives as a consequence, if not properly forecasted and addressed (Baptist et al., 2007).

For forest fires no correlation could be established for transitions between land cover classes in the level 1 and the level 2 classification. For grasslands known to be yearly burned such as Lamkauli, Baghaura and Khauraha (figure 2) this measure is important to prevent succession. These grasslands have therefore been present for a relatively long time, at least since 1964. Smaller patches of grass close to these grasslands have mostly disappeared, especially east of Baghaura and north of Lamkauli. The reason why these patches disappeared and *phantas* such as Baghaura and Lamkauli are maintained as grasslands is presumably because of the lack of annual fires and anthropogenic cutting for these surrounding patches.

Lacking is precise annual knowledge on anthropogenic disturbances. Persistent presence of short grasslands on the channel bars south west in the park, is visible in the level 2 classification. This is close to the built-up area and accompanied with field observations the short grasslands here are a likely a consequence of grazing of livestock.

V. What are possible causes of changes in the vegetation pattern near the Karnali floodplain in Bardia National Park?

To answer the main research question, the causality of the relation between drivers and changes in the land cover pattern is discussed. The established correlations between the land cover dynamics and the environmental drivers does not imply causation, but with knowledge of the system the main drivers of change in the vegetation pattern can be inferred.

Before 2009, large transitions of grassland to bare were observed in years with extreme discharge events (in 2000, 2008 and 2009). After 2009, these successional resets were not observed anymore while discharges measured at Chisapani in 2013 and 2014 were of a greater magnitude than the earlier measured discharges. The shift in river course in 2009 is therefore considered as the cause of reduced (peak) discharges in the Geruwa branch, resulting in less successional resets nearby to the Geruwa river. Consequently, more successional growth is observed with increased coverages of grassland and forest.

In years 2007 and 2014, years with extreme precipitation, transitions from grassland to bare occurred along the perennial streams. Large discharges in the perennial streams during extreme precipitation events are therefore considered as the driver for successional resets along these streams.

From 2014 to 2015, a successional setback of forest cover is observed throughout the area in both the level 1 and level 2 classifications. From the level 2 classification is derived that the decrease in forest area in 2015 coincides with increased coverage of shrubland and dry tall grassland. Since then a regeneration of forest occurs. This event is not coinciding with a disturbance event from the datasets used in this study, so no relation to the environmental drivers was established. Possible explanations are intensive anthropogenic cutting and burning occurred in 2015, or extensive forest fires took place.

Anthropogenic disturbances are considered the main drivers for maintaining the *phanta* grasslands such as Lamkauli and Baghaura. Historical analysis shows that these phantas have been present for at least since 1964 and for Lamkauli probably at least since 1927. For these phantas it is known that annual anthropogenic cutting and burning occurs (Dinerstein, 1979a; Brown, 1995). Before Bardia was established as National Park, a larger extent of savannah type grasslands was present, based on the

aerial photograph of 1964 (Appendix D) and its classified land cover map. Supposedly, because of absence of anthropogenic disturbances and slow westward shift of the Geruwa river in the last decennia of the 20th century, these grasslands declined in coverage. The still present phantas such as Lamkauli, Baghaura and Khauraha are present because successional growth is mainly deterred by anthropogenic measures.

5.3 In context with literature and regional findings

5.3.1 Historic context

In a historical context, comparison of the grasslands of the level 1 classification to the land cover map created for 1964 indicates that the Lamkauli, Baghaura and Khauhara *phantas* have been present for at least a couple of decades. Going further back in time, the Lamkauli grassland can be traced back to a village that is mapped on the topographic map of 1927 as Lathwa. This is not the case for Baghaura and Khauraha. Based on the aerial photographs from 1964 (Appendix D) no villages are present within the park, except a tiny agricultural area close to Chisapani. According to Brown (1997) the Baghaura and Lamkauli phantas haven been cultivated between 1965 and 1975, one year after the date of aerial photographs 1964.

5.3.2 Regional context

In a regional context, the shift of the river course in 2009 resulted in an increase of water coverage during the dry period along the western branch of the Karnali river (Kauriala river), with a decreasing trend of forest coverage and lower coverage of grassland along this branch, as calculated in section 4.6.2. The fluvial disturbance factors seemed to have increased in this river whereas those disturbances seem to have decreased along the Geruwa branch.

For the Babai river, eastward of the Geruwa river, the level 2 classification is applied. Especially disturbances in the vegetation pattern are observed in 2014 and 2017, coinciding with large precipitation events. For these years is also known that extensive flooding of the Babai river occurred (Chhetri et al., 2020). From 1993 to 2019, for the Babai river it is expected to have seen decreased coverage of grasslands because of the replacement of several villages when the park was established. However, in this study this is not investigated further with the level 1 classification model. An increase in extreme precipitation events in the region (Bajracharya, 2014; Karki et al., 2017) could mean that the magnitude of fluvial disturbances caused by the Babai river and perennial streams increases. This would be favorable for maintaining a degree of heterogeneity and also grassland habitat of endangered faunal species.

For a long time, plans of creating an hydropower dam in the Karnali river near Chisapani have been around, which could have significant consequences on the floodplain vegetation in Bardia National Park. It is thought that installment of the dam will have consequences for discharge and sediment supply. Variation in magnitude of discharge will decrease as observed in other locations where dams have been built (Beck and Basson, 2003). This would result in smaller peak discharges downstream. The decreased peak discharges would also impact the morphodynamical changes of the Geruwa river. Changes in river morphology are postulated to happen during extreme discharges with recurrence intervals of 5 years or

larger (Richardson and Thorne, 2001). If the magnitude of extreme discharges decreases, it is less likely that the river course will shift to the Geruwa branch, so that it becomes the dominant discharge branch of the Lower Karnali system again. Installment of the dam would than make the present-day situation more permanent, and a shift to higher successional levels of vegetation is expected. From a sedimentation supply perspective, smaller amounts of sediment are expected to reach Bardia National Park, resulting in narrowing of the river channel (Beck and Basson, 2003).

5.3.3 Earlier studies in Bardia

The outcome of this study is compared to earlier findings in Bardia National Park and for other places in the terai with similar characteristics. No other study considered annual land cover maps for studying the space-time dynamics of land cover in the Terai Zone. The studies that assessed land cover changes used three to six moments in time to assess changes. In Canada and in the Netherlands, studies have used annual imagery for studying land cover dynamics, to which the results of this study can be compared.

The land cover data of 1976 (Dinerstein) and 1997 (Sharma) indicated a decrease in tall floodplain grasslands and savannah grasslands, and an increase in forest, both successional and Sal forest. This is in line with the trend found in this study for the period between 1964 and 2000, in which a loss of grasslands and increase of forest is observed.

5.3.4 In context with studies in the Terai Zone

Other parks in the (Indian) Terai where a shift in river course occurred are the Manas reserve and Jaldapara Wildlife Sanctuary. In the Manas reserve, the coverage of alluvial grasslands decreased (46.8%) along the river branch with reduced discharges, while a 74.8% increase in savannah type of grasslands was observed. Water sources became scarce and a shift to drier vegetation types occurred in the reserve. These changes are somewhat different from those observed at Bardia National Park. In Bardia National Park, the succession from alluvial grasslands is observed to transition directly to riverine forest instead of savannah grassland (short grassland in this report), except if disturbances occur (Dinerstein, 1979b). In the Jaldapara Wildlife Sanctuary a shift in course of the Torsa river during floods in 1968 is seen as one of the primary factors for decreased coverage of grassland and increase in woodland. These are both scenarios that could happen to Bardia National Park if the shift of the river course is permanent.

5.3.5 In context with similar studies outside of the Terai Zone

As described in the literature review, the study of Hermosilla et al. (2018) used an elaborate method of post processing using a framework of changes between annual land covers. Accuracy obtained was 70,3% with a Random Forest classification model, resembling the accuracy achieved in this study for the level 2 classification with a comparable choice of land cover classes. Post-processing in the study of Hermosilla included a Hidden Markov Model, and logical land cover transition rules, significantly reducing errors in land cover change.

In the Netherlands a similar study was conducted, specific on floodplain vegetation (Harezlak et al., 2020). The vegetation in the floodplain has been mapped using a 35-year Landsat series, with 5-year steps in time taken with 5-year composites. Although this reduces the temporal resolution for analysis, the obtained accuracy is somewhat higher (77%). For analysis Ternary graphs with unchanged,

retrogression and succession on the axes was an adequate analysis for considering dynamics of land cover. Compared to these studies the achieved accuracies of this study are of the same magnitude.

5.3.6 Implications for ecology and measurement practices

The coverage of wet tall grasslands is relatively extensive at present, which is beneficial for species dependent on these grasslands, such as hog deer and rhinoceros. For faunal species dependent on dispersed grasslands in the landscape the habitat suitability is thought to have decreased over the last decades. With the reduced fluvial disturbances by the Geruwa river, land cover will shift to later successional stages in the vicinity of the channel belt. This makes anthropogenic interventions a greater necessity to maintain a large enough degree of disturbances for the early- to mid-successional stages of vegetation to be maintained in the vicinity of the channel belt. Without interventions, it is expected that on a longer timescale the now extensive alluvial tall grasslands will transition to more woody species with ultimately a homogenic riverine forest. However, if anthropogenic disturbances are extensive, the now alluvial tall grasslands could turn into grasslands with short grassland (more *Imperata cylindrica* dominated), such as Lamkauli and Baghaura, based on successional relationships from literature (Dinerstein, 1979b; Lehmkuhl, 2000).

5.4 Future research

For future research in the park it is interesting to focus on a more detailed level of vegetation types. UAVs (Unmanned Aerial Vehicles) are considered very useful for mapping floodplain vegetation at very high accuracies (Van Iersel et al., 2018; Van Iersel, 2020), considering vegetation height (0.17 - 0.33 m accuracy) and greenness. This would enable detailed monitoring of growth of grasses and transitions to other types of vegetation, although this has not yet been explored on more detailed grassland communities. Increased accuracies could be achieved by using satellite imagery with a higher spatial and temporal resolution (e.g. Sentinel) or imagery taken by UAVs, although the latter is more costly.

Driving factors not considered here, but proven to have impact on the vegetation pattern are soil moisture and substrate. Including these, along with forest fires and anthropogenic disturbances would make the understanding of space-time land cover dynamics in Bardia more complete. The impact of forest fire was shallowly considered in this study. To gain more insights into the impact of forest fires on the vegetation pattern, it is advised to study forest fire events on a smaller spatial and temporal scale. Detailed logging of anthropogenic measurements could increase understanding of the impact of anthropogenic disturbances on land cover dynamics.

For other parks in the Terai, the used methodology could successfully be implemented for assessing the annual development of the vegetation pattern, while the monetary costs are minimal. Two parks of interest are for example Chitwan National Park, where grasslands have been recorded to decline in area, and the Katerniaghat wildlife sanctuary located downstream of Bardia National Park. The reduced impact of the Geruwa river is likely of impact for the Katerniaghat wildlife sanctuary as well, and of interest is the consequence of the shift in river course for the vegetation there. Moreover, with the assumption that the composition of the vegetation types does not change, the classification model created for 2019 could be used for years to come to monitor the land cover development, preferably with the advised optimizations incorporated.

6. Conclusion

The land cover dynamics could successfully be connected to environmental drivers. The drivers considered are discharge and flooded area of the Karnali river, precipitation, and forest fires. The relation between environmental drivers on the space-time dynamics of the land cover in Bardia National Park is studied by creating annual land cover maps and by comparing the changes in land cover to variations in datasets of environmental drivers. The accuracy of the produced maps is sufficient to draw general conclusions on the land cover dynamics.

The general pattern of grassland patches experienced a decline in heterogeneity, based on landscape fragmentation metrics. The outcome indicates the following for grassland patches: a decrease in number, a decrease in length of the perimeter, an increase in connectivity and a compaction of the shape. These findings indicate encroachment of the grassland patches and loss of landscape heterogeneity. Furthermore, the aerial coverage of grasslands was largest in 2019 compared to other years in the studied timespan, which is from 1993 to 2019 and separately 1964). From 1993 to 2019, grasslands have covered almost the whole extent of the active river channels at least one moment in time, which indicates that no forest stand is older than 27 years in and close to the stream channel.

Before the shift in river course in 2009, extreme hydrologic events (in 2000, 2008 and 2009) coincide with considerable transitions of grassland to bare, where the coverage of grassland is revegetated over time after the event. For extreme discharges of the Karnali river measured at Chisapani, these transitions happen close to and near the Geruwa river, which is the eastern branch of the Lower Karnali system.

The shift in river course of the Geruwa river is considered to be of significant influence on the peak discharges and therefore on the vegetation pattern. After 2009, no successional resets coincided with extreme discharges of the Karnali river, while discharges measured at Chisapani in 2013 and 2014 were of a greater magnitude than the earlier measured discharges. The fluvial disturbances have been reduced and extensive revegetation of the riverbed by early successional vegetation along and within the stream channel is observed, accompanied with a steady shift to later successional stages of vegetation. The decline of fluvial disturbances along the Geruwa river is supported by applying the classification model to the Kauriala river, the western branch of the Lower Karnali system. Since the shift to this branch in 2009, a loss of grass and forest and increase of bare and water cover is observed there.

In years 2007 and 2014, years with extreme precipitation events, transitions from grassland to bare occurred along the perennial streams. Large discharges in the perennial streams during extreme precipitation events are therefore considered as the driver for successional resets along these streams.

From 2014 to 2015, a successional setback of forest cover is observed throughout the area in both the level 1 and level 2 classifications, while shrubland and dry tall grassland increased in coverage. This event This event is not coinciding with a disturbance event from the datasets used in this study, so no relation to the environmental drivers was established. Possible explanations are intensive anthropogenic cutting and burning occurred in 2015, or extensive forest fires took place not recorded by the fire dataset based on MODIS imagery.

Anthropogenic disturbances are considered the main drivers for maintaining the *phanta* grasslands such as Lamkauli and Baghaura, on which annual anthropogenic cutting and burning occurs. Historical analysis shows that these phantas have been present for at least since 1964 and for Lamkauli presence is

recorded in 1927. Before Bardia was established as National Park, larger extent of savannah type grasslands were present, based on the land cover map of 1964 and literature. Supposedly, because of absence of anthropogenic disturbances and slow westward shift of the Geruwa river in the last decennia of the 20th century, grasslands declined in coverage especially east of Baghaura and north of Lamkauli. The still present *phantas* such as Lamkauli, Baghaura and Khauraha are present because successional growth is mainly deterred by anthropogenic measures.

The changing land cover pattern with expected increase in later successional stages of vegetation in the vicinity of the Geruwa river in the next decade highlights the necessity to maintain a degree of disturbance processes to conserve the early to mid-successional vegetation types beneficial for faunal species in Bardia National Park.

Increased annual data on anthropogenic activities, a more elaborate evaluation of forest fires and other environmental drivers such as soil moisture and substrate, or using imagery with a higher spatial or temporal resolution such as Sentinel satellites imagery or UAVs will increase the understanding of the space-time dynamics of the land cover pattern in Bardia National Park.

7. References

Acharya, R. 2002. Comparison of change detection techniques in Chitwan District of Nepal. Change: 1–12.

Adhakari, B.R. 2013. Flooding and Inundation in Nepal Terai: Issues and Concerns. Hydro Nepal J. Water, Energy Environ. 12: 59–65. doi: 10.3126/hn.v12i0.9034.

AgiSoft PhotoScan Standard. 2016. http://www.agisoft.com/downloads/installer/.

Ahmad, A., and S. Quegan. 2013. Comparative analysis of supervised and unsupervised classification on multispectral data. Appl. Math. Sci. 7(73–76): 3681–3694. doi: 10.12988/ams.2013.34214.

Areendran, G., K. Raj, S. Mazumdar, and A. Sharma. 2017. Land use and land cover change analysis for Kosi river wildlife corridor in Terai Arc landscape of Northern India: Implications for future management. Trop. Ecol. 58(1): 139–149.

Arieira, J., D. Karssenberg, S.M. De Jong, E.A. Addink, E.G. Couto, C. Nunes Da Cunha, and J.O. Skøien. 2011. Integrating field sampling, geostatistics and remote sensing to map wetland vegetation in the Pantanal, Brazil. Biogeosciences 8(3): 667–686. doi: 10.5194/bg-8-667-2011.

Baidya, N.G., D.R. Bhuju, and P. Kandel. 1970. Land Use Change in Buffer Zone of Chitwan National Park, Nepal between 1978 and 1999. Ecoprint An Int. J. Ecol. 16: 79–86. doi: 10.3126/eco.v16i0.3478.

Bajracharya, R. 2014. Study of climate change in Bardiya district, Nepal: impact and adaptation in agriculture (a case study from Kalika VDC). BSc thesis, Kathmandu University.

Baptist, M.J., V. Babovic, J.R. Uthurburu, M. Keijzer, R.E. Uittenbogaard, A. Mynett, and A. Verwey. 2007. On inducing equations for vegetation resistance. J. Hydraul. Res. 45(4): 435–450. doi: 10.1080/00221686.2007.9521778.

Beck, J.S., and G.R. Basson. 2003. The hydraulics of the impacts of dam development on the river morphology. Water Res. Com. Rep. No. 1102/1/03, South Africa. (1102): 287.

Beeri, O., R. Phillips, J. Hendrickson, A.B. Frank, and S. Kronberg. 2007. Estimating forage quantity and quality using aerial hyperspectral imagery for northern mixed-grass prairie. Remote Sens. Environ. 110(2): 216–225. doi: 10.1016/j.rse.2007.02.027.

Belgiu, M., and L. Drăgu. 2016. Random forest in remote sensing: A review of applications and future directions. ISPRS J. Photogramm. Remote Sens. 114: 24–31. doi: 10.1016/j.isprsjprs.2016.01.011.

Berghuis, A.H. 2019. Msc Thesis: Groundwater research in Nepal for tiger conservation, A reconnaissance study to groundwater dynamics in an alluvial mega-fan in Bardiya National Park (Terai), focusing on the interaction between groundwater and the Karnali river. MSc thesis, U.

Bey, A., A.S.P. Díaz, D. Maniatis, G. Marchi, D. Mollicone, S. Ricci, J.F. Bastin, R. Moore, S. Federici, M. Rezende, C. Patriarca, R. Turia, G. Gamoga, H. Abe, E. Kaidong, and G. Miceli. 2016. Collect earth: Land use and land cover assessment through augmented visual

interpretation. Remote Sens. 8(10): 1–24. doi: 10.3390/rs8100807.

Bhattarai, B.P., and P. Kindlmann. 2012. Habitat heterogeneity as the key determinant of the abundance and habitat preference of prey species of tiger in the Chitwan National Park, Nepal. Acta Theriol. (Warsz). 57(1): 89–97. doi: 10.1007/s13364-011-0047-8.

Biswas, T. 2010. A Spatio-Temporal Analysis of Landscape Change within the Eastern Terai, India : Linking Grassland and Forest Loss to Change in River Course and Land Use. Ph.D.thesis, Utah State University.

Biswas, T., R.D. Ramsey, J.A. Bissonette, and J. Symanzik. 2014. Integration of two spectral indices to monitor loss of moist grasslands within the Jaldapara Wildlife Sanctuary, India. Int. J. Remote Sens. 35(3): 1038–1063. doi: 10.1080/01431161.2013.875631.

Bolton, M. 1976. Royal Karnali Wildlife Reserve Management Plan. National P. FAO/UNDP, Rome.

Breiman, L. 2001. Random forests. Mach. Learn. 45(1): 5–32. doi: 10.1023/A:1010933404324.

Brown, K. 1995. Plain tales from the grasslands: extraction, management and conservation of natural resources in Royal Bardia National Park, Nepal. Work. Pap. - Cent. Soc. Econ. Res. Glob. Environ. (GEC 95-14).

Brown, K. 1997. The political ecology of biodiversity, conservation and development in Nepal's Terai: Confused meanings, means and ends. Ecol. Econ. 24(1): 73–87. doi: 10.1016/S0921-8009(97)00587-9.

CBS. 2014. National Population and Housing Census 2011 - Chitwan. Gov. Nepal 06: 1–278. http://cbs.gov.np/image/data/Population/VDC-Municipality in detail/35 Chitwan_VDCLevelReport.pdf.

Champion, F., and S. Seth. 1968. A revised survey of the forest types of India. Indian Forest Records. Manager of Publications. Delhi, India.

Chhetri, T.B., Y.P. Dhital, Y. Tandong, L.P. Devkota, and B. Dawadi. 2020. Observations of heavy rainfall and extreme flood events over Banke-Bardiya districts of Nepal in 2016–2017. Prog. Disaster Sci. 6: 100074. doi: 10.1016/j.pdisas.2020.100074.

Chitale, V.S., and M.D. Behera. 2014. Analysing land and vegetation cover dynamics during last three decades in Katerniaghat wildlife sanctuary, India. J. Earth Syst. Sci. 123(7): 1467–1479. doi: 10.1007/s12040-014-0496-y.

Clements, F.E. 1916. Plant succession; an analysis of the development of vegetation. Carnegie Institution of Washington.

CNP. 2016. Grassland Habitat Mapping in Chitwan National Park. Chitwan National Park, Kasara, Chitwan.

Crist, E.P., and R.C. Cicone. 1984. Application of the Tasseled Cap concept to simulated Thematic Mapper data. Photogramm. Eng. Remote Sens. 50(3): 343–352.

Department of Hydrology and Meteorology. Department of Hydrology and Meteorology (no date). Real time data available at: http://www.hydrology.gov.np/#/basin/35?_k=hfoi0v (2020).

DHM. 2017. Observed Climate Trend Analysis of Nepal in the Districts and Physiographic Regions of Nepal (1971-2014). Dep. Hydrol. Meteorol. Nepal: 101.

Dinerstein, E. 1979a. An ecological survey of the royal Karnali-Bardia Wildlife Reserve, Nepal. Part II: Habitat/Animal Interactions. Biol. Conserv. 15(2): 127–150. doi: 10.1016/0006-3207(79)90030-2.

Dinerstein, E. 1979b. An ecological survey of the royal Karnali-Bardia Wildlife Reserve, Nepal. Part I: Vegetation, modifying factors, and successional relationships. Biol. Conserv. 15(2): 127–150. doi: 10.1016/0006-3207(79)90030-2.

Dinerstein, E. 1980. An ecological survey of the Royal Karnali-Bardia Wildlife Reserve, Nepal. Part III: Ungulate populations. Biol. Conserv. 18(1): 5–37. doi: 10.1016/0006-3207(80)90063-4.

DNPWC and DFSC. 2018. Status of Tigers and Prey in Nepal. Department of National Parks and Wildlife Conservation & Department of Forests and Soil Conservation. Ministry of Forests and Environment. Kathmandu, Nepal.

Edwards, E. 1983. A broad-scale structural classification of vegetation for practical purposes. Bothalia 14(3/4): 705–712. doi: 10.4102/abc.v14i3/4.1231.

Eisenberg, J.F., and J. Seidensticker. 1976. Ungulates in southern Asia: A consideration of biomass estimates for selected habitats. Biol. Conserv. 10(4): 293–308. doi: 10.1016/0006-3207(76)90003-3.

FAO. 2016. Map accuracy assessment and area estimation : a practical guide. Natl. For. Monit. Assess. Work. Pap. E(46): 69. http://www.fao.org/3/a-i5601e.pdf.

FIRMS - Active Fire Data. https://firms.modaps.eosdis.nasa.gov/active_fire/#firms-shapefile (accessed 1 March 2020).

Da Gama Leitão, H.C., and J. Stolfi. 2002. A multiscale method for the reassembly of two-dimensional fragmented objects. IEEE Trans. Pattern Anal. Mach. Intell. 24(9): 1239–1251. doi: 10.1109/TPAMI.2002.1033215.

Ghimire, B., K. Bhujel, and K. Rijal. 2014. Fire hazard zonation of Bardia National Park , Nepal : A disaster preparedness approach. : 27–33.

Gómez, C., J.C. White, and M.A. Wulder. 2016. Optical remotely sensed time series data for land cover classification: A review. ISPRS J. Photogramm. Remote Sens. 116: 55–72. doi: 10.1016/j.isprsjprs.2016.03.008.

Gorelick, N., M. Hancher, M. Dixon, S. Ilyushchenko, D. Thau, and R. Moore. 2017. Google Earth Engine: Planetary-scale geospatial analysis for everyone. Remote Sens. Environ. 202: 18–27. doi: 10.1016/j.rse.2017.06.031.

Hall, F.G., D.E. Strebel, J.E. Nickeson, and S.J. Goetz. 1991. Radiometric rectification: Toward a common radiometric response among multidate, multisensor images. Remote Sens. Environ. 35(1): 11–27. doi: 10.1016/0034-4257(91)90062-B.

Harezlak, V., G.W. Geerling, C.K. Rogers, W.E. Penning, D.C.M. Augustijn, and S.J.M.H. Hulscher. 2020. Revealing 35 years of landcover dynamics in floodplains of trained lowland rivers using satellite data. River Res. Appl. (September 2019): 1–9. doi: 10.1002/rra.3633.

Hasmadi, M., P. Hz, and S. Mf. 2009. Evaluating supervised and unsupervised techniques for land cover mapping using remote sensing data. Geogr. - Malaysian J. Soc. Sp. 5(1): 1–10.

Hermosilla, T., M.A. Wulder, J.C. White, N.C. Coops, and G.W. Hobart. 2015a. An integrated Landsat time series protocol for change detection and generation of annual gap-free surface reflectance composites. Remote Sens. Environ. 158: 220–234. doi: 10.1016/j.rse.2014.11.005.

Hermosilla, T., M.A. Wulder, J.C. White, N.C. Coops, and G.W. Hobart. 2015b. Regional detection, characterization, and attribution of annual forest change from 1984 to 2012 using Landsat-derived time-series metrics. Remote Sens. Environ. 170: 121–132. doi: 10.1016/j.rse.2015.09.004.

Hermosilla, T., M.A. Wulder, J.C. White, N.C. Coops, and G.W. Hobart. 2018. Disturbance-Informed Annual Land Cover Classification Maps of Canada's Forested Ecosystems for a 29-Year Landsat Time Series. Can. J. Remote Sens. 44(1): 67–87. doi: 10.1080/07038992.2018.1437719.

Hijmans, R.J., J. van Etten, M. Mattiuzzi, M. Sumner, J.A. Greenberg, O.P. Lamigueiro, A. Bevan, E.B. Racine, and A. Shortridge. 2011. Raster: raster: Geographic data analysis and modeling. R Packag. version: 2–0. http://cran.stat.unipd.it/web/packages/raster/%5Cnhttp://cran.at.r-project.org/web/packages/raster/raster.pdf (accessed 28 June 2020).

Hu, Y., and Y. Hu. 2019. Land cover changes and their driving mechanisms in Central Asia from 2001 to 2017 supported by Google Earth Engine. Remote Sens. 11(5). doi: 10.3390/rs11050554.

Hupp, C.R., and W.R. Osterkamp. 1996. Riparian vegetation and fluvial geomorphic processes. Geomorphology 14(4 SPEC. ISS.): 277–295. doi: 10.1016/0169-555X(95)00042-4.

Van Iersel, W. 2020. A bird's-eye view on river floodplains: Mapping and monitoring land cover with remote sensing. PhD thesis, Utrecht University.

Van Iersel, W., M. Straatsma, E. Addink, and H. Middelkoop. 2018. Monitoring height and greenness of non-woody floodplain vegetation with UAV time series. ISPRS J. Photogramm. Remote Sens. 141: 112–123. doi: 10.1016/j.isprsjprs.2018.04.011.

Inskipp, C., and T. Inskipp. 1983. Report on a survey of Bengal Floricans Houbaropsis bengalensis in Nepal and India, 1982. International Council for Bird Preservation.

Jnawali, S.R., and P.W. Wegge. 1993. Space and habitat use by a small re-introduced population of greater one–horned rhinoceros in RBNP–a preliminary report.

Jnawali, S.R., and P. Wegge. 2000. Importance of tall grasslands in megaherbivore conservation. p. 84–91. *In* Grassland ecology and management in protected areas of Nepal. Proceedings of a Workshop, Royal Bardia National Park, Thakurdwara, Bardia, Nepal, 15-19 March, 1999. Volume 2: Terai protected areas. International Centre for Integrated Mountain Development.

Karki, R., S. Ul Hasson, U. Schickhoff, T. Scholten, and J. Böhner. 2017. Rising Precipitation Extremes across Nepal. Climate 5: 4. doi: 10.3390/cli5010004.

Kelley, L.C., L. Pitcher, and C. Bacon. 2018. Using google earth engine to map complex shade-grown coffee landscapes in northern Nicaragua. Remote Sens. 10(6). doi: 10.3390/rs10060952.

Kennedy, R.E., S. Andréfouët, W.B. Cohen, C. Gómez, P. Griffiths, M. Hais, S.P. Healey, E.H. Helmer, P. Hostert, M.B. Lyons, G.W. Meigs, D. Pflugmacher, S.R. Phinn, S.L. Powell, P. Scarth, S. Sen, T.A. Schroeder, A. Schneider, R. Sonnenschein, J.E. Vogelmann, M.A. Wulder, and Z. Zhu. 2014. Bringing an ecological view of change to landsat-based remote sensing. Front. Ecol. Environ. 12(6): 339–346. doi: 10.1890/130066.

Van Kooten, E.E. 2019. Changes in the Lower Karnali river by human activities and its possible role on sub-tropical tall grasslands in Bardia National Park, Nepal. M.Sc. thesis, Utrecht Univeristy.

Langley, S.K., H.M. Cheshire, and K.S. Humes. 2001. A comparison of single date and multitemporal satellite image classifications in a semi-arid grassland. J. Arid Environ. 49(2): 401–411. doi: 10.1006/jare.2000.0771.

Lawrence, R.L., S.D. Wood, and R.L. Sheley. 2006. Mapping invasive plants using hyperspectral imagery and Breiman Cutler classifications (RandomForest). Remote Sens. Environ. 100(3): 356–362. doi: 10.1016/j.rse.2005.10.014.

Lehmkuhl, J. 1989. The ecology of south-Asian tall-grass communities (PhD. thesis, Washington, Seattle, WA). PhD dissertation, University of Washington, Seattle, WA.

Lehmkuhl, J.F. 1994. A classification of subtropical riverine grassland and forest in Chitwan National Park, Nepal. Vegetatio 111(1): 29–43. doi: 10.1007/BF00045575.

Lehmkuhl, J.F. 2000. The organisation and human use of Terai riverine grasslands in the Royal Chitwan National Park, Nepal. Grassl. Ecol. Manag. Prot. areas Nepal. Proc. a Work. R. Bardia Natl. Park. Thakurdwara, Bardia, Nepal, 15-19 March, 1999. Vol. 2 Terai Prot. areas (Lehmkuhl): 37–49.

Li, X., and A.G.O. Yeh. 1998. Principal component analysis of stacked multi-temporal images for the monitoring of rapid urban expansion in the Pearl River Delta. Int. J. Remote Sens. 19(8): 1501–1518. doi: 10.1080/014311698215315.

Lo, C.P., and L.J. Watson. 1998. The influence of geographic sampling methods on vegetation map accuracy evaluation in a swampy environment. Photogramm. Eng. Remote Sensing 64(12): 1189–1200.

Lorenz, C.M., G.M. Van Dijk, A.G.M. Van Hattum, and W.P. Cofino. 1997. Concepts in river ecology: implications for indicator development. Regul. Rivers Res. Manag. 13(6): 501–516. doi: 10.1002/(SICI)1099-1646(199711/12)13:6<501::AID-RRR479>3.0.CO;2-1.

Mas, J.F., and E. Vega. 2012. Assessing yearly transition probability matrix for land use/land cover dynamics. Accuracy 2012 - Proc. 10th Int. Symp. Spat. Accuracy Assess. Nat. Resour. Environ. Sci.: 345–350.

McGarigal, K. 199AD. FRAGSTATS: spatial pattern analysis program for quantifying landscape structure (Vol. 351). US Department of Agriculture, Forest Service, Pacific Northwest Research Station.

McGarigal, K. ;Cushma. 2002. FRAGSTATS: Spatial Pattern Analysis Program for Categorical Maps. Computer software program produced by the authors at the University of Massachusetts, Amherst. http://www. umass. edu/landeco/research/fragstats/fragstats. html.

McGarigal, K. 2014. Landscape Pattern Metrics. *In* Wiley StatsRef: Statistics Reference Online. John Wiley & Sons, Ltd, Chichester, UK.

Moe, S.R., and P. Wegge. 1994. Spacing behaviour and habitat use of axis deer (Axis axis) in lowland Nepal. Can. J. Zool. 72(10): 1735–1744. doi: 10.1139/z94-234.

Myneni, R.B., F.G. Hall, P.J. Sellers, and A.L. Marshak. 1995. Interpretation of spectral vegetation indexes. IEEE Trans. Geosci. Remote Sens. 33(2): 481–486. doi: 10.1109/36.377948.

Nagarkoti, A. 2012. a Comparative Study of Abundance of Tiger Prey Base in Bardia-Katarniaghat (Khata) Corridor and South-West Corner of Bardia National Park. M.Sc. thesis, Norwegion Univ. Life Sci.

Nordberg, M.L., and J. Evertson. 2005. Vegetation index differencing and linear regression for change detection in a Swedish mountain range using Landsat TM® and ETM+® imagery. L. Degrad. Dev. 16(2): 139–149. doi: 10.1002/ldr.660.

Odden, M. 2007. Tigers, leopards and their prey in Bardia National Park, Nepal. Tigers, leopards their prey Bardia Natl. Park. Nepal (January 2007): 36 pp. doi: 10.13140/RG.2.2.29496.75527.

Odden, M., P. Wegge, and T. Storaas. 2005. Hog deer Axis porcinus need threatened tallgrass floodplains: A study of habitat selection in lowland Nepal. Anim. Conserv. 8(1): 99–104. doi: 10.1017/S1367943004001854.

Pal, M. 2005. Random forest classifier for remote sensing classification. Int. J. Remote Sens. 26(1): 217–222. doi: 10.1080/01431160412331269698.

Peet, N.B. 1997. Biodiversity and the management of tall grassland in Nepal. Ph.D., University of East Anglia.

Peet, N.B., A.R. Watkinson, D.J. Bell, and B.J. Kattel. 1999a. Plant diversity in the threatened sub-tropical grasslands of Nepal. Biol. Conserv. 88(2): 193–206. doi: 10.1016/S0006-3207(98)00104-9.

Peet, N.B., A.R. Watkinson, D.J. Bell, and U.R. Sharma. 1999b. The conservation management of Imperata cylindrica grassland in Nepal with fire and cutting: An experimental approach. J. Appl. Ecol. 36(3): 374–387. doi: 10.1046/j.1365-2664.1999.00405.x.

Planet Team. 2017. Planet Application Program Interface: In Space for Life on Earth. San Francisco, CA. https://api.planet.com.

Plexida, S.G., A.I. Sfougaris, I.P. Ispikoudis, and V.P. Papanastasis. 2014. Selecting landscape metrics as indicators of spatial heterogeneity-Acomparison among Greek landscapes. Int. J. Appl. Earth Obs. Geoinf. 26(1): 26–35. doi: 10.1016/j.jag.2013.05.001.

Pokheral, S.K. 1993. Floristic composition, biomass production, and biomass harvest in the grasslands of the Royal Bardia National Park, Bardia, Nepal. M.Sc. thesis, Agric. Univ. Norw.

Pontius, G., and S. Khallaghi. 2019. Intensity.analysis: Intensity of Change for Comparing Categorical Maps from Sequential Intervals. https://cran.r-project.org/ package=intensity.analysis.

Prajapati, A. 2008. Nutrient Analysis of important food tree species of Asian Elephant (Elephas maxiums) in hot-dry season in Bardia National Park, Nepal. (January): 57.

Puri, G.S. 1961. Indian Forest Ecology (vol.2). Oxford B. Station.: 390.

Richardson, W.R., and C.R. Thorne. 2001. Multiple thread flow and channel bifurcation in a braided river: Brahmaputra-Jamuna River, Bangladesh. Geomorphology 38(3–4): 185–196. doi: 10.1016/S0169-555X(00)00080-5.

Rock, B.N., J.E. Vogelmann, D.L. Williams, A.F. Vogelmann, and T. Hoshizaki. 1986. Remote Detection of Forest Damage. Bioscience 36(7): 439–445. doi: 10.2307/1310339.

Rouse, J.W., R.H. Hass, J.A. Schell, and D.W. Deering. 1973. Monitoring vegetation systems in the great plains with ERTS.

Roy, D.P., V. Kovalskyy, H.K. Zhang, E.F. Vermote, L. Yan, S.S. Kumar, and A. Egorov. 2016. Characterization of Landsat-7 to Landsat-8 reflective wavelength and normalized difference vegetation index continuity. Remote Sens. Environ. 185: 57–70. doi: 10.1016/j.rse.2015.12.024.

Sarma, P.K., B.P. Lahkar, S. Ghosh, A. Rabha, J.P. Das, N.K. Nath, S. Dey, and N. Brahma. 2008. Land-use and land-cover change and future implication analysis in Manas National Park, India using multi-temporal satellite data. Curr. Sci. 95(2): 223–227.

Schroeder, T., W. Cohen, C. Song, … M.C.-R. sensing of, and U. 2006. Radiometric correction of multi-temporal Landsat data for characterization of early successional forest patterns in western Oregon. Elsevier.

Seidensticker, J. 1976. Ungulate populations in Chitawan Valley, Nepal. Biol. Conserv. 10(3): 183–210. doi: 10.1016/0006-3207(76)90034-3.

Sertel, E., R.H. Topaloğlu, B. Şallı, I.Y. Algan, and G.A. Aksu. 2018. Comparison of landscape metrics for three different level land cover/land use maps. ISPRS Int. J. Geo-Information 7(10). doi: 10.3390/ijgi7100408.

Sharma, B.K. 1999. Wildlife habitat mapping by using Geographic Information Systems (GIS) in the Karnali floodplain of Royal Bardia National Park in lowland Nepal. M.Sc. thesis, Norwegian University of Life Sciences.

Shetty, S. 2019. Analysis of Machine Learning Classifiers for LULC Classification on Google Earth Engine Analysis of Machine Learning Classifiers for LULC Classification on Google Earth Engine. : 1–65.

Sinclair, H.D., S. Brown, B.R. Adhikari, M. Attal, A. Borthwick, M. Budimir, M. Creed, E.H. Dingle, S. Dugar, D. Gautam, N. Gourmelen, S.M. Mudd, S. Neupane, R. Pedreschi, K.N. Ruwanpura, J. Sharma, A. Sneddon, and M. Uprety. 2017. Improving understanding of flooding and resilience in the Terai, Nepal. : 1–5. https://infohub.practicalaction.org/oknowledge/handle/11283/620609.

Skidmore, A.K. 1999. Accuracy assessment of spatial information. p. 197–209. *In* Springer, Dordrecht.

Støen, O.G., and P. Wegge. 1996. Prey selection and prey removal by tiger (Panthera tigris) during the dry season in lowland Nepal. Mammalia 60(3): 363–373. doi: 10.1515/mamm-1996-0303.

Stuart, N., T. Barratt, and C. Place. 2006. Classifying the neotropical savannas of Belize using remote sensing and ground survey. p. 476–490. *In* Journal of Biogeography.

Tadono, T., H. Ishida, F. Oda, S. Naito, K. Minakawa, and H. Iwamoto. 2014. Precise Global DEM Generation by ALOS PRISM. ISPRS Ann. Photogramm. Remote Sens. Spat. Inf. Sci. II–4(May): 71–76. doi: 10.5194/isprsannals-ii-4-71-2014.

Thapa, T.B. 2011. Habitat Suitability Evaluation for Leopard (Panthera Pardus) Using Remote Sensing and GIS in and Around Chitwan National Park, Nepal. PhD thesis, Saurashtra University.

Thapa, K., S. Nepal, G. Thapa, S.R. Bhatta, and E. Wikramanayake. 2013. Past, present and future conservation of the greater one-horned rhinoceros Rhinoceros unicornis in Nepal. Oryx 47(3): 345–351. doi: 10.1017/S0030605311001670.

Thorne, C.R., A.P.G. Russell, and M.K. Alam. 1993. Planform pattern and channel evolution of the Brahmaputra River, Bangladesh. Geol. Soc. Spec. Publ. 75(1): 257–276. doi: 10.1144/GSL.SP.1993.075.01.16.

Turner, M.G., and R.H. Gardner. 2015. Landscape ecology in theory and practice: Pattern and process, second edition. Springer.

Upreti, B.N. 1994. Royal Bardia national park. National Conservation Strategy Implementation Project, National Planning Commission, HMG Nepal, in collaboration with IUCN--The World Conservation Union. National Conservation Strategy Implementation Project.

USAID. 2018. Lower Karnali Watershed Health Report. Water: 1–23. www.chesapeakebay.net/action/howtotips.

Vesipa, R., C. Camporeale, and L. Ridolfi. 2017. Effect of river flow fluctuations on riparian vegetation dynamics: Processes and models. Adv. Water Resour. 110: 29–50. doi: 10.1016/j.advwatres.2017.09.028.

Vogels, M.F.A., S.M. de Jong, G. Sterk, and E.A. Addink. 2017. Agricultural cropland mapping using black-and-white aerial photography, Object-Based Image Analysis and Random Forests. Int. J. Appl. Earth Obs. Geoinf. 54: 114–123. doi: 10.1016/j.jag.2016.09.003.

Wegge, P., S.R. Jnawali, T. Storaas, and M. Odden. 1999. Grasslands and large mammal conservation in the lowland Terai: a preliminary

synthesis based on field research conducted in Royal Bardia National Park, Nepal. p. 50–57. *In* Grassland ecology and management in protected areas of Nepal. Proceedings of a Workshop, Royal Bardia National Park, Thakurdwara, Bardia, Nepal, 15-19 March, 1999. Volume 2: Terai protected areas. International Centre for Integrated Mountain Development.

White, J.C., M.A. Wulder, G.W. Hobart, J.E. Luther, T. Hermosilla, P. Griffiths, N.C. Coops, R.J. Hall, P. Hostert, A. Dyk, and L. Guindon. 2014. Pixel-based image compositing for large-area dense time series applications and science. Can. J. Remote Sens. 40(3): 192–212. doi: 10.1080/07038992.2014.945827.

Xie, Y., Z. Sha, and M. Yu. 2008. Remote sensing imagery in vegetation mapping: a review. J. Plant Ecol. 1(1): 9–23. doi: 10.1093/jpe/rtm005.

Xiong, J., P.S. Thenkabail, J.C. Tilton, M.K. Gumma, P. Teluguntla, A. Oliphant, R.G. Congalton, K. Yadav, and N. Gorelick. 2017. Nominal 30-m cropland extent map of continental Africa by integrating pixel-based and object-based algorithms using Sentinel-2 and Landsat-8 data on google earth engine. Remote Sens. 9(10): 1–27. doi: 10.3390/rs9101065.

Yang, X., M.C.J. Damen, and R.A. Van Zuidam. 1999. Satellite remote sensing and GIS for the analysis of channel migration changes in the active Yellow River Delta, China. ITC J. 1(2): 146–157. doi: 10.1016/S0303-2434(99)85007-7.

Young, N.E., R.S. Anderson, S.M. Chignell, A.G. Vorster, R. Lawrence, and P.H. Evangelista. 2017. A survival guide to Landsat preprocessing. Ecology 98(4): 920–932. doi: 10.1002/ecy.1730.

Zanter, K. 2019. Landsat Collection 1 Level 1 Product Definition. United States Geological Survey.

Zhu, Z., S. Wang, and C.E. Woodcock. 2015. Improvement and expansion of the Fmask algorithm: Cloud, cloud shadow, and snow detection for Landsats 4-7, 8, and Sentinel 2 images. Remote Sens. Environ. 159: 269–277. doi: 10.1016/j.rse.2014.12.014.

8. Appendices

I. Appendices in this report

A. Land cover maps of level 1
B. Land cover perpendicular to Geruwa river
C. Error matrices
D. 1964 composite of aerial photographs
E. Topographic maps

II. Digital appendices

F. Input data

- Training samples
- Discharge dataset
- Precipitation dataset
- Flood extent files
- Forest fire dataset
- Validation dataset

G. Scripts (Goole Earth Engine & RStudio)

- Creation of satellite composites
- Classification of land cover maps
- Land cover perpendicular to floodplain
- Transition matrices
- Sankey plot
- Validation
- Landscape fragmentation metrics
- Rasterization of the 1964 map

H. Output data

- Land cover maps
- Excel sheets with all data 'complete-overview' (transition data, calculated environmental indicators etc)

I. Additional data

- Topographic maps
- Aerial photographs (1964) of Bardia National Park and Chitwan National Park

A. Land cover maps of the level 1 classification

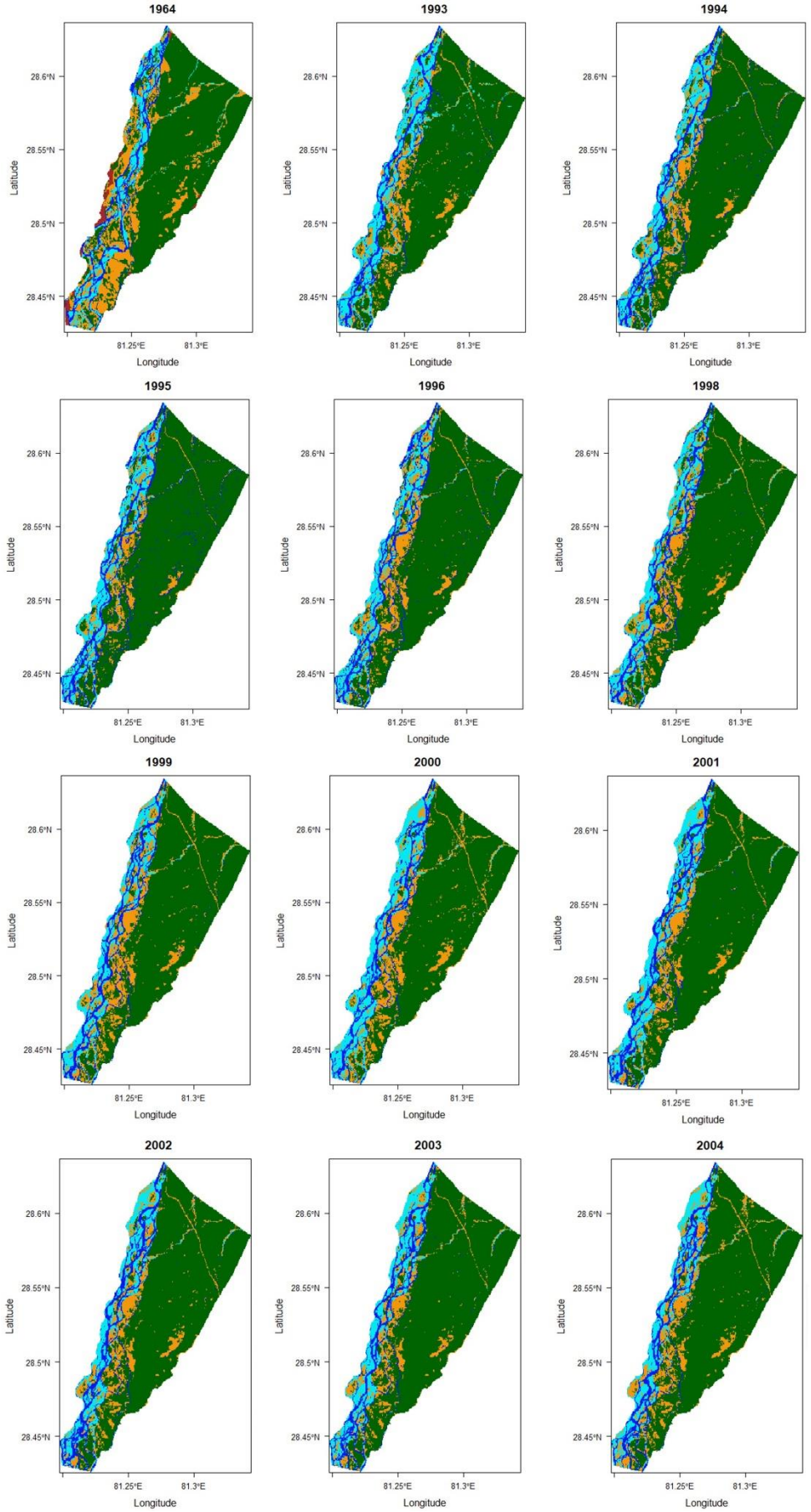

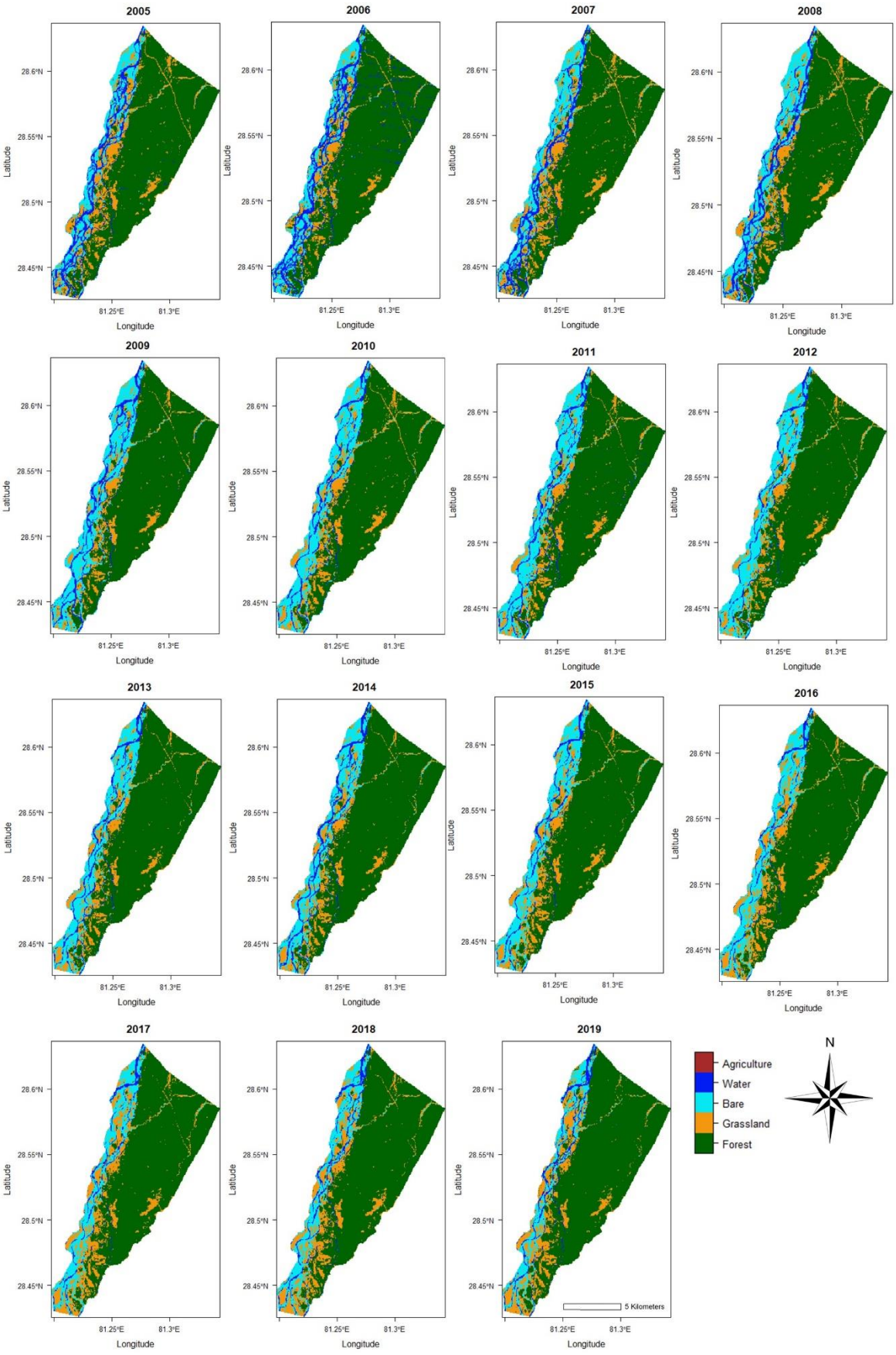
2005
2006
2007
2008
2009
2010
2011
2012
2013
2014
2015
2016
2017
2018
2019
Latitude
Longitude
28.6°N
28.55°N
28.5°N
28.45°N
81.25°E
81.3°E
Agriculture
Water
Bare
Grassland
Forest
N
5 Kilometers

B. Land cover perpendicular to Geruwa river

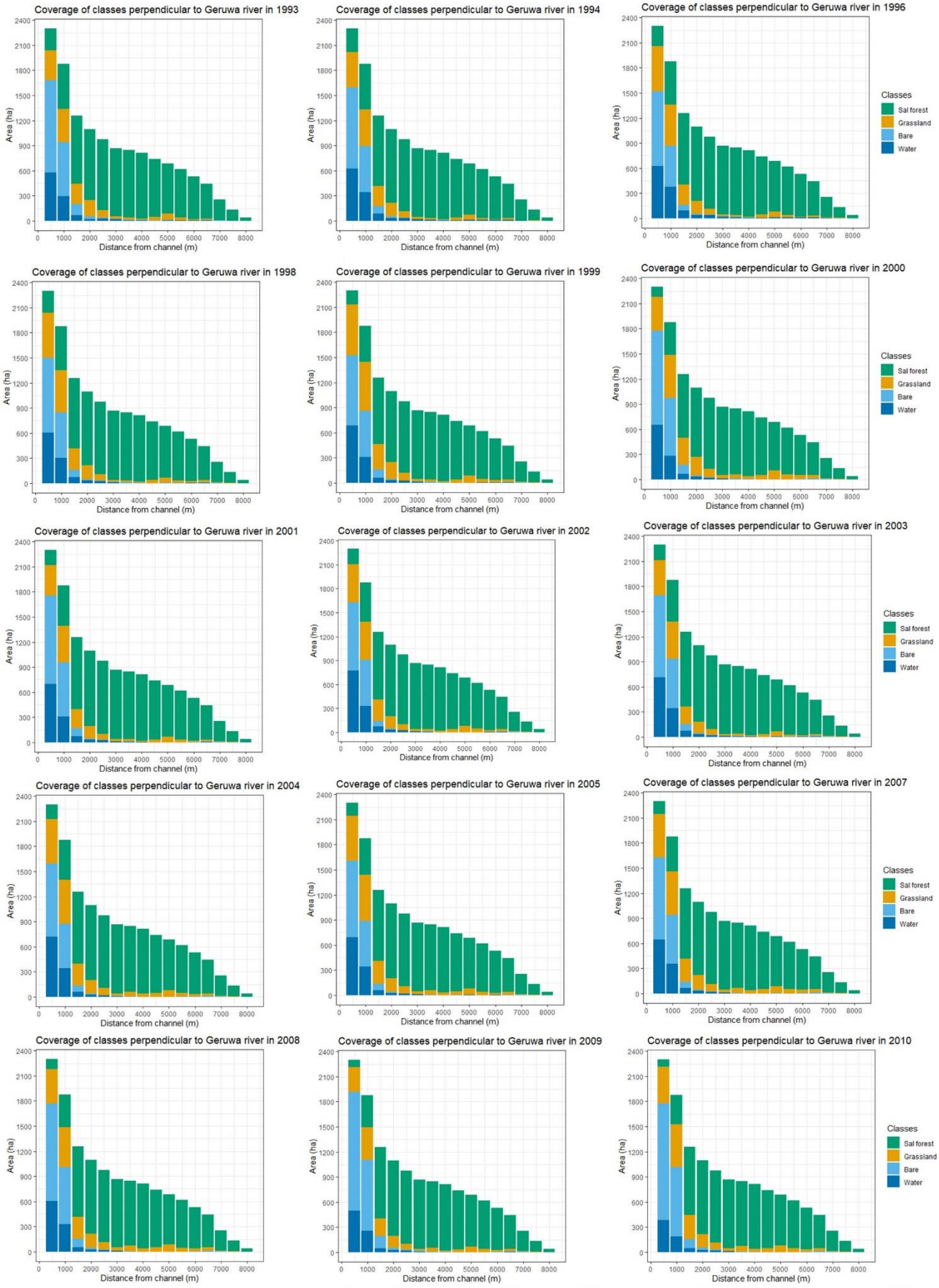

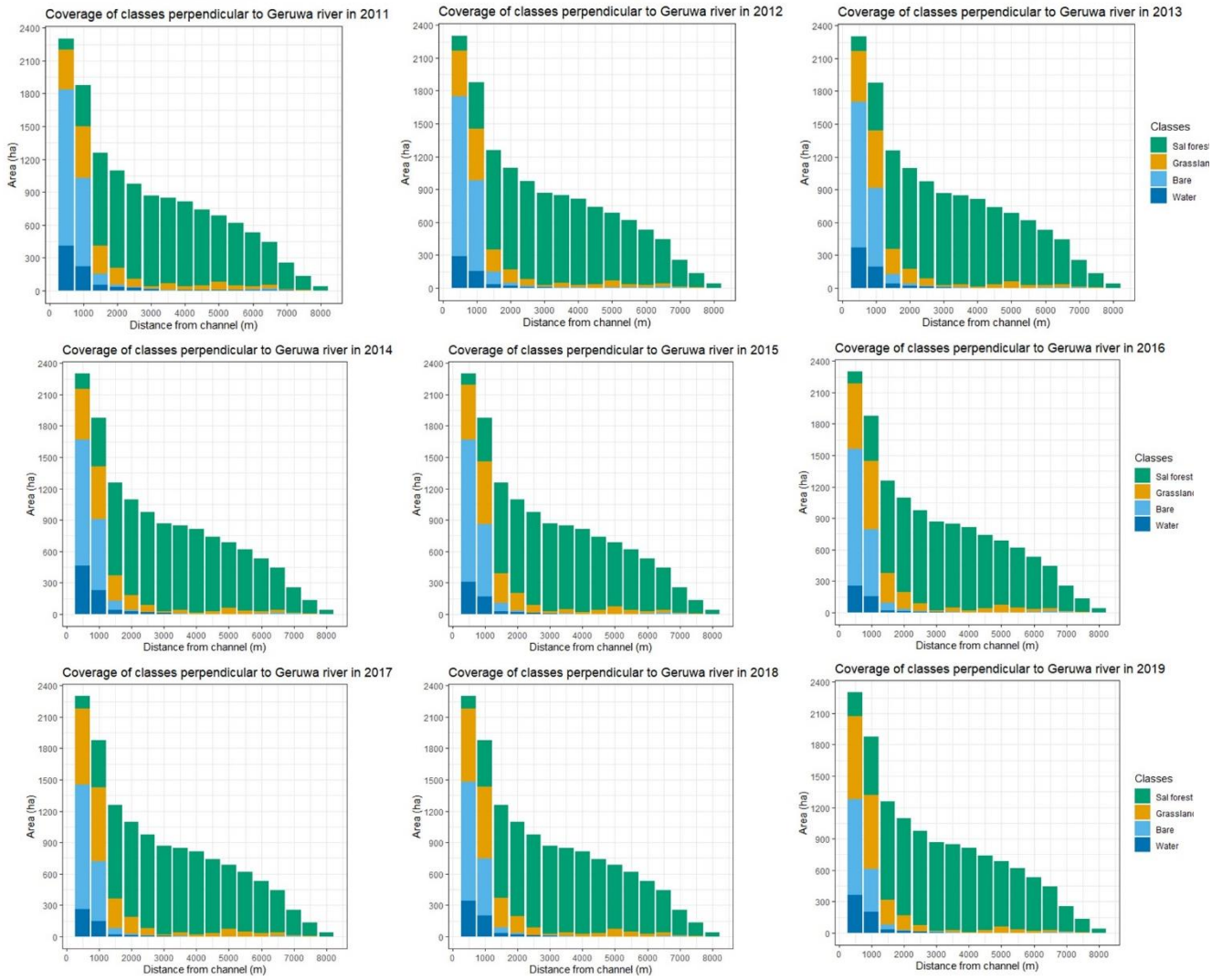
Coverage of classes perpendicular to Geruwa river in 2011
Coverage of classes perpendicular to Geruwa river in 2012
Coverage of classes perpendicular to Geruwa river in 2013
Coverage of classes perpendicular to Geruwa river in 2014
Coverage of classes perpendicular to Geruwa river in 2015
Coverage of classes perpendicular to Geruwa river in 2016
Coverage of classes perpendicular to Geruwa river in 2017
Coverage of classes perpendicular to Geruwa river in 2018
Coverage of classes perpendicular to Geruwa river in 2019
Area (ha)
Distance from channel (m)
Classes
Sal forest
Grassland
Bare
Water

C. Error matrices

2000	Forest	Grassland	Bare	Water	Sum	UA
Forest	45	4	0	0	49	91.8
Grassland	3	20	0	0	23	87.0
Bare	0	7	10	5	22	45.5
Water	1	4	2	5	12	41.7
Sum	49	35	12	10	106	
PA	91.8	57.1	83.3	50.0		**75.5**

p-value	1.43E-07	**CI95**	0.66	0.83	**kappa**	0.64

2010	Forest	Grassland	Bare	Water	Sum	UA
Forest	45	5	0	0	50	90.0
Grassland	1	14	0	0	15	93.3
Bare	1	1	22	5	29	75.9
Water	1	0	0	11	12	91.7
Sum	48	20	22	16	106	
PA	93.8	70.0	100.0	68.8		**86.8**

p-value	3.06E-15	**CI95**	0.79	0.93	**kappa**	0.81

2011	Forest	Grassland	Bare	Water	Sum	UA
Forest	45	6	0	0	51	88.2
Grassland	1	13	0	0	14	92.9
Bare	0	1	20	7	28	71.4
Water	0	0	1	12	13	92.3
Sum	46	20	21	19	106	
PA	97.8	65.0	95.2	63.2		**84.9**

p-value	1.10E-13	**CI95**	0.77	0.91	**kappa**	0.78

2018	Forest	Grassland	Bare	Water	Sum	UA
Forest	46	4	0	1	51	90.0
Grassland	5	20	1	1	27	74.0
Bare	0	5	10	4	19	52.6
Water	0	2	0	7	9	77.8
Sum	51	31	11	13	106	
PA	90.2	64.5	90.9	53.8		**78.3**

p-value	3.78-e09	**CI95**	0.69	0.86	**kappa**	0.67

2019 level 1	Forest	Grassland	Bare	Water	Sum	UA
Forest	38	5	0	0	43	88.4
Grassland	3	34	0	0	37	91.9
Bare	0	4	6	0	10	60.0
Water	1	1	1	5	8	62.5
Sum	42	44	7	5	98	
PA	90.5	77.3	85.7	100.0		**84.7**

2019 level 2	Sal forest	Wet tall grassland	Short grassland	Bare	Water	Shrub land	Riverine forest	Dry tall grassland	Sum	UA
Sal forest	23	0	0	0	0	0	0	0	23	100.0
Wet tall grassland	0	5	2	1	0	0	0	1	9	55.6
Short grassland	0	1	19	1	0	2	0	2	25	76.0
Bare	0	1	1	8	0	0	0	0	10	80.0
Water	0	0	0	0	8	0	0	1	9	88.9
Shrubland	0	1	2	0	0	3	2	1	9	33.3
Riverine forest	1	1	1	0	0	0	10	0	13	76.9
Dry tall grassland	0	1	4	0	0	3	2	6	16	37.5
Sum	24	10.	29	10.0	8	8	14	11	114. 0	
PA	95.8	50.0	65.5	80.0	100.0	37.5	71.4	54.5		**71.93**

2019 level 2 *Second validation run*	Sal forest	Wet tall grassland	Short grassland	Bare	Water	Shrub land	Riverine forest	Dry tall grassland	Sum	UA
Sal forest	18	0	0	0	0	1	0	0	19	94.7
Wet tall grassland	0	7	0	0	0	1	0	0	8	87.5
Short grassland	0	1	12	1	0	0	1	2	17	70.6
Bare	0	1	1	9	1	0	1	0	13	69.2
Water	0	1	0	0	5	0	2	0	8	62.5
Shrubland	0	0	2	0	0	1	4	2	9	11.1
Riverine forest	1	0	0	1	1	0	8	0	11	72.7
Dry tall grassland	0	0	3	0	0	1	0	6	10	60.0
Sum	19	10	18	11	7	4	16	10	95	
PA	94.7	70.0	66.7	81.8	71.4	25.0	50.0	60.0		**69.5**

2019 level 2 *Third validation run*	**Sal forest**	**Wet tall grassland**	**Short grassland**	**Bare**	**Water**	**Shrub land**	**Riverine forest**	**Dry tall grassland**	**Sum**	**UA**
Sal forest	24	0	0	0	0	0	0	0	24	100.0
Wet tall grassland	0	8	1	1	0	0	0	0	10	80.0
Short grassland	0	1	14	1	0	0	0	1	17	82.4
Bare	0	3	1	11	0	0	0	0	15	73.3
Water	0	1	0	0	11	0	0	0	12	91.7
Shrubland	1	0	1	0	0	2	1	3	8	25.0
Riverine forest	1	0	1	1	0	0	13	0	16	81.3
Dry tall grassland	0	1	6	0	0	1	1	5	14	35.7
Sum	26	14	24	14	11	3	15	9	116	
PA	92.3	57.1	78.6	78.6	100.0	66.7	86.7	55.6		**75.7**

D. Composite of aerial photographs from 1964

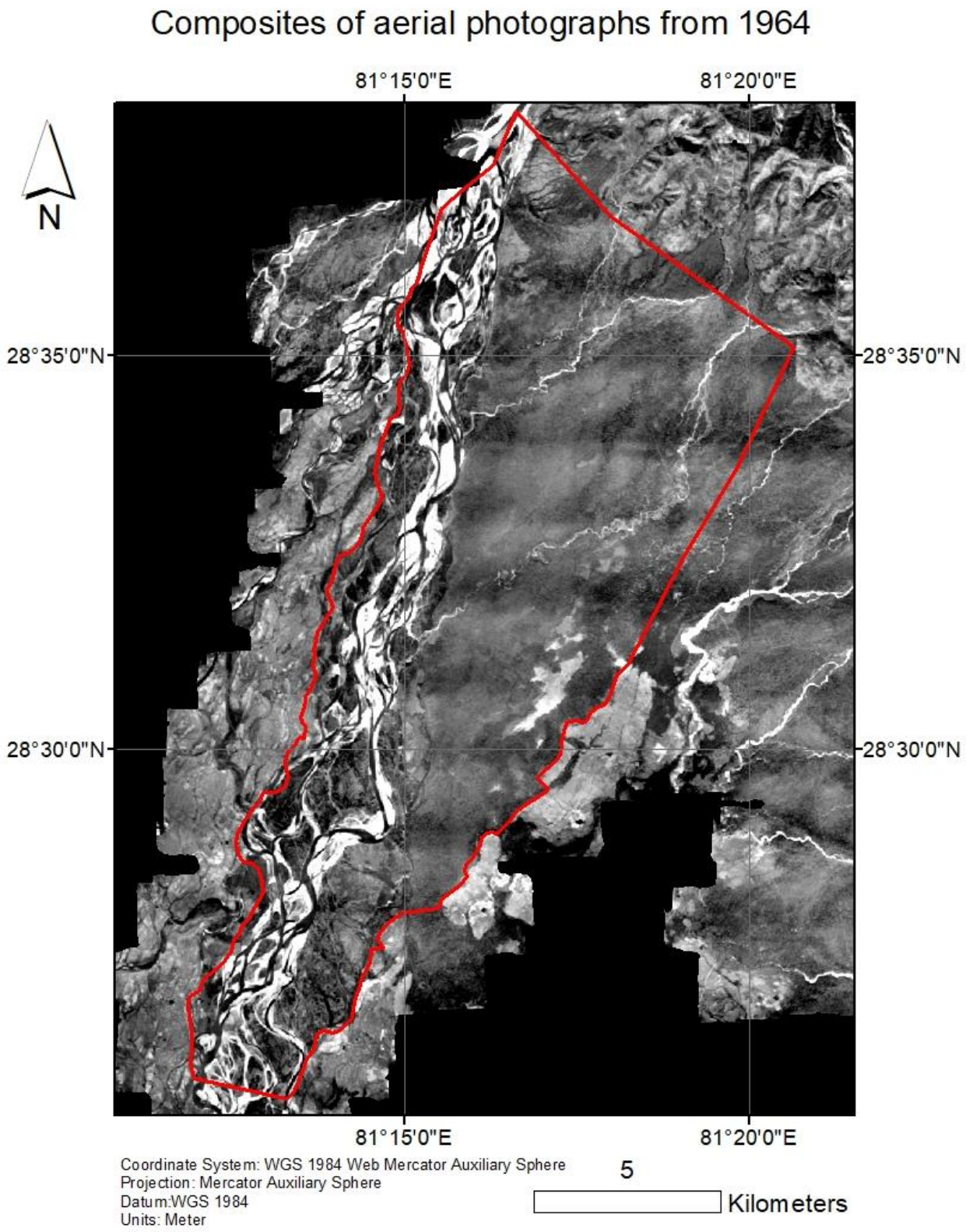

E.. Topographic maps of 1927 and 1984


JOINT OPERATIONS GRAPHIC
SCALE 1:250,000
SCALE 1:250,000
NEPĀLGANJ, NEPAL; INDIA
SERIES 1501
SHEET NH 44-15
EDITION 1
ELEVATIONS IN METERS
CAUTION